NOTE TO USERS

uOttawa

L'Université canadienne
Canada's university

FACULTÉ DES ÉTUDES SUPÉRIEURES ET POSTOCTORALES

uOttawa

L'Université canadienne
Canada's university

FACULTY OF GRADUATE AND POSDOCTORAL STUDIES

Susannah Krack

AUTEUR DE LA THÈSE / AUTHOR OF THESIS

M.Sc. (Earth Sciences)

GRADE / DEGREE

Department of Earth Sciences

FACULTÉ, ÉCOLE, DÉPARTEMENT / FACULTY, SCHOOL, DEPARTMENT

Effect of growth phase and metabolic activity on the surface charge of *Escherichia coli* K-12 and on its adhesion to quartz and lepidocrocite

TITRE DE LA THÈSE / TITLE OF THESIS

D. Fortin

DIRECTEUR (DIRECTRICE) DE LA THÈSE / THESIS SUPERVISOR

CO-DIRECTEUR (CO-DIRECTRICE) DE LA THÈSE / THESIS CO-SUPERVISOR

EXAMINATEURS (EXAMINATRICES) DE LA THÈSE / THESIS EXAMINERS

D. Lean

T. Patterson

Gary W. Slater

LE DOYEN DE LA FACULTÉ DES ÉTUDES SUPÉRIEURES ET POSTDOCTORALES /
DEAN OF THE FACULTY OF GRADUATE AND POSTDOCORAL STUDIES

Effect of growth phase and metabolic activity on the surface charge of *Escherichia coli* K-12 and on its adhesion to quartz and lepidocrocite

By

Susannah Krack

Thesis submitted to the School of Graduate Studies and Research

In partial fulfillment of the requirements for the of Master of Science (M.Sc) degree in

the Department of Earth Sciences, University of Ottawa, Ottawa, Ontario, Canada

K1N 6N5

Your file Votre référence
ISBN: 0-494-11317-0
Our file Notre référence
ISBN: 0-494-11317-0

To my parents, Maurice and Sheila

General Abstract

There are a number of bacteria associated with livestock, one of which is *Escherichia coli* O157:H7, a pathogenic bacterium often found associated with animal feces, which has the potential to contaminate groundwater in many rural areas. Adhesion onto soil particles is also an important biogeochemical process controlling bacterial transport that is influenced by a number of interrelated variables including pH, ionic strength, solution chemistry, soil mineralogy, bacterial growth phase and metabolic activity. The main objectives of this thesis were to first assess the surface reactivity of *E. coli* K-12 (a model non-pathogenic bacterium) as a function of bacterial growth phase and activity and second, to determine the extent of *E. coli* adhesion to quartz and Fe-oxide, two common soil minerals, as a function of pH, using batch experiments. The titration results showed that lepidocrocite had the highest buffering capacity, then bacteria, and quartz the lowest. Among the various cell treatments, results showed that overall, metabolically active cells in their mid-exponential phase showed the highest buffering capacity, whereas metabolically active cells in their mid-stationary growth phase showed the lowest buffering capacity. Non-metabolically active cells had intermediate buffering capacities. Adhesion results first showed that E. *coli* adhesion to lepidocrocite was pH dependent. Adhesion increased with decreasing pH because lepidocrocite possess a net positive charge at low pH while the cells are negatively charged. In the quartz systems, pH had little to no effect on cell adhesion likely because both the cell wall and the quartz surface displayed a net negative charge in the pH range studied here. Results also showed that adhesion to lepidocrocite was greater with cells in the exponential growth phase than in the stationary growth phase, likely as a result of more protonated sites on the surface of

the cells. Growth phase did not appear to affect the adhesion of *E. coli* to quartz. The results also showed that metabolic activity played a role in adhesion, especially when the adhesion was performed in the growth medium. Cells that were not reproducing and not metabolically active adhered better to both minerals, particularly in the lepidocrocite system. The enhanced adhesion in the presence of inactive cells was caused by the inhibited proton motive force. Overall, electrostatic interactions accounted for most of the mineral-bacteria interactions observed in our study. The Fe-oxides are the most likely minerals to play a role in reducing the transport of *E. coli* in natural environments due to their net positive charge under environmental conditions. However, in order to quantify the surface reactivity of the cells and minerals, surface complexation models (SCM) are needed to calculate the type and concentration of binding sites available on the cell and minerals.

Résumé

Escherichia coli est un pathogène souvent présent dans le fumier. Cette bactérie peut facilement contaminer les nappes phréatiques de plusieurs régions rurales. Plusieurs processus biogéochimiques peuvent affecter le transport des bactéries, tout particulièrement leur adhésion a des particules de sol. Ce processus est influencé par de nombreuses variables inter-reliées, incluant le pH, la force ionique et la chimie de la solution, la minéralogie du sol, la phase de croissance bactérienne et l'activité métabolique. Les objectifs principaux de cette thése étaient dans un premier temps, d'évaluer la réactivité de la surface de la bactérie *E. coli.* K-12 (une bactérie représentative non-pathogénique) en fonction de ses phases de croissance ainsi qu'en fonction de son activité métabolique. Le deuxième but était de déterminer jusqu'à quel point *E. coli* adhère aux particules de quartz et d'oxydes de fer, deux minéraux communs des sols, et ce en fonction du pH. Les résultats ont indiqué que La lépidocrocite avait la plus haute capacité tampon, suivi par les bactéries et le quartz. Parmi les différents traitements de cellules, les résultats ont démontré que les cellules actives d'un point de vue métabolique et existant en phase de croissance exponentielle avaient la plus haute capacité tampon tandis que les cellules dans la phase stationnaire avaient la plus basse capacité tampon. Les cellules non-actives avaient une capacité tampon intermédiaire. Les expériences d'adhésion avec ces mêmes bactéries et minéraux ont indiqué dans un premier temps que l'adhésion des cellules *E. coli* à la lépidocrocite était dépendente du pH. Le niveau d'adhésion a augmenté lorsque le pH a diminué parce que la lépidocrocite a une charge nette positive à bas pH tandis que les cellules sont chargées négativement. Dans le système du quartz, le pH a eu très peu d'effet sur

l'adhésion des cellules, tout probablement parce que la paroi cellulaire ainsi que la surface du quartz étaient chargées négativement dans la gamme de pH étudiée. Les résultats ont aussi démontré que l'adhésion des cellules à la lépidocrocite était plus intense pour les cellules en phase de croissance exponentielle qu'avec celles en phase stationnaire. Ceci est probablement le résultat du plus grand nombre de sites de protonation existant à la surface des cellules. La phase de coissance des bactéries *E. coli* n'apparait pas avoir eu d'effet sur leur adhésion au quartz. Les résultats ont aussi indiqué que l'activité métabolique a joué un rôle important dans l'adhésion, surtout lorsque l'adhésion se faisait dans le milieu de culture. Les cellules qui ne se reproduisaient pas et qui n'étaient pas actives métaboliquement ont mieux adhéré aux deux minéraux (tout particulièrement la lépidocrocite) que les cellules dans les autres phases de croissance et d'activité métabolique. L'augmentation de l'adhésion en présence des cellules inactives a été causée par le fait que la force motive des protons dans la paroi cellulaire était inhibée. En résumé, les interactions électrostatiques semblent être responsables de la plupart des interactions minéraux-bactéries observées dans notre étude. Les oxydes de fer, avec leur charge nette positive sous des conditions environnementales normales, sont possiblement les minéraux qui joueront le rôle le plus important dans le transport des bactéries *E. coli* dans un environnement naturel. Finalement, afin de quantifier la réactivité de la surface des cellules et des minéraux, des modèles de complexation de surface (MCS) sont nécessaires pour calculer le type et la concentration des sites de sorption sur les cellules et les minéraux.

Acknowledgements

I thank Dr. Fortin for her constant support, encouragement, and supervision without which, this thesis would not have been possible. I also thank OGS for partial funding of my salary. I thank Dr. Frances Pick for her assistance with the epifluorescence microscope and DAPI counting method, and Dr. David Lean for allowing me to use his lab facilities. I extend my tremendous gratitude to Dr. Daughney, for his regular help all along this project, particularly in the theoretical aspects. Thank you also to the professors and staff of the Earth Science Department, who created a pleasant environment to work in.

I would also like to extend my appreciation to my parents, for their encouragement and support, financial and emotional, particularly through difficult times. I am also grateful to Michelle Nugent for her valuable advice, and help with translation. A special thanks to Mike Shuker for being a constant source of encouragement, and to Louie Beans for breaking the tension in moments when nothing else could.

This project was funded by a research grant from the Ontario Ministry of Food and Agriculture, the Ontario Cattlemen's Association and the Ontario Pork Association to D. Fortin and C. Daughney.

Table of Contents

Chapter 2

Surface Reactivity of *E. coli* cells and pure phase minerals quartz (SiO_2) and Lepidocrocite (γ FeOOH) as interpreted through acid-base titrations.

Chapter 3

The effect of Growth Phase and Metabolic State on Adhesion between *E. coli* and pure phase minerals quartz (SiO_2) and Lepidocrocite (γ FeOOH).

List of Tables

Chapter 1

Chapter 2

Chapter 3

List of Figures

Chapter 1

Chapter 2

Chapter 3

General Introduction

The following manuscript is a paper format thesis designed to better identify the factors that influence the movement of *Escherichia coli* in natural soil and water environments and predict its transport. Specifically, the adhesion between *E. coli* and two soil representative minerals; quartz and lepidocrocite will be investigated. Adhesion of bacteria and minerals is of fundamental importance because adhered cells will move at a rate that is slower than the advective velocity of the groundwater.

The first chapter is a review of the background literature available on the chemical and physical properties of the bacterial cells and minerals in question, and on previous studies on adhesion between cells and other surfaces. The second chapter provides insight into the surface reactivity and buffering capacity (acid-base properties) of *E. coli* cells and quartz and lepidocrocite surfaces. This is crucial because the first step to investigating the adhesion of *E. coli* cells to minerals is to characterize the surface functional groups on the cell wall and mineral surfaces and determine the proton binding capacity of the *E. coli* cells.

The present study hypothesizes that the growth phase and metabolic state will affect the surface reactivity of *E. coli* cells (Chapter 2). Chapter 2 investigates the acid-base behaviour of *E. coli* K-12 (grown in a chemically defined medium containing nitrate and phosphate) as a function of growth phase and at the surface characteristics of lepidocrocite and quartz. Chapter 3 provides the detailed investigation of adhesion between *E. coli* cells and the minerals, including the effect of pH, growth phase and metabolic activity on adhesion of *E. coli* to quartz and lepidocrocite (γ-FeOOH). In chapter 3, it is further speculated that the changes in surface reactivity will affect the

adhesion between the cells and pure phase quartz and lepidocrocite. The results of the study will be used in future surface complexation models that will be used to better predict *E. coli* transport in aquifers and soils impacted by agricultural activities.

Chapters 2 and 3 are written as scientific papers, which will be submitted to peer-reviewed journals. As such, some redundancy (i.e., background literature in the introduction and discussion) is unavoidable.

Chapter 1

The effect of nutrient availability on the biogeochemical processes affecting adhesion between bacteria and minerals

Abstract

Mineral-bacteria adhesion affects bacterial transport in soils and is controlled by many interrelated variables, including availability of nutrients, pH, ionic strength, solution composition, mineralogy, bacterial growth phase and metabolic activity. In prior adhesion studies, the effect of pH was found to be variable and depended on the species and strain of bacteria being used in the study and on what type of surface was being used. Adhesion was found to increase with increasing hydrophobicity in some studies and decrease with increasing hydrophobicity in other studies. If the two surfaces (bacteria and mineral) have opposing charges, then increasing the ionic strength of the solution tends to decrease the adsorption. If the two surfaces have similar charges, then adsorption tends to increase with increasing ionic strength. Most studies have found that bacteria adsorb better in the exponential growth phase where they are most motile. Those with appendages also adsorbed better as they have a greater motility and can come in contact with surfaces more easily. They also have a greater surface area and higher surface charge, which also increase adsorption. Bacteria were also found to adhere better under limited nutrient availability.

1.0 Introduction

Groundwater contamination is a prevalent issue that is becoming a crisis in many areas of the world. Here in Canada, it is a serious concern because a large number of cities and communities rely on groundwater as their source of drinking water. One of the most dangerous threats facing areas of high population is the transport of deadly pathogens to the drinking water systems. The Walkerton tragedy (Ontario, May 2000) forced politicians to re-think their drinking water regulations and implement better monitoring strategies. *Escherichia coli* O157:H7, a pathogenic bacterium associated with manure, entered the groundwater aquifer through leaching by rain and surface water.

About 30% of the drinking water requirements in Ontario are provided by groundwater. In rural areas, people depend almost entirely on private wells for drinking water (Goss et al., 1998). Diffuse, or non-point sources of *E. coli*, such as the leaching from manure used as fertilizer, direct contamination by livestock, or poorly located and maintained septic beds, can threaten aquifer recharge areas, as they provide bacteria present in groundwater with an excess of nutrients (Rudolph et al, 1998).

Goss et al. (1998) and Rudolph et al. (1998) studied the contamination of well water in rural areas across Ontario. The studies focused on townships where at least 50% of the total land use was for agricultural purposes. The maximum acceptable concentration (MAC) of coliform bacteria specified by the Ontario Ministry of Health is 5 colonies per 100 ml (none of which should be *E. coli*). Table 1.1 shows data from the two studies, which tested wells for *E. coli* and related contamination. It was observed that over the winter and summer months, between 16.6% and 36.5% of the wells exceeded the Ontario guidelines.

Table1.1. Well contamination in Ontario (Modified from Goss et al., 1998)

Contaminant	No. of wells tested	Exceeds objectives	
		Winter (%)	Summer (%)
Total Coliform	1208	30.0±2.6	32.2±2.7
E. coli	**598**	**19.7±3.3**	**25.3±3.6**
Fecal coliform	268	16.8±4.6	24.3±5.2
Total coliform or fecal coliform	598	31.6±3.8	36.5±3.9
Total coliform, *E. coli* or fecal coliform	1208	33.1±2.7	35.4±2.8

The hydrological processes that affect the transport of bacteria through soils have been studied extensively. The critital factors that have been identified are pore size, pore velocity, and flow rate (Douglas et al., 1994). On the other hand, biogeochemical factors also influence in bacterial transport, and they have been overlooked.

The present thesis examines the relationship between nutrient availability and the biogeochemical factors that affect the adhesion of *E. coli* to common soil minerals. This first chapter is a literature review of the physiological and physico-chemical parameters affecting cell adhesion to mineral surfaces.

2.0 Physiological factors affecting Bacteria-Mineral Adhesion

Adhesion of bacteria to minerals is a very important biogeochemical mechanism that can aid in retarding the movement of bacteria through soil and prevent the contamination of water. Adhesion and adsorption as terms are often used interchangeably. For the purpose of this review, adsorption is specifically defined as the attachment of a solute to the surface of a solid, or as the accumulation of solutes (usually dissolved ions) around a solid-solution interface (Drever, 1997), while adhesion occurs on a larger scale between bacteria and minerals as opposed to dissolved ions (metals).

There are several interrelated variables that control the adhesion of bacteria to minerals in soil. These include soil mineralogy, pH, ionic strength, bacterial growth phase and metabolic activity. We describe here the physiological factors, including the bacterial cell wall structure, bacterial growth and nutrients. The physico-chemical factors are described in section 2.2. The availability of phosphorus, carbon and nitrogen as nutrients supplied from manure can affect these variables, thereby influencing adhesion.

2.1 Bacterial Cell Wall Structure and reactivity

Bacterial cells are prokaryotes. All cells have a cell membrane, which is enclosed within the cell wall and gives the cell its form and strength, protecting them from osmotic stress (Chapelle, 2001). Cell membranes, or cytoplasmic membranes, act as the boundary between the inside of the cell and the external environment, and serve to regulate the chemical environment in and around the cell (Chapelle, 2001). Proteins contained in the cell membrane regulate the transport of chemicals into and out of the cells (Chapelle, 2001, Fortin et al., 1998). The cell membrane consists of approximately 60% proteins and 40% phospholipids (Chapelle, 2001). Some of the proteins allow the transport of sugars into the cell, which are used as a source of energy. Other proteins can aid in transferring electrons within the cell (Chapelle 2001; Daughney and Fortin, 2001).

There are two different types of cell walls, gram-positive, and gram-negative, which differ in structure and complexity. These differing properties are important when studying adsorption of minerals to the cell wall because they result in differences in charge magnitude, which in turn affect the amount of attraction between the cell wall and charged surface (Beveridge and Fyfe, 1985). Under natural pH conditions (i.e., 3-9), most bacteria have a net negative charge (Daughney and Fortin, 2001).

Gram-positive cell walls are composed of a thick layer of peptidoglycan (Figure 1.1). Peptidoglycan is a 3D polymer formed of sugars and amino acids, which are cross-linked with peptide bridges and provides most of the strength of the cell wall (Daughney and Fortin, 2001 and references therein). The peptidoglycan is rich in the carboxyl and phosphoryl functional groups (Chapelle, 2001). Additional secondary polymers may also be present within the peptidoglycan and they are also rich in carboxyl groups, increasing the negative net charge of bacteria (Chapelle, 2001; Daughney and Fortin, 2001). *Bacillus subtilis* is a perfect example of a gram-positive bacterium.

Gram-negative cell walls have a multilayered structure consisting of a thinner layer of peptidoglycan surrounded by a two membrane layer, i.e., a layer of phosphlipids called the outer membrane (Figure 1.1), and an inner plasma membrane (Beveridge and Koval, 1981). The inner part of the outer membrane contains phospholipids rich in phosphoryl groups, whereas the outer part is composed of lipopolysaccharides (LPS), which contains both phosphoryl and carboxyl groups. The space between the cell membrane and the peptidoglycan is called the periplasmic space (Chapelle 2001). *E. coli* is a perfect example of a gram-negative bacterium.

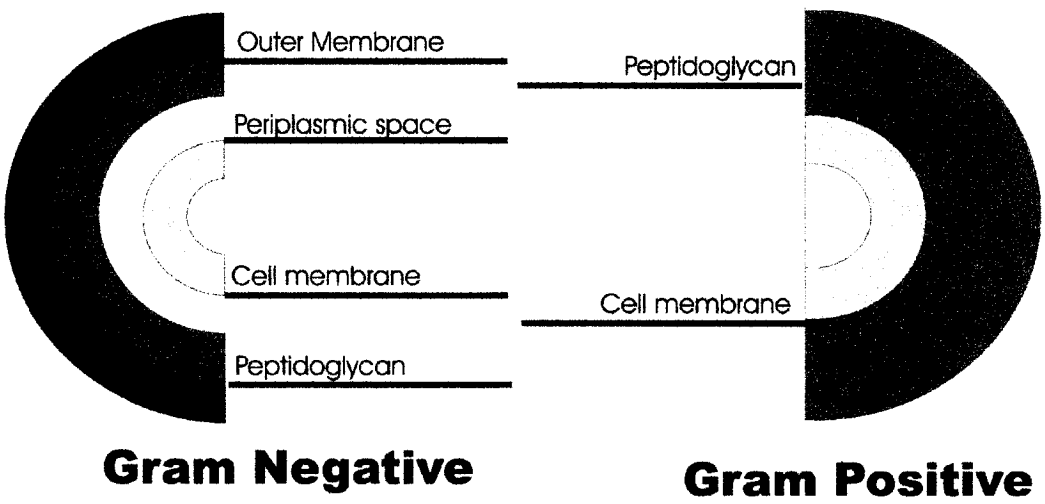

Figure 1.1. Cell wall structure. A: gram-negative cell wall, B: gram-positive cell wall (adapted from Chapelle, 2001).

Both gram-positive and gram-negative cell walls have high negative charge density as the outer membrane and peptidoglycan are negatively charged and attract electropositive cations. The adhesion potential between a gram-positive bacterium and a gram-negative bacterium differs in that there are different concentrations of surface functional groups which change the surface charge on the bacteria (Beveridge and Fyfe, 1985; Truesdail et al, 1998). Due to the thicker layer of peptidoglycan on the gram-positive cell, there is a higher concentration of functional groups that carry a negative charge (Truesdail et al 1998). This increases the overall negative charge on the gram-positive cell wall, which enhances the potential for adhesion to a positively charged surface.

A study by Ong et al (1999) has shown that gram-negative bacteria have a higher concentration of lipopolysaccharides (LPS), which is a structural component of the outer membrane. LPS are composed of complex lipids anchored to the cell membrane and are used in the barrier function of the outer membrane (Strain et al., 1983). LPS contain functional groups, mainly phosphoryl groups, which contribute to the overall surface charge of the cell. LPS may help gram-negative bacteria better adhere to negatively charged surfaces than gram-positive cells (Ferris and Beveridge, 1984). It is postulated that metals may also form bridges between LPS molecules thereby stabilizing the outer membrane (Ferris and Beveridge, 1984; Langley and Beveridge, 1999).

In the case of *E. coli* K12, the LPS are located asymmetrically on the outer half of the membrane and have a complete core, but lack the O-antigenic side chains known to *E. coli* O157:H7, the virulent strain (Beveridge and Koval, 1984). The principle sites for

cation binding are located in the polar head groups of the phospholipids, the available sites on the LPS and the acidic groups of the exposed polypeptides (Beveridge and Koval, 1983). Gram-negative cell envelopes have been found to bind less metal than Gram-positive cell walls by approximately 10% (Beveridge and Koval, 1983).

With respect to anion binding to bacterial cell walls, there is generally less information in the literature, especially for *E. coli*. Since bacterial cell walls are electronegative, anion binding is unlikely to occur because of electrostatic repulsion. In the case of gram-positive cells, such as *B. subtilis*, Urrutia and Beveridge (1993) demonstrated that silicate anions were likely bound to amino groups within the cell wall. Urrutia and Beveridge (1994) also showed that the binding of silicate anions could also occur through cation bridging.

2.2 Growth Phase and Metabolic State

The growth phase of bacteria has been studied quite extensively as a potential factor of adhesion between bacteria and metals, and between bacteria and common soil minerals. However, the results are not in good agreement. The relationships between cell metabolic state and adhesion are also variable and poorly constrained (Kjelleberg and Hermansson, 1984; DeFlaun et al., 1990; Fletcher 1977; van Schie and Fletcher, 1999).

Bacteria reach three phases of growth. The first stage is the exponential or log growth phase, followed by the stationary phase and then a decline or death phase. Figure 1.2 depicts a typical bacterial growth curve. The growth phase where maximum binding to glass beads occurs is controversial. It has been suggested (Kjelleberg and Hermansson 1984) that cells adsorb to glass beads best when they are inactive, i.e., during the

stationary phase or when they are dead, but most studies have established the opposite, i.e., that cells adhere best to surfaces during the log or exponential growth phase (DeFlaun et al., 1990; Fletcher 1977; van Schie and Fletcher, 1999).

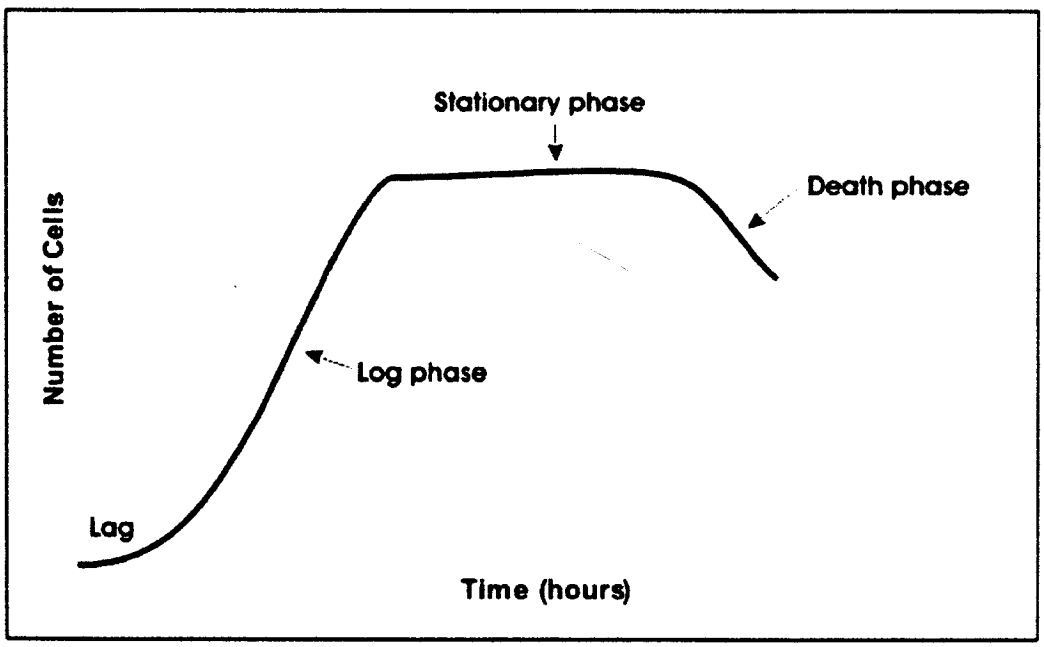

Figure 1.2. Typical growth curve of bacterial cultures.

DeFlaun et al. (1990) studied the adhesion of *Pseudomonas fluorescens* and *E. coli* to fine sandy loam. The study determined that the logarithmically growing cells adhered in greater numbers to the sediments than those in the stationary phase. This is reasonable because bacteria, such as *Bacillus subtilis* cells, in exponential phase display approximately four times more carboxyl sites, twice as many phosphoryl sites and 1.5 times more amine sites than those in stationary phase (Daughney et al, 2001). DeFlaun et al (1990) also found that the cells adsorbed better when they were thoroughly washed. The same conclusions were drawn by Fletcher (1977), who found that with a marine pseudomonad, log phase cultures had the greatest adsorption to polystyrene followed by the stationary and death-phase cultures. The authors postulated that changes in cell

motility and changes in the cell surface polymer composition during the various growth phases could explain the adhesion differences. Motility is the movement of a cell through the use of appendages such as a flagellae, fimbriae or pili (Chapelle, 2001). Motility increases the chance that the bacteria might encounter a potential surface for adhesion, while non-motile bacteria would only encounter a surface through the natural movement of currents or Brownian motion (Fletcher, 1977). Motility is highest during the exponential growth phase, and then declines with the onset of the stationary phase. Cell motility continues to decline through the stationary phase and the death phase (Fletcher, 1977). Figure 1.3 illustrates the relationship between cell concentration and the number of attached cells onto polystyrene. These results indicate that the greatest number of attached bacteria occurs when the cells are in their log growth phase.

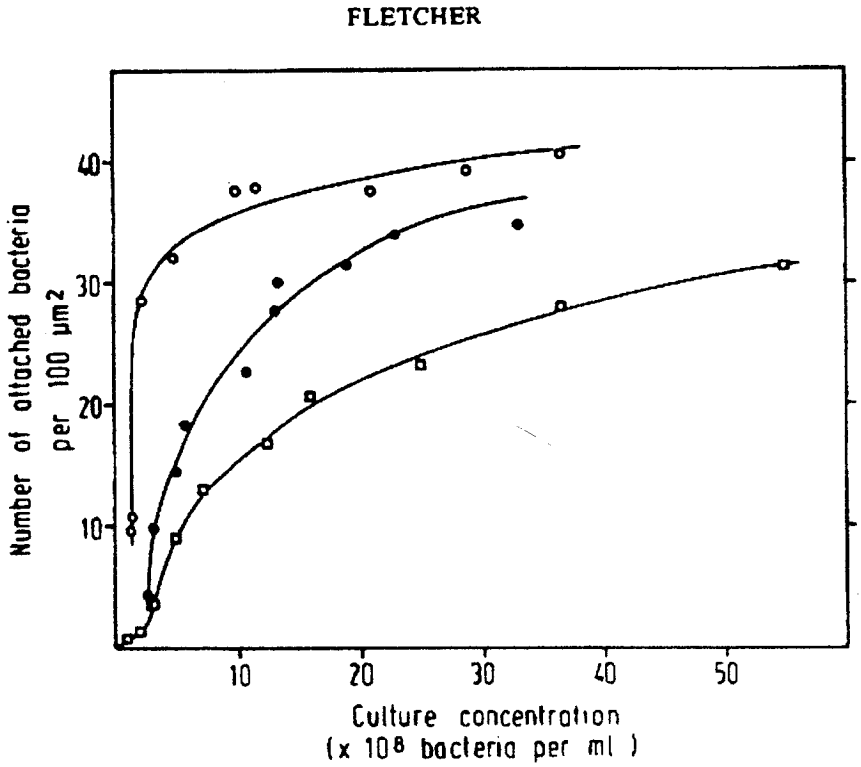

Figure 1.3. The relationship between cell concentration and the number of cells attached to polystyrene after 2 hrs. Empty circles =log phase, filled =stationary phase, empty squares=death phase (Modified from Fletcher, 1977).

In a 1999 study by Van Schie and Fletcher, it was found that *Desulfovibrio sp.* Strain G11 only adhered to glass cover slips and amorphous iron coated glass cover slips in small numbers during the exponential growth phase, whereas they did not adhere at all during the stationary phase. Using microscopic observations, the same authors determined that the log phase cells were highly motile while the cells in the stationary phase showed no motility. Although the relationships between biological variables and cell adhesion remain complex and sometimes unclear, it is likely that growth phase and/or metabolic state will affect the transport of *E. coli* through soils.

2.3 Nutrient Availability

Given the fact that growth phase appears to affect cell adhesion to surfaces, it can be assumed that the availability of nutrients would also impact this process since they are necessary for cell survival and likely dictate growth phase of a microbial population. A number of studies (Humphrey et al, 1983; DeFlaun et al, 1990; Fletcher 1977; Kjelleberg and Hermansson, 1984) have looked at the effect of cell starvation on the adhesion of bacteria to different substrata.

Experimental studies have found that some bacteria undergo changes in surface characteristics in response to starvation (Humphrey et al 1983). Some cells were reduced in volume by up to 70% (Humphrey et al, 1983). Rod shaped bacteria, such as *E. coli* were found to become smaller as a result of starvation while coccoidal strains did not (Humphrey et al, 1983). It was also found that the hydrophilic (having an affinity for water) strains of bacteria tended to decrease in size while the hydrophobic (water repelling) strains actually increased in size when deprived of nutrients. The study by Humphrey et al. (1983) concluded that cells deprived of nutrients initially experienced an increase in adhesion.

Kjelleberg and Hermansson (1984) used seven different marine bacterial strains to determine their ability to adhere to glass during starvation. This study also reported changes in cell surface characteristics, most apparently in cell size and cell wall hydrophobicity. Cell size was found to decrease within a very short time, and continued to decrease over a 22-hour period. Fragmentation of the bacteria occurred whereby the cells divided without growth, which increased the number of bacteria but decreased their overall size. Almost all of the bacterial strains showed an increase in hydrophobicity (the

property of being water repellent) in response to starvation, which in some cases resulted in an increase of adhesion and in other cases, in a decrease in adhesion (Kjelleberg and Hermansson, 1984). The same study also reported that while four strains of bacteria increased their adhesion in response to starvation after twenty-two hours, the other three strains had an initial increase in adhesion after the first five hours, followed by a decline after twenty-two hours. In a different study, DeFlaun et al. (1990) determined that a minimal salt medium was a better growth medium for attachment than a nutrient-rich broth, suggesting that limiting nutrient availability had a positive effect on adsorption.

Daughney et al. (2000) determined that cells growing in the presence of abundant nutrients at exponential growth phase had a higher concentration of proton active surface functional groups than those in either stationary or sporulated phase and therefore had a more negative electrostatic charge under circum-neutral pH conditions. The increased negative charge may increase adhesion to positively charged mineral surfaces, such as iron oxy-hydroxides.

3.0 Physico-chemical Factors affecting Bacteria-Mineral Adhesion

The important physico-chemical factors affecting cell adhesion are pH, ionic strength, hydrophobicity and soil mineralogy. Other factors include temperature, pore water content, cell shape and mineral grain size. However, their impact on cell adhesion has been studied less and therefore will not be addressed in this review.

3.1 Soil mineralogy

The mineralogical variables include the type of minerals present in the soil, their morphology, surface area and reactivity. Quartz (SiO_2) is the most common mineral in the earth's crust. It is also an important component of soils, along with Fe-oxides, feldspars and micas. Fe-oxides (such as amorphous $Fe(OH)_3$, goethite (α-FeOOH), lepidocrocite (γ-FeOOH) and hematite (Fe_2O_3)) tend to occur as discrete particles in soils or as coating on mineral surfaces, such as quartz. Quartz possesses a low surface area of approximately 0.2 m^2g^{-1} and has a net negative charge under most soil conditions (Yee et al, 2001). Iron oxides have a larger surface area ranging from 15-260m^2g^{-1} with the surface area increasing as the pH of a system falls from 7 to 5, and usually have a net positive charge under pH neutral conditions (Cornell and Schwertmann, 1996). Clay particles vary in size and composition and show a wide range of surface area (Walker et al, 1989). The adhesion of bacterial cells to mineral surfaces strongly depends on the electrostatic forces between the two surfaces. The relationship between surface charge and pH is described in the following section.

3.2 pH

Bacterial adhesion to mineral surfaces is governed in large part by the electrostatic forces between the cell and the mineral. These electrostatic forces are influenced by the surface charge on the bacteria and the mineral, which is in turn governed by the composition of the solution, ionic strength and pH (Van Loosedrecht et al, 1989). Both bacterial cells and mineral surfaces display different types and concentrations of proton-active surface functional groups that give them a pH and ionic strength dependant electrostatic charge (Daughney et al., 1998; Yee et al, 2000). The pH

influence on the charge differs between different strains of bacteria and between different minerals, making it very difficult to correlate research and make any general conclusions.

Bacteria possess various exposed functional groups on their cell wall (Beveridge and Fyfe, 1985). These functional groups possess an acid-base behavior, i.e, they can gain or loose protons depending on the pH conditions (Fein et al., 1997). In a low pH solution, the sites become protonated due to the high concentration of protons making the surface more positive. At high pH, where there are relatively few hydrogen ions, the sites become de-protonated rendering the surface more negative. The pH at which the charge is neutral is called the pH of zero point of charge, where the number of negative sites is balanced by an equal amount of positive sites (Morel and Hering, 1993).

Figure 1.4 illustrates the relationship between *B. subtilis*, a Gram-positive rod shaped bacterium, and changes in pH. The bacterial surface charge becomes more negative as the pH increases following the de-protonation of the various functional groups (Fein et al., 1997). Daughney and Fein (1998) showed that carboxyl and hydroxyl groups contribute more to the surface charge, as they are more ionisable (Daughney and Fein, 1998).

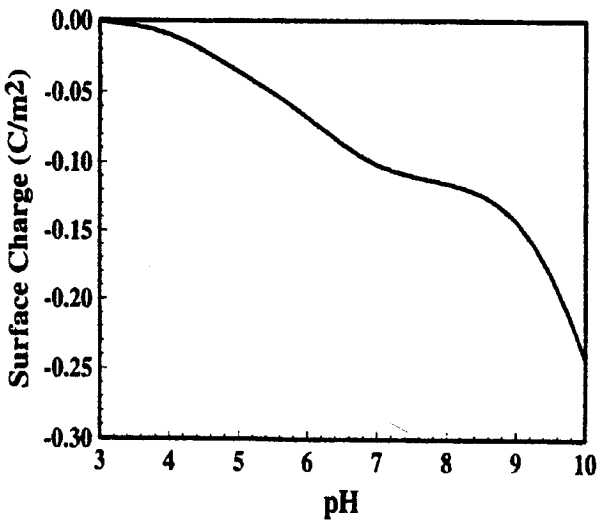

Figure 1.4. Surface charge of *Bacillus subtilis* as a function of pH (modified from Daughney et al., 2001)

Minerals also display a surface charge given by the dissociation of chemisorbed water molecules on their surface and mineralogical defects (Morel and Hering, 1993). Quartz has a negative surface charge throughout the pH range of natural waters (4<pH<9) (Yee et al, 2000). The authors studied the adhesion of *B. subtilis* onto quartz (SiO_2) and corundum (Al_2O_3). They showed that the adsorption of *B. subtilis* onto quartz was relatively weak and did not significantly change in response to changes in pH (Figure 1.5). They reasoned that quartz has a low negative surface charge, causing repulsion. On the other hand, the adhesion of *B. subtilis* onto corundum was much more significant since the bacterial surface is negatively charged above pH 2.2 and the surface of corundum is positively charged. Consequently, the attraction between the two was the strongest in the pH range of the experiment.

In a different study, using *B. subtilis, P. fluorescens* and silica (to mimic sandy soil or groundwater environments), Kinoshita et al. (1993) found that changing the pH

from 5.5 to 7.0 had little effect on *B. subtilis* adhesion, and that the attachment of *P. fluorescens* onto silica was greater at pH of 7.0 than at pH 5.5. At higher pH conditions (7.0 to 8.0), *Psudomonas fluorescens* slowly became desorbed due to the electrostatic repulsion between the two surfaces.

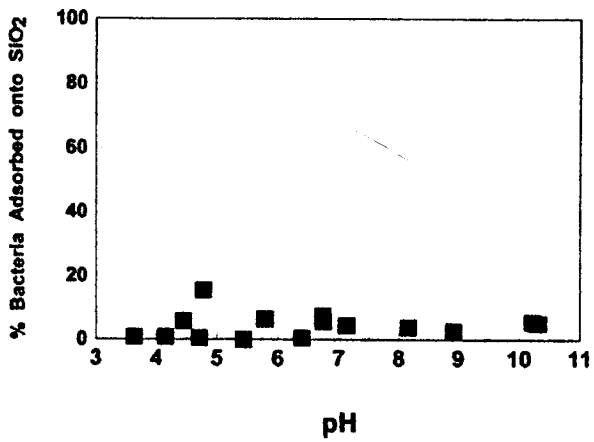

Figure 1.5. pH dependence of *Bacillus subtilis* sorption onto quartz (modified from Yee et al. 1999)

E. coli cells are negatively charged above a pH 3 due to de-protonated carboxyl and phosphoryl functional groups suggesting that adhesion onto positively charged mineral surfaces should be favored (Walker et al, 1998). No studies have quantified *E. coli* adhesion to mineral surfaces, but a recent study has modeled metal sorption onto *E. coli* cells. Figure 1.6 shows the adsorption behavior of Cd^{2+} onto pure cultures of various gram-positive and gram-negative bacterial species, including *E. coli* (Yee and Fein, 2001). As expected, the adsorption of positively charged Cd^{2+} onto negatively charged bacteria increases with pH (Yee and Fein, 2001).

The interaction between bacteria and mineral surfaces can be evaluated by adhesion isotherms, which describe the relationship between the amount of substance adsorbed per unit of mass, where the system is at a constant temperature (Morel and

Herring, 1993). The Volmer and Langmuir theories assume that adhesion is reversible and that there is no lateral interaction between adhered cells (Daughney and Fortin, 2001; Morel and Hering, 1993). Reversibility can be tested by first obtaining conditions where adhesion is favorable and determining the number of attached cells, followed by changing the conditions (pH and ionic strength) to those unfavorable for adhesion and re-assessing the number of attached cells. Van Loosdrecht et al (1989) showed that the adhesion of *E. coli* to quartz is fully reversible. Yee et al (2000) determined that that adhesion of *Bacillus subtilis* to corundum is also reversible. The same could not be determined for quartz because no relationship to pH or ionic strength could be determined for adhesion of *B. subtilis* to quartz. The effect of pH on adhesion is highly variable and differs between minerals as well as between different strains of bacteria.

While pH is a significant factor governing adsorption and de-sorption of bacteria in soils, it is impossible to use only pH to describe adsorption in a natural environment containing numerous strains of bacteria and a variety of minerals including oxides, quartz and metals which all behave differently. The following section describes the effect of ionic strength onto surface charge and adhesion.

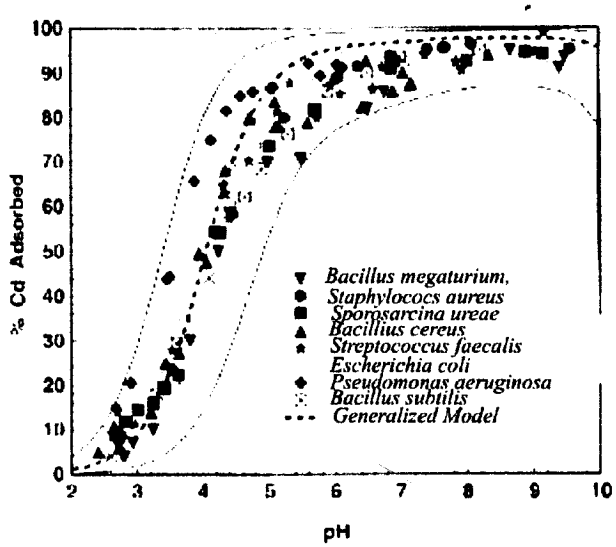

Figure 1.6. Cd adsorption onto various bacterial species as a function of pH (modified fromYee and Fein, 2001).

3.3 Ionic Strength

Cell surfaces are usually negatively charged in the pH range of natural groundwater, as are most minerals in nature, leading to a repulsive response between cell and mineral surfaces. This repulsive nature depends on the distance of attractive forces, which is influenced by the ionic strength of the aqueous phase (Daughney and Fein, 2001; Loosdrecht et al 1989; Yee et al, 1999). There are significant differences in the effect of ionic strength on bacteria and mineral surface charge.

Several models exist to describe the relationship between ionic strength and adsorption, but most studies appear to favour the double-layer model, also referred to as the diffuse double-layer model (DDLM) for the adsorption between two oppositely charged surfaces (Yee et al, 1999; Kinoshita et al, 1991). The double layer model represents the interfacial region between two charged surfaces, with an inner layer of charge determining ions and an outer layer of ions of opposing charge, as illustrated in

Figure 1.7 a. If the two surfaces in question have opposing charges, with few ions in solution, the overall net charge on the charged surface is still quite strong and the attractive forces extend further away from this surface. The higher the electrolyte concentration, the more ions will be attracted to the charged sites and the overall net charge will be reduced, thus reducing how far the electrostatic attraction will extend into the solution (Figure 1.7 b and c). In simple terms, the higher the ionic strength, the thinner the double layer becomes, decreasing the electrostatic interactions and thereby decreasing the potential for adsorption.

This concept was exemplified in a study by Yee et al (1999), on the adhesion between *B. subtilis* and corundum. At pH 6, *B. subtilis* cells were negatively charged and the corundum was positively charged. The authors showed that at low ionic strength, the double layers associated with both surfaces were thick and the attractive fields extended out further into solution, therefore increasing the potential for adsorption. With increasing ionic strength, the higher concentration of electrolytic ions reduced the overall net charge of the surface and decreased the thickness of the electric double layer between the bacteria and mineral surfaces, thereby reducing adsorption.

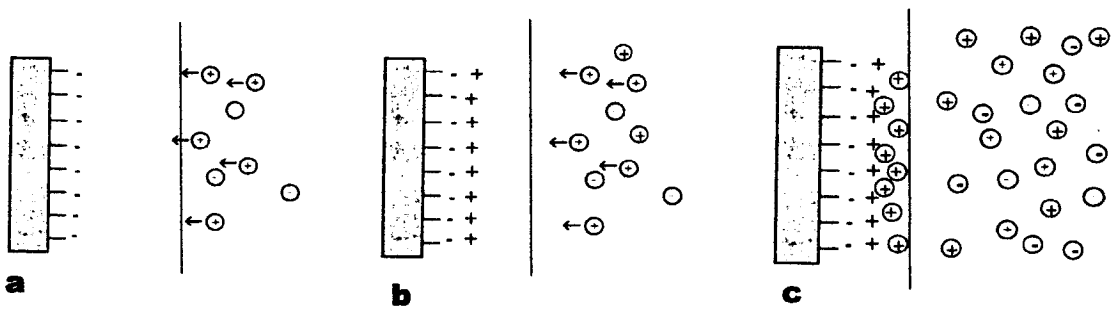

Figure 1.7. The effect of increasing ionic strength (a-c) on the electrostatic interactions between oppositely charged surfaces.

Fein et al (1997) and Yee et al (1999) determined that there was a pronounced negative correlation between ionic strength and cell adhesion to aluminum oxide, which has a positive charge comparable to that of iron hydroxides. They established that an increased ionic strength reduced adhesion in otherwise favorable conditions. Scholl and Harvey (1992) and Lukasik et al (1999) have shown that cells preferentially adhered to iron or aluminum oxides rather than quartz. They indicated that the chemical composition of the soil water (pH, ionic strength) and the mineralogy of the soil (quartz vs. iron oxides) may dramatically affect the transport of *E. coli* through soils. This, however was not quantitatively investigated. Such experiments are presented in chapter 3 of this thesis.

The influence of ionic strength on adhesion between two negative surfaces, which is most often the case in natural systems, is rather difficult to quantify. A simple model that addresses this situation is the DLVO (Deraguin-Landau-Verwey-Overbeek) theory, which accounts for the long- range electrostatic forces, the short-range van der Waals and hydrophobic forces, and describes the potential energy of interaction between the bacteria and mineral surfaces as a function of their separation distance (Yee and Fein, 2001). This theory accounts for the change in potential energy with changing ionic strength by addressing the thickness of the electric double layers as discussed for the diffuse double layer model.

According to DLVO theory, bacterial adsorption will occur at higher ionic strength at the point where Van Der Waals attractive forces overcome the repulsion due to overlapping electric double layers of the bacterium and mineral surfaces (Hermansson, 1999). Bacteria with a negative charge will begin to be attracted to the negatively charged

surface as the van der Waals forces overcome the repulsion from the bacteria and mineral surfaces (Scholl and Harvey, 1992; Shafer et al, 1998; Loosdrecht et al 1989). In this case, an increase in ionic strength would potentially increase the potential for adhesion. This was confirmed in the study of Loosdrecht et al (1989) using 5 bacterial strains of varying hydrophobicities, and polystyrene as an adhesion surface. Polystyrene had a negative charge in the pH range of the study, as did the bacterial strains. It was found that an increase in adhesion occurred when the electrolyte strength was increased. The thickness of the diffuse layer surrounding a charged particle varies according to ionic strength; with increasing ionic strength, the thickness decreases (Hermansson, 1999).

Fontes et al (1991) determined that an increase in ionic strength enhanced the ability of bacteria to adhere to quartz sand. However, the authors stated that increasing the ionic strength increased the availability of ions in solution to form bridges between the charged sites on both the quartz and the bacterial cell surface, allowing the bacteria to get closer to the mineral surface. They also speculated that ionic strength might enhance aggregation of bacteria cells. Other studies, including the one by Jewett et al. (1995), found that high ionic strength decreased bacterial adhesion.

3.4 Hydrophobicity

Hydrophobicity is the property of being water-repellent causing the surface in question to repel and not absorb water. Bacterial adhesion to mineral surfaces is controlled by hydrophobic forces between the cell and the mineral and by molecular scale interactions that depend on the surface structures of the cell (van Loosdrecht et al., 1978).

Bacterial surfaces contain hydrophobic substances, such as lipids, that can render the surface hydrophobic, meaning that they repel water.

Bacterial hydrophobicity is defined by Gannon et al (1991) as the net surface charge of the cells. Other studies have described hydrophobicity in terms of a surface free energy, which is calculated from the contact angle of a drop of liquid on a given surface as illustrated in Figure 1.8 (van Loosdrecht et al, 1987). In this study, the surface was the bacterial cell wall. The contact angle θ (Figure 1.9) is a function of the surface free energies of the three surfaces, the suspending liquids, and bacteria, and provides a relative measurement of hydrophobicity. Hydrophobicity relates to the surface free energy, which tends to decrease with increasing hydrophobicity (Loosdrecht et al, 1987). Hydrophobicity can be determined by partitioning bacteria between two aqueous phases; a polyethelyne glycol (PEG) phase and a dextran (DEX) phase. Most cells will move to one phase depending on their surface free energy (Loosdrecht et al 1989).

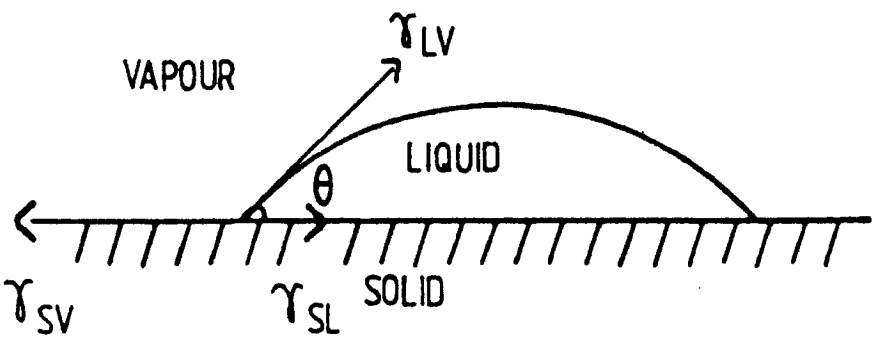

Figure 1.8. Relationship between the contact angle and different interfacial tensions, where gSL, gSV, gLV = surface tension of the Solid-Liquid interface, the solid vapour interface, and the liquid-vapour interface respectively. (van Loosdrecht et al, 1987).

Some studies have found that the extent of adhesion increases with increasing hydrophobicity of the bacteria (Absolom, 1983; Stenstrom 1989). A study by Fletcher

and Loeb (1979) showed that the number of attached bacteria increased with respect to the contact angle (Figure 1.9). Other studies cited in Fletcher and Loeb (1979) have found that bacteria preferred hydrophilic surfaces. In addition, hydrophobicity was found be higher in cells that were fimbriated or that had appendages (Stenstrom and Kjelleberg 1985). Hydrophobicity can also vary with changes in pH and ionic strength (Jewitt, 1995).

Hydrophobicity is difficult to quantify because there is a lot of variation in surface characteristics within different bacterial strains and also within a single strain (Stenstrom, 1989). The hydrophobicity and morphology of the cells are controlled by several biological variables, such as the growth conditions and metabolic state.

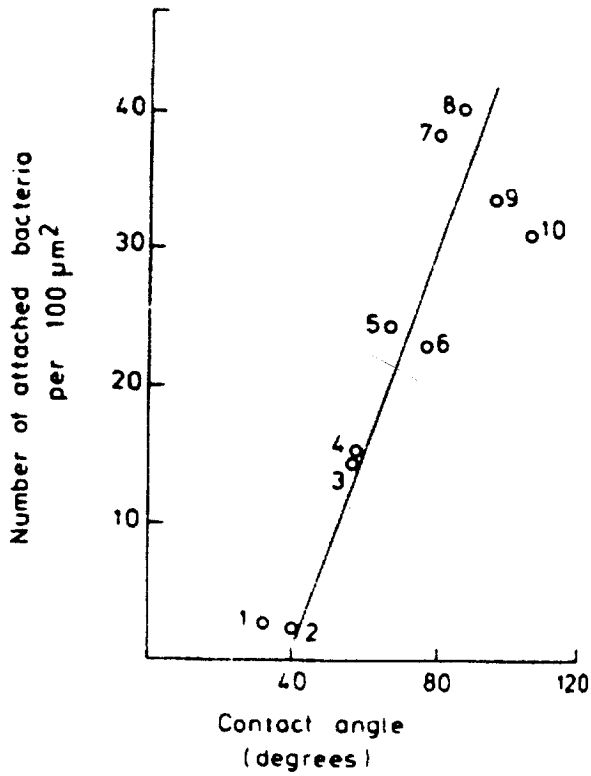

Figure 1.9. Relationship between the number of adsorbed bacteria and the contact angle for various substrata (modified from Fletcher and Loeb, 1979).

It is possible that cell size and shape, as well as length, density and composition of fimbriae, lipopolysaccharide (LPS) side chains, extracellular polysaccharides (EPS) and other appendages, may affect the hydrophobic properties of the cells (Humphrey et al, 1982; Kjelleberg et al, 1982; Ferris and Beveridge, 1999; Gannon et al 1991). The presence of appendages, such as fimbrils, flagellum, and exopolymers, increases the surface area of a bacterium. Strenstrom and Kjelleberg (1985) indicated that the presence of fimbrils in *Salmonella typhimurium* resulted in a higher surface hydrophobicity and negative charge than non-fimbriated strains, therefore increasing the potential for adhesion to a series of minerals. The relationship between the presence of fimbriae and

increased binding of the cell surface was indicated by the linear relationship between the high hydrophobicity of the fimbriated cells and the degree of adhesion. For all of the minerals used in the experiments (quartz, albite, feldspar, and magnetite) with the exception of biotite, the adhesion was found to be considerably more in the fimbriated cells. Strenstrom and Kjelleberg (1985) suggested that the increased number of binding sites along the fimbriae resulted in a higher degree of adhesion because of the increased bond energy represented at each binding site. The higher negative and positive surface charges associated with the fimbriated cells also corresponded to higher degrees of adhesion. The fimbriae were negatively charged but also possessed exposed positive groups that contributed to overcoming the repulsive forces of two negatively charged surfaces (Strenstrom and Kjelleberg 1985). An earlier study by Kjelleberg and Hermansson (1984) determined that bacteria that were irreversibly adsorbed were those that had fimbrils.

4.0 Conclusions

Bacterial transport in soil is an important area of study as it can directly affect groundwater quality. People rely on groundwater as a source of drinking water, therefore it is important to be able to predict the transport of pathogenic bacteria (such as *E. coli* O157:H7) in aquifers and soils. Several parameters have been found to influence the rate of transport of bacteria through soils, including adsorption or adhesion of bacterial cells onto mineral surfaces.

Adhesion between bacteria and minerals has not been studied as extensively as that of bacteria and metals. However, several of the factors affecting metal sorption onto

bacteria are also involved in cell adhesion onto mineral surfaces. Such factors include hydrophobicity of the cell wall, pH, ionic strength, nutrient availability and growth phase.

It is clear that several biological, chemical and mineralogical variables can affect bacterial adhesion to soil particulate matter. However, there are no studies to date that relate the concentration and availability of nutrients on the chemical, mineralogical and biological factors that govern bacterial adhesion to mineral surfaces.

The present study hypothesizes that the growth phase and metabolic state will affect the surface reactivity of *E. coli* cells (Chapter 2). Chapter 2 investigates the acid-base behaviour of *E. coli* K-12 (grown in a chemically defined medium containing nitrate and phosphate) as a function of growth phase and at the surface characteristics of lepidocrocite and quartz. In chapter 3, it is further speculated that the changes in surface reactivity will affect the adhesion between the cells and pure phase quartz and lepidocrocite. The results of the study will be used in future surface complexation models that will be used to better predict *E. coli* transport in aquifers and soils impacted by agricultural activities.

5.0 References

Absolom, Darryl.R; Lamberti, F.V.; Policove, Z.; Singg, W.; vanOss, C.J and A.W. Newman. 1983. Surface thermodynamics of bacterial adhesion. *Appl. Environ. Microb.* 46(1), 90-97.

Chapelle, Francis H. *Ground-Water Microbiology and Geochemistry.* Pages 32-37. John Wiley & Sons, Inc. New York : 2001.

Cornell, R.M and Schwertmann, U. 1996. *The Iron Oxides: Structure, Properties, Reactions, Occurrence and Uses.* Pages 221-225. VCH Publishers, New York: 1996.

Cunliffe, C.A., C. Alexander and E.N. Vulfson. Bacterial Adhesion at Synthetic Surfaces. *Appl. Environ. Microb.* 65(11), 4995-5002.

Daughney, C. and D. Fortin. 2001. Mineral adsorption by bacteria. *Encyclopedia of Surface and Colloid Science*, Marcel Dekker, Inc.

Daughney.CJ. and J.B. Fein. 1998. The effect of ionic strength on the adsorption of H+, Cd^{2+}, Pb^{2+}, and Cu^{2+} ions by *Bacillus subtilis* and *Bacillus Licheniformis:* a surface complexation model. *Journal of Colloid and Interface science.* 198, 53-77.

Daughney, C.J., Fein, J.B. and N. Yee. 1998. A comparison of the thermodynamics of metal adsorption onto two common bacteria. *Chemical Geology.* 144, 161-176.

Dawson, P., Humphrey, B.A. and K.C. Marshall. 1981. Adhesion: A Tactic in Survival Strategy of a Marine Vibrio During Starvation. *Current Microbiology*. 6, 195-199.

DeFlaun,M.F., Tamzer, A.S., McAteer, A.L., Marshall, B. and S.B. Levy.1990. Development of an adhesion assay and characterization of an adhesion-deficient mutant of *pseudomonas fluorescens*. *Appl. Environ. Microb.* 56, 112-119.

Dong, H. ,Rothmel, R., Onstott, T., Fuller, M.E., DeFlaun, M., Streger, S., Dunlap, R., and M. Fletcher. 2002. Simultaneous transport of Two Bacterial strains in intact cores from Oyster, Virginia: Biological effects and numerical modeling. *Appl. Environ. Microb.* 68(5), 2120-2132.

Drever, James I. The Geochemistry of Natural Waters: Surface and Groundwater Environments. Pages 343-357. Prentice Hall. New York:1997.

Fein J.B., Daughney, C.J., Yee, N. and T.A. Davis. 1997. A chemical equilibrium model for metal adsorption onto bacterial surfaces. *Geochim. Cosmochim. Acta,* 61(16), 3319-3328.

Fletcher, M. 1977. The effects of culture concentration and age, time, and temperature on bacterial attachment to polystyrene. *Can. J. Microb.* 23(1), pp. 1-6.

Fletcher, Madilyn and G.I. Loeb. 1979. Influence of substratum characteristics on the attachment of a marine pseudomonad to solid surfaces. *Appl. Environ. Microb.* 37(1): 67-82.

Fontes, D.E.; Mills, A.L.; Hornberger, G.M. and J.S. Herman. 1991. Physical and chemical factors influencing transport of microorganisms through porous media. *Appl. Environ. Microb.* 57(9), 2473-2481.

Gannon, J.T., Manilal, V.B. and M. Alexander. 1991. Relationship between Cell Surface Properties and Transport of Bacteria through Soil. *Environ. Sci. Technol.* 57, 190-193.

Goss, M.J., Barry, D.A.J., and D.L. Rudolph. 1998. Contamination in Ontario farmstead domestic wells and it's association with agriculture: 1. Results from drinking water wells. *J. Contam. Hydrol.* 32, 267-293.

Harvey, R.W., and S.P. Garabedian. 1991. Use of Colloid Filtration Theory in modeling movement of bacteria through a contaminated sandy aquifer. *Environ. Sci. Technol.* 25, 178-185.

Hermansson, M. 1999. The DLVO theory in microbial adhesion. *Colloids and surfaces B: Biointerfaces.* 14, 105-119.

Humphrey B., Kjelleberg, S. and K.C. Marshall. 1983. Responses of marine bacteria under starvation conditions at a solid-water interface. *Appl. Environ. Microb.* 45(1), 43-47.

Jewitt, D.G.; Hilbert, T.A.; Logan, B.E.; Arnold, R.G. and R.C. Bales. 1995. Bacterial transport in labratory columns and filters : influence of ionic strength and pH on collision efficiency. *Wat. Res.* 29(7), 1673-1680.

Kinoshita, Takashi.; Bales, R.C.; Yahya, M.T.; and C.P. Gerba. 1993. Bacteria transport in a porous medium : retention of bacillus and pseudomonas on silica surfaces. *Wat. Res.* 27(8), 1295-1301.

Kjelleberg, Staffan and Malte Hermansson. 1984. Starvation- induced effects on bacterial surface characteristics. *Appl. Environ. Microb.I* 48(3), 497-503.

Lukasik, J.; Cheng, Y.H.; u, F.; Tamplin, M.; and S.R. Farrah. 1999. Removal of microorganisms from water by columns containing sand coated with ferric and aluminium hydroxides. *Wat. Res.* 33(3), 769-777.

Rudolph, D.D., Barry, D.A.J. and M.J. Goss. 1998. Contamination in Ontario Farmstead domestic wells and its association with agriculture: 2. Results from multilevel monitoring well installations. *J. Contam. Hydrol.* 32, 295-311.

Schafer, A.; Ustohal; P.; Harms, H.; Stauffer, F.; Dracos, T. and A.J.B. Zendher. 1998. Transport of bacteria in unsaturated porous media. *J. Contam. Hydrol.* 33, 149-169.

Scholl, Martha. A. and Ronald W. Harvey. 1992. Laboratory investigations on the role of sediment surface and groundwater chemistry in the transport of bacteria through a contaminated sandy aquifer. *Environ. Sci. Technol.* 26, 1410-1417.

Strenstrom, T.A. 1989. Bacterial hydrophobicity, an overall parameter for the measurement of adhesion potential to soil particles. *Appl. Environ. Microb.* 55, 142-147.

Stenstrom, T.A. and S. Kjelleberg. 1985. Fimbriae mediated nonspecific adhesion of Salmonella typhymurium to mineral particles. *Arch. Microbiol.* 143, 6-10.

Truesdail, S.E., Lukasik J., Farrah, S.R., Shah, D.O., and R.B. Dickinson. 1998. Analysis of bacterial deposition on metal (hydr)oxide-coated sand filter media. *Journal of Colloid and Interface Science.* 203, 369-378.

VanLoosdrecht, M.C.M; Lyklema, J.; Norde, W.; Schraa, G.; and A.J.B. Zehnder. 1987. The role of bacterial cell wall hydrophobicity in adhesion. *Appl. Environ. Microb.* 53(8), 1893-1897.

VanLoosdrecht, M.C.M; Lyklema, J.; Norde. And A.J.B. Zehnder. 1989. Bacterial adhesion : a physicochemical approach. *Microb. Ecol.* 17, 1-15.

Van Schie. P.M. and M. Fletcher. 1999. Adhesion of biodegradative anaerobic bacteria to solid surfaces. *Appl. Environ. Microb.* 65(11), 5082-5088.

Walker, S.G., Flemming, C.A., Ferris, F.G., Beveridge, T.J and G.W. Bailey. 1989. Physicochemical Interaction of *Escherichia coli* Cell Envelopes and *Bacillus subtilis* cell walls with two clays and ability of the composite to immobilize heavy metals from solution. *Appl. Environ. Microb.* 55(11), 2976-2984.

Yea-Ling, Ong., Razatos, A., Georgiou, G., and Mukul M. Sharma. 1999. Adhesion forces between *E. coli* bacteria and biomaterial surfaces. *Langmuir.* 15, 2719-2725.

Yee, Nathan.; Fein, J.B. and C. Daughney. 1999. Experimental study of the pH, ionic strength, and reversability behaviour of bacteria- mineral adsorption. *Geochim. Cosmochim. Acta,* 64(4), 609-617.

Yee, N. and J. Fein. 2001. Cd adsorption onto bacterial surfaces: A universal adsorption edge? *Geochim. Cosmochim. Acta,* 65(13), 2037-2042.

Zvyagintsev, D.G. and V.S. Guzev. 1977. Relationship between adsorption of microorganisms and the stage of their development. *Microbiologiia,* 46(2), 295-299.

Chapter 2

Surface charge of *Escherichia coli* K-12 as a function of growth phase and metabolic activity compared to the surface charge of quartz and lepidocrocite

Abstract

The objectives of this study are to first study how *E. coli* K12 affects the chemical conditions of a chemically defined growth medium (M9) and second, to determine the surface charge of the cells as a function of growth phase and metabolic activity. The last objective is to study the surface charge of quartz and lepodocrocite, two common soil minerals. pH, Eh, DOC, DIC and the concentration of phosphate (PO_4^{3-}) and nitrate (NO_3^-) were monitored to track changes in the chemistry of the M9 medium resulting from the growth of *E. coli*. Results first showed that the growth of E. *coli* acidified the growth medium as a result of the complete and incomplete oxidation of glucose and the production of organic acids. DOC levels slightly decreased during the exponential growth phase of *E. coli*, while DIC levels increased possibly in response to the partial consumption of glucose and to the production of CO_2. The cells consumed phosphate and nitrate during early growth, but then released soluble phosphate and nitrate back into the medium near the end of their stationary growth phase (likely as organic P and N). Acid-base titrations of lepidocrocite suspended in $NaNO_3$ electrolyte showed that the iron oxide had a higher buffering capacity than quartz, which is consistent with values reported in the literature. Acid-base titrations of *E. coli* cells first showed that the buffering capacity increased with the quantity of cells in suspension. Second, metabolically active cells in their mid-exponential phase showed the highest buffering capacity, whereas metabolically active cells in their mid-stationary growth phase demonstrated the lowest buffering capacity. Non-active cells had intermediate buffering capacities. Changes in the structure and chemical composition of the cell wall during growth were likely responsible for the differences. In order to fully characterize the

surface reactivity of the cell and mineral surfaces, surface complexation models (SCM) are required to calculate the type and concentration of binding sites available on the cell and minerals.

1.0 Introduction

A serious concern with soil and groundwater contamination is the transport of pathogenic bacteria. *Escherichia coli* is a common bacterial species associated with manure produced by agricultural activities (Rudolph et al, 1998). Manure is susceptible to leaching by rain and surface water, making it a common groundwater contaminant in rural areas (Rudolph et al, 1998; Goss et al. 1998). Contamination of groundwater by pathogenic bacteria, such as *E. coli* O157:H7, poses a risk to human and environmental health, as shown by the Walkerton tragedy of May 2000.

Adhesion of bacteria to minerals is of fundamental importance because adhered cells will move at a rate that is slower than the advective velocity of the groundwater. The first step to investigating the adhesion of *E. coli* cells to minerals is to characterize the surface functional groups on the cell wall and mineral surfaces and determine their proton binding capacity.

Quartz is the most common mineral in earth's crust. It is the principal constituent of most soils and the main component of aquifers that are typically tapped for water in rural communities (Murck et al, 1996). Quartz along with other silicate minerals, generally display a net negative charge in the natural pH range of soils (Yee et al, 2001). Iron oxides represent another important component of soils, but they are less abundant than quartz. They occur as oxide, hydroxide or oxyhydroxide minerals in soils and aquifers and coat the surfaces of minerals like quartz (Murck et al, 1996). Iron oxides usually carry a positive to neutral electric charge under pH neutral conditions (Cornell and Schwertmann, 1996).

It has been established that in natural soils, bacterial cells carry a negative charge (Daughney and Fortin, 2001). If adhesion is controlled by both electrostatic and hydrophobic reactions, bacterial adhesion will be less in the presence of soil minerals that are negatively charged, but enhanced in the presence of minerals with a positive charge. Bacterial cell walls typically have an assortment of organic surface functional groups, including carboxyl, phosphate, amine and hydroxyl sites (Fein et al, 1997). To quantify the adhesion of bacteria to minerals, it is necessary to characterize these functional groups by determining the number and type of functional group present, the total surface area of bacteria available, and the absolute concentrations and deprotonation constants of the proton active surface functional groups on the cell wall (Daughney and Fein, 1997; Yee et al, 1999).

Previous studies (Yee et al, 1999; Yee et al, 2001; Daughney and Fein, 1997, Daughney et al, 2001, Fein et al, 1997) have shown that chemical equilibrium surface complexation models (SCMs) effectively quantify the acid–base titration data for both the bacteria and the minerals. Specifically, they allow the determination of the absolute concentration and deprotonation constants for the cell surface functional groups and the functional groups present on the mineral surfaces. In SCM, interactions between protons and the solid surfaces are described with a set of chemical reactions, each with a unique thermodynamic stability constant. The models are then extended to encompass the measurements of surface electric potential (Zeta potential) of each surface.

Acid-base titrations of active *E. coli* K-12 cells at mid-exponential and mid-stationary growth phases will be compared with titrations of non-metabolically active cells at the same growth phases to assess if growth phase and metabolic activity affect the

buffering capacity. Daughney et al (2001) found that *Bacillus subtilis* cells in exponential phase displayed approximately four times more carboxyl sites, twice as many phosphoryl sites and 1.5 times more amine sites than those in stationary phase. DeFlaun et al. (1990) determined that logarithmically growing *Pseudomonas fluorescens* and *E. coli* adhered in greater numbers to sandy loam than those in the stationary phase. Here, similar titrations of quartz and lepidocrocite will also be conducted to determine their relative buffering capacity.

The objectives of this manuscript are to examine the proton binding capability *E. coli* K12 cells and evaluate the surface reactivity of the cells in different growth phases and metabolic states, and two minerals; quartz and lepidocrocite. The data obtained from this study will provide the background information essential for the quantification of adhesion between *E. coli* and these two minerals (Chapter 3).

2.0 Materials and Methods

2.1 Growth protocol

E. coli K-12 cells kept on solid Tripticase Soy Agar (TSA) were obtained from T.J. Beveridge (University of Guelph, Ontario). *E. coli* K-12 is a laboratory strain, which lacks the O antigen portion of the lipopolysaccharide layer (LPS), an important component of the cell wall of Gram negative bacteria. (Stevenson et al., 1994). However, it represents a good analogue for more pathogenic strains, such as *E. coli* O157:H7. The cells were cultured in 100 ml of autoclave sterilized Trypticase Soy Broth (TSB) for 48 hours at 37°C, and then 5 ml of the pre-culture were transferred into 100 ml of M9, a

chemically defined medium (Table 2.1). *E. coli* slowly adapted to the new growth medium and reproducible growth curves were obtained. An attempt was made to grow the cells in M9 medium containing 10 times less phosphate and nitrate, but the growth curves were not reproducible, therefore all experiments were performed using M9 with its original composition. Growth curves were also obtained for cultures that were poisoned by streptomycin sulfate in order to stop the metabolic activity and the reproduction. The antibiotic (0.1g/L and 0.01g/L) was added at mid-exponential phase.

The optical density of the *E. coli* cultures was determined by reading the absorbance at 600 nm with a Beckman DU-65 spectrophotometer. In addition, the purity of the *E. coli* K-12 culture was verified after each experiment by plating it on TSA.

Table 2.1: Chemical composition of the growth medium (M9)

Components	Concentration (mol/L)
Na^+	1.707×10^{-3}
PO_4^{3-}	2.699×10^{-4}
K^+	2.205×10^{-4}
Cl^-	2.745×10^{-3}
NH_4^+	1.865×10^{-3}
Ca^{2+}	1.000×10^{-4}
NO_3^-	4.837×10^{-4}
Mg^{2+}	1.001×10^{-3}
SO_4^{2-}	1.001×10^{-3}
DOC (glucose)	0.242
pH	7.00

2.2 Growth Chemistry

The chemistry of the liquid growth medium during *E. coli* growth was monitored in order to assess how the cells modified their environment. Specifically, pH, Eh, nitrate and phosphate concentrations, and dissolved organic and inorganic carbon (DIC and DOC, respectively) were measured at various intervals during growth.

2.2.1 pH

pH was measured during the growth of *E. coli* using a VWR SP 21 scientific pH probe. The pH meter was calibrated prior to use with standardized VWR pH 4, pH 7 and pH 10 buffers at the start of each day and after every 5 hours of inactivity. The pH buffer standards were changed once a week to maintain precision. The pH was measured at the same time of the optical density over the course of approximately 60-100 hours. To ensure that the culture remained sterile during the measurements, a small sub sample of approximately 5 ml was withdrawn using a sterilized pipette tip.

2.2.2 Eh

The redox potential (Eh) was measured at the same intervals as pH using a calibrated Corning Redox Platinum Comb electrode. The probe was calibrated using standardized redox buffers at 234 mV and 300 mV.

2.2.3 Phosphate Concentration

A 5ml sample was withdrawn from the main culture using a 5ml precision pipette and a sterile pipette tip and placed into a clean beaker. The sub-sample was diluted with

ultrapure water (1:100 dilution), filtered (0.20 μm Acrodisc Syringe Filter) and analyzed with the PhosVer3 reagent using a HACH spectrophotometer (HACH DR/2010).

2.2.4 Nitrate Concentration

A 10ml sample was withdrawn from the main culture using and placed into a clean beaker. The sub-sample was filtered (0.20μm Acrodisc syringe filter) and analyzed with the NitraVer 5 nitrate reagent using a HACH spectrophotometer (HACH DR/2010).

2.2.5 Dissolved Organic Carbon (DOC) and Dissolved Inorganic Carbon (DIC)

Exactly 10 ml of suspension were removed from the culture and filtered (0.20μm Acrodisc filter). Samples were then stored at 4°C and later analyzed with the 1010 model Total Organic Carbon Analyzer/ Auto-sampler calibrated with monopotasium salt standards (5ppm, 10ppm, 25ppm, 50ppm). Prior to analysis, samples were diluted (1ml sample, 49ml distilled de-ionized water).

2.2.6 Dry weight calibration

Titration data must be normalized to the dry weight of bacteria (g/ml); therefore a calibration curve was necessary. To calibrate the optical density values to the representative dry weight of *E coli*, cultures were grown in 1L flasks to mid-exponential and mid-stationary phase and then washed four times in distilled de-ionized (DDI) water. Cells were pelleted by centrifugation at 6000rpm for ten minutes and washed in DDI water. After each wash, cells were re-centrifuged at 6000rpm for 10 minutes and the

supernatant was discarded. After the final wash, the cells were re-suspended in a given amount of DDI water to provide an optical density between 0.8 and 1.5 ensuring adequate weight. Three to five aliquots of 15 ml were added to aluminum weigh boats, ensuring that the actual weights were recorded to the highest possible level of precision. The sub samples were dried in an oven at 60°C for 48 hours and then re-weighed at room temperature. A dry weight calibration curve was created from the results, and was used to calibrate all of the titration data.

2.3 Mineral Preparation

The quartz and lepidocrocite used in the experiments were obtained from Alpha Aesar (Silicon (IV) oxide, 99.995% and Iron (III) hydroxide, gamma FeO(OH)). The mineralogy and purity of the mineral phases was assessed by XRD. Both mineral phases were confirmed to be pure and were identified as quartz and lepidocrocite (γ-FeOOH).

The minerals were washed using a 0.01M $NaNO_3$ solution. The electrolyte was removed by centrifugation at 500 rpm for 3 minutes. The washing procedure was repeated 5 times for both the quartz and the lepidocrocite. The quartz was dried at 60°C for 48, while the lepidocrocite was dried in an anaerobic chamber for 5 days. The surface area of the lepidocrocite and quartz was determined by BET isotherm analysis at the University of Ottawa on a Micromeritics ASAP 2010. The surface area of lepidocrocite and quartz was 165.2 m^2/g and 0.142 m^2/g, respectively (Appendix 2.1).

2.4 Acid –base titrations of *E. coli* suspensions

The titration of *E. coli* suspensions was performed directly in the M9 growth medium or in 0.01M $NaNO_3$ electrolyte. The titrations were performed on *E. coli* cells harvested at either mid-exponential or mid-stationary growth phase. For titrations of cells poisoned by streptomycin sulfate (non metabolically active and non-reproducing cells), the antibiotic was added approximately 1.5 hours prior to the titration. For titrations in the electrolyte, the cells were washed four times by centrifugation in 0.01M $NaNO_3$. After the final rinsing, the cells were suspended in approximately 200 ml of the electrolyte to obtain an optical density between 0.250 and 0.750. For titrations of *E. coli* in the growth medium, bacteria were harvested at either mid-exponential or mid-stationary growth phase and a known weight of suspension was measured directly into the titration beaker after measuring the optical density.

For all titrations, a known weight of suspension (approximately 40g) was placed in a sealed titration vessel and purged of CO_2 by N_2 bubbling for 30 minutes. Throughout the titrations, a positive pressure of N_2 was maintained. Titrations were conducted using an automated titrator (Radiometer-Copenhagen TTT85/ABU 80) to pH 8 with aliquots of standardized, CO_2 free NaOH (0.01N) after a stability of 0.1mV/sec was obtained. The suspension was brought back to pH 4 with a weighed amount of standardized HCl (0.1N) immediately after the initial titration, and then titrated back to pH 8 in order to assess reversibility.

2.5 Acid – base titrations of minerals

Quartz was suspended in 0.01M $NaNO_3$ electrolyte at a concentration of 10g/L and 100g/L and titrated as outlined in section 2.4. Lepidocrocite was titrated in concentrations of 5g/L and 10g/L.

2.6 Calculation of [H⁺] added

Titration curves for both the cells and the minerals were plotted on a graph showing the pH versus the concentration of H^+ added. Microsoft Excel spreadsheets were used to calculate the change in $[H^+]$ added per unit of pH using the equation 1,:

$$[H^+]\text{ added} = [\text{Acid Added}]\times\frac{V_{AA}}{(V_{SUSP}+V_{AA}+V_{BA})} - [\text{Base Added}]\times\frac{V_{BA}}{(V_{SUSP}+V_{AA}+V_{BA})}$$

$$=0.1\times\frac{V_{AA}}{(V_{SUSP}+V_{AA}+V_{BA})} - 0.01\times\frac{V_{BA}}{(V_{SUSP}+V_{AA}+V_{BA})} \quad (1)$$

where V_{AA} and V_{BA} are the volume of acid added and base added respectively and V_{SUSP} is the volume of the bacterial suspension being titrated. Concentrations are expressed in mol/L and volume in liters. In order to compare the various cell treatments, the concentration of $[H^+]$ added was normalized with respect to the dry weight of cells (g). A more detailed explanation on the titration spreadsheets and calculation of $[H^+]$ added is available in Appendix 2.2.

2.7 Uncertainty associated with the calculation of [H⁺] added

The error, or uncertainty associated with the precision of the instruments used (i.e., burette, balance, pH meter) on the calculation of $[H^+]$ added was calculated for each point for each titration curve according to equation 2 (Skoog et al, 1997):

$$\frac{U_Y}{Y} = \sqrt{\frac{U_a^2}{A^2} + \frac{U_b^2}{B^2} + \frac{U_c^2}{C^2} + \ldots}, \qquad (2)$$

where U_Y is equal to the uncertainty associated with the calculation of value Y ($[H^+]$ added) and where $U_{a, b, c...}$ is the error associated with value A, B, C etc obtained from instrument reading.

A spreadsheet was created in Microsoft Excel to calculate the uncertainty for each point on a given titration curve. Appendix 2.3 shows an example for the calculation of one set of data on a titration curve. The results indicated that the error caused by the precision of the instruments was minimal.

3.0 Results

3.1 *E. coli* growth

In the M9 medium, at 37°C, the active *E. coli* cells took approximately 20-24 hours to reach the exponential growth phase, and 48-60 hours to reach the stationary growth phase, as illustrated in Figure 2.1. The use of streptomycin at two different concentrations stopped the cells from growing and reproducing (Figure 2.2). The higher concentration of 0.1g/L was chosen as the standard concentration for the antibiotics for

all experiments to ensure maximum potency. It was determined from these experiments that the cells ceased to reproduce after approximately 2 hours after the addition of the antibiotic, therefore in experiments using metabolically inactive, non-reproducing cells, the cultures were harvested for titrations 2 hours after adding the streptomycin.

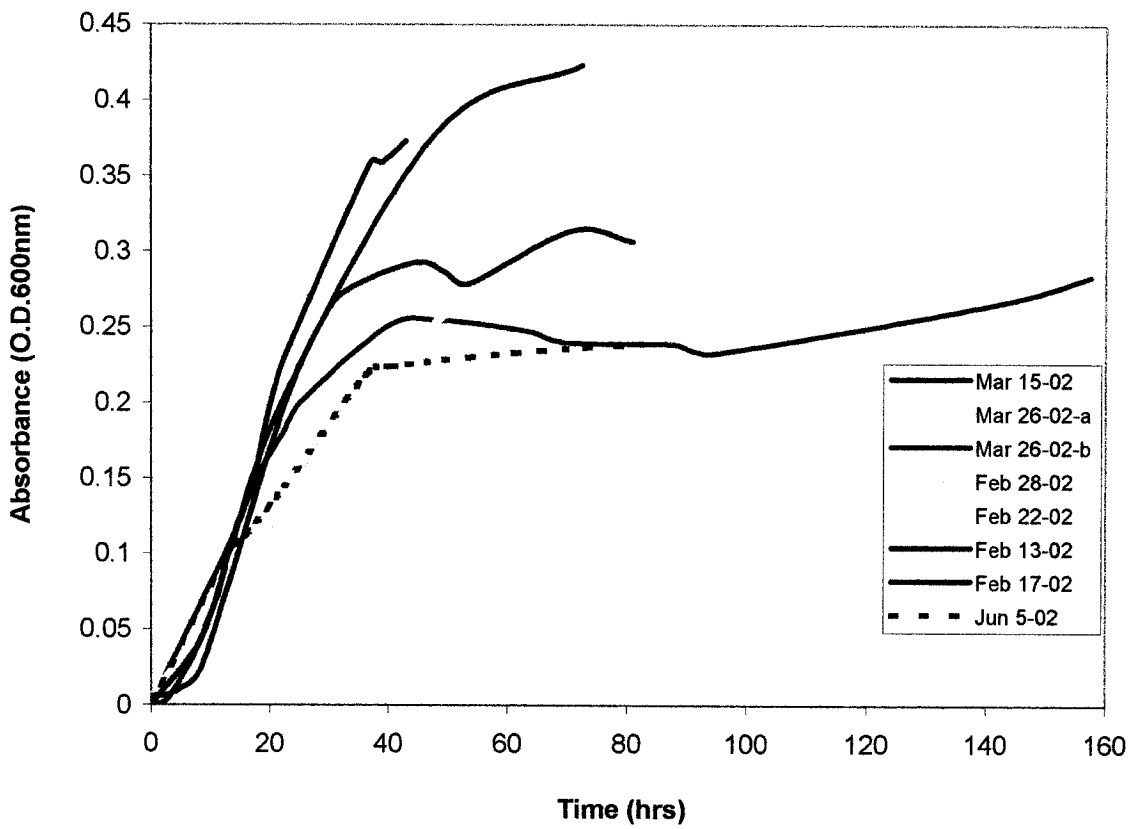

Figure 2.1. Growth curves of *E. coli* cells in M9 medium over a period of 40 to 140 hours. Results obtained from individual cultures from January 2002 to May 2002.

3.2 Growth Chemistry

3.2.1 pH

The growth medium became acidic as the cell population increased from the exponential to mid-stationary phase (Figure 2.3). The final pH of the spent medium after 48-60 hours decreased from a starting pH of approximately 7 to a pH between 3.5-4.0.

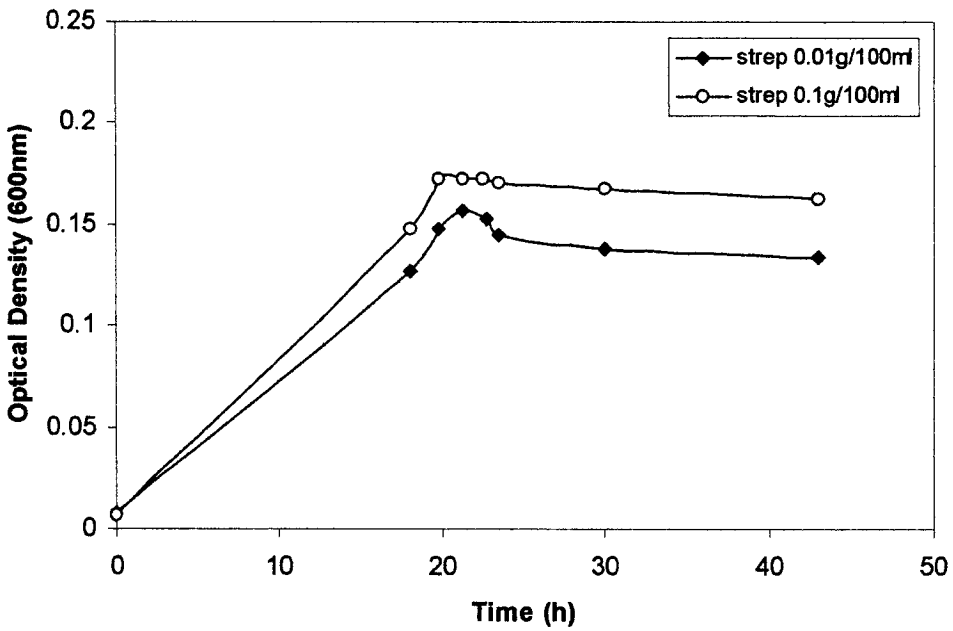

Figure 2.2. Growth curves of two separate *E. coli* cell suspensions in M9 medium poisoned by streptomycin after 20 hours of growth. After 20 hours, the cells became metabolically inactive and non-reproducing.

3.2.2 Redox Potential

The redox potential fluctuated during growth (Figure 2.3). There was commonly a large variation in the redox potential during the exponential growth phase. The Eh then stabilized to a slight increasing trend in the stationary phase.

3.2.3 Nutrient Levels

Nitrate and phosphate levels in the spent medium also varied as a function of growth phase, as shown in Figure 2.3. During the exponential and stationary growth phases, both nitrate and phosphate levels declined, indicating that the cells consumed

both of the nutrients during growth. In the late stationary phase, there was a slight increase in both nutrients to be discussed further in section 4.

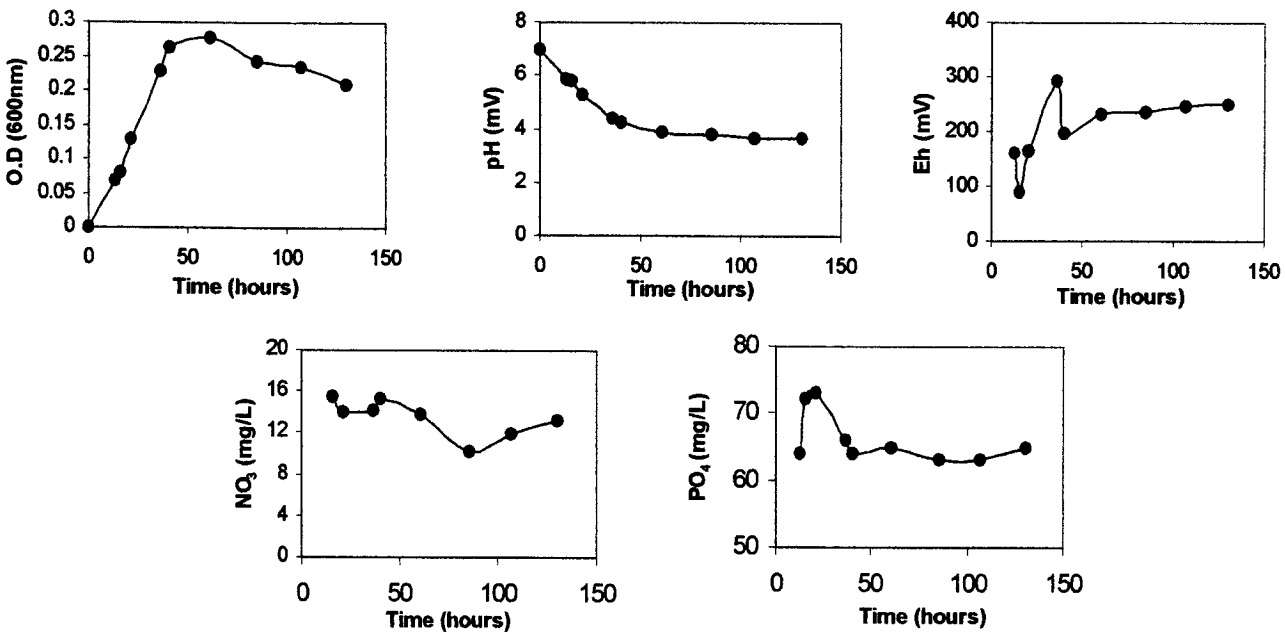

Figure 2.3. Growth curve of active *E. coli* cells in M9 medium and concurrent chemical changes in the medium as a function of time.

3.2.4 Dissolved Organic/Inorganic Carbon

DIC concentrations increased from exponential to mid-stationary phase, followed by and increase from mid to late stationary and death phase, whereas DOC concentrations in the M9 growth medium decreased from exponential to stationary phase (Figure 2.4). From mid-stationary phase to late stationary and death phase, the DOC levels however increased.

3.3 Dry Weight – Optical Density Correlation

The results linking the optical density to the dry weight of the cells indicate that the approach is reliable, as indicated by the high correlation coefficient (R^2 = 0.9666) (Figure 2.5). Optical density measurements were transformed into dry weights to normalize the titration data to biomass.

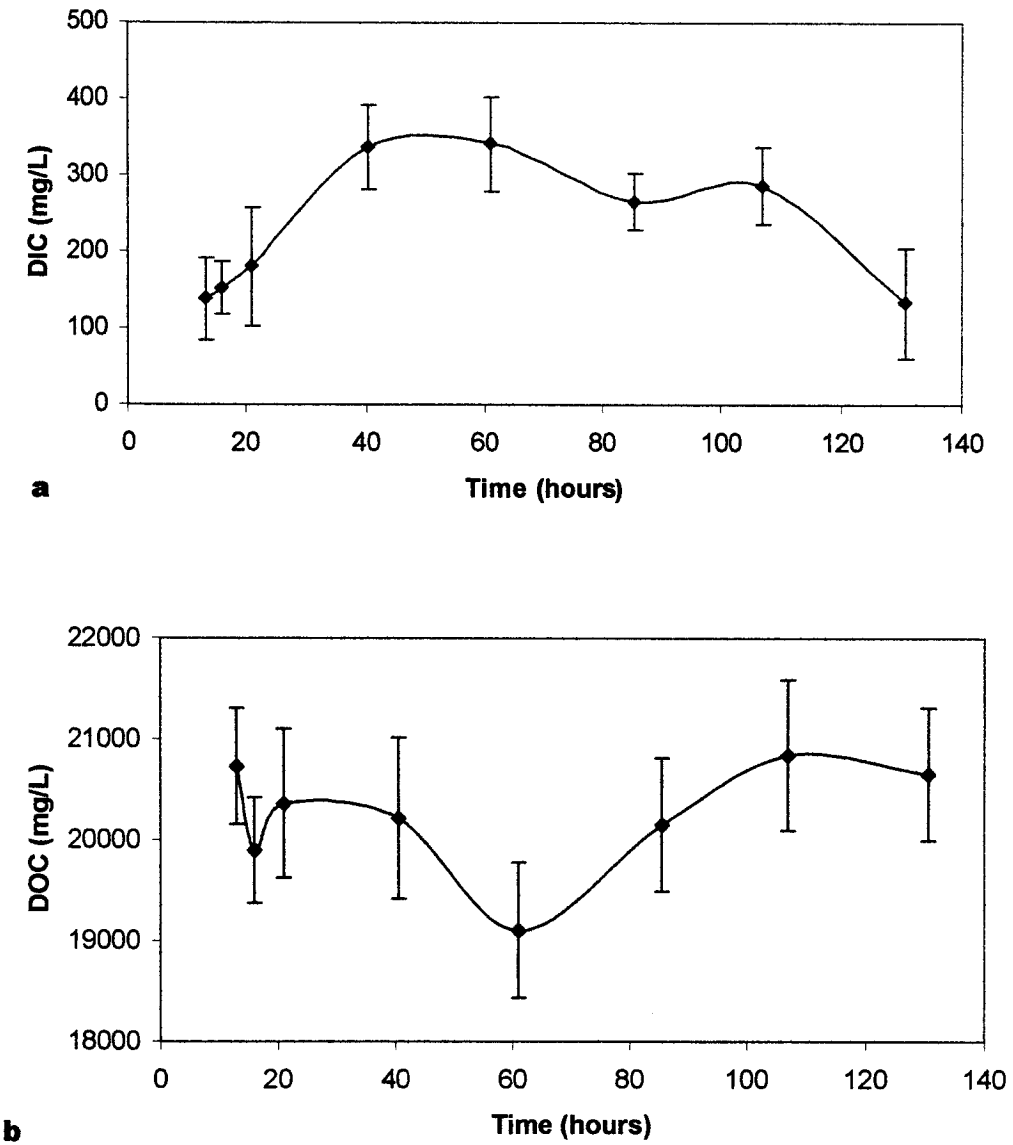

Figure 2.4. Dissolved organic carbon (DOC) (a) and inorganic carbon (DIC) (b) concentrations in the M9 growth medium during the growth of active *E. coli* cells.

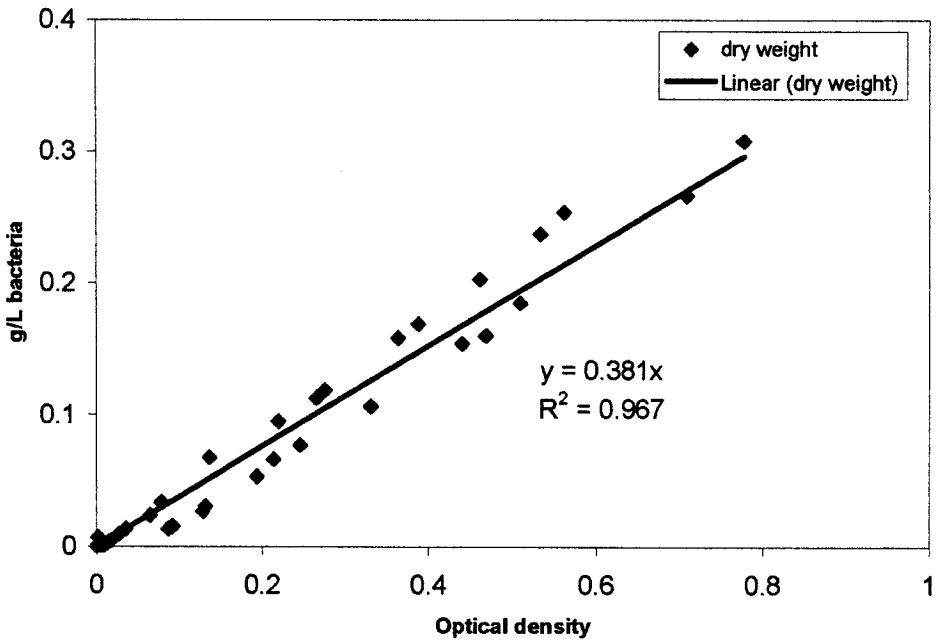

Figure 2.5 Optical Density vs. dry weight of bacteria calibration curve used to determine dry weight of bacteria for each titration.

3.4 Acid -Base Titrations of *E. coli*

3.4.1 Titrations of *E.* coli in M9 medium

Results from titrations of *E.* coli in the M9 medium showed that the suspension (i.e., M9 medium with cells) had a high buffering capacity (Figures 2.6 to 2.8). The titrations are expressed as the change in pH as a function of the amount of acid (H^+ ions) added. The results indicate that cell suspensions from the same growth phase (Figure 2.6 a and b), but with various dry weights, possessed slightly different buffering capacities, but no consistent trend was observed between the quantity of cells and the concentration of [H^+] added (higher buffering capacity should be expected from higher quantities of cells). The comparison of titration curves of cells in their mid-exponential and mid-stationary growth phases, for which the dry weight was identical, showed that the

buffering capacity of both suspensions was slightly different (Figure 2.7), most noticeably below pH 4.5 and above pH 6.5, where the exponential phase cells had enhanced buffering.

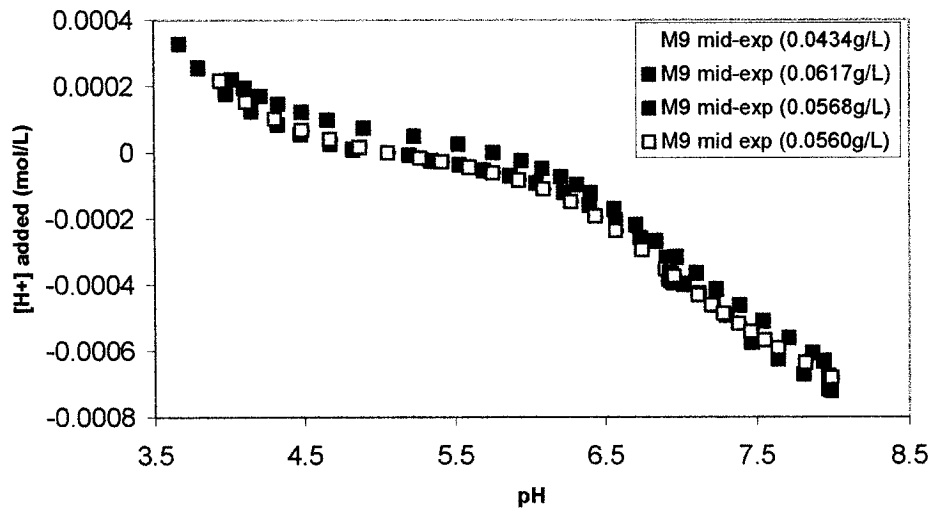

a

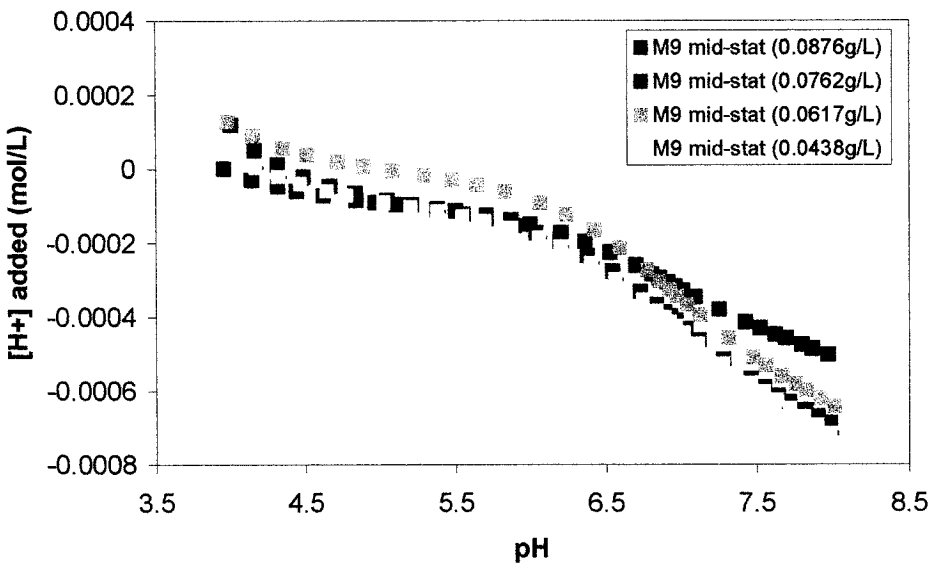

b

Figure 2.6. **a.** Acid-base titrations of active *E. coli* cells (of various dry weights) in mid exponential growth phase in M9 medium. **b.** Acid-base titrations of active *E. coli* cells (of various dry weights) in mid stationary growth phase in M9 medium.

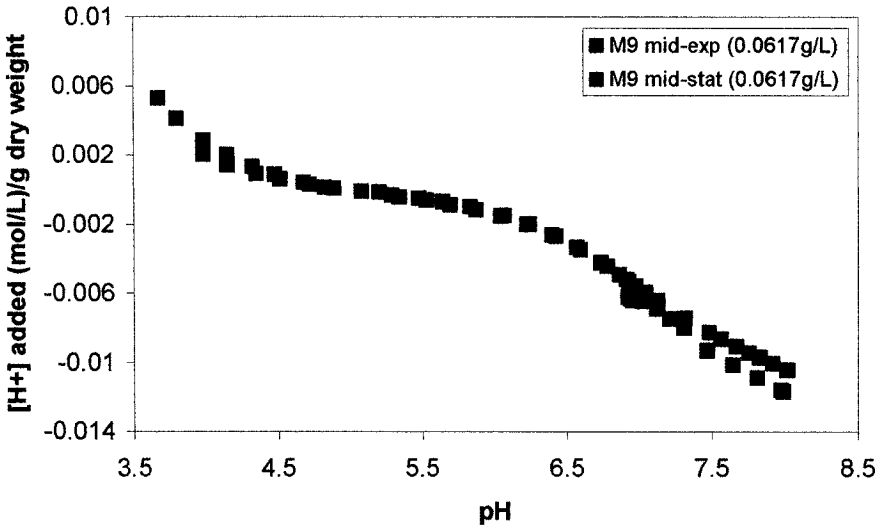

Figure 2.7. Comparison between acid-base titrations performed using active cell suspensions of identical dry weights (0.0617g/L) in the exponential growth phase and cells in the stationary phase in M9 medium.

Reverse titrations of the cells in their mid-exponential and mid-stationary growth phases in the M9 medium indicated that the titrations were fully reversible (Figure 2.8). In addition, titration of the spent M9 medium (after the cells were removed) showed that the medium itself had a strong buffering capacity (Figure 2.8). Since the spent medium (i.e., medium without cells) had a similar buffering capacity as the cells in the growth medium, it became necessary to remove the cells from the medium and titrate them in a neutral electrolyte.

3.4.2 Titrations of *E.* coli in 0.01 M $NaNO_3$ electrolyte

The strong buffering capacity of the M9 medium is shown in Figure 2.9. The $NaNO_3$ electrolyte showed no buffering in comparison to the medium, indicating that any buffering observed in titrations with *E. coli* in the electrolyte should be due to the cells themselves. Titration curves in $NaNO_3$ were either expressed as $[H^+]$ added as a function of pH to show the reproducibility of the titration curves and the effect of dry

weight on the buffering capacity, or as $[H^+]$ added normalized with respect to dry weight of bacteria in order to fully assess the effect of growth phase and metabolic state on the buffering capacity.

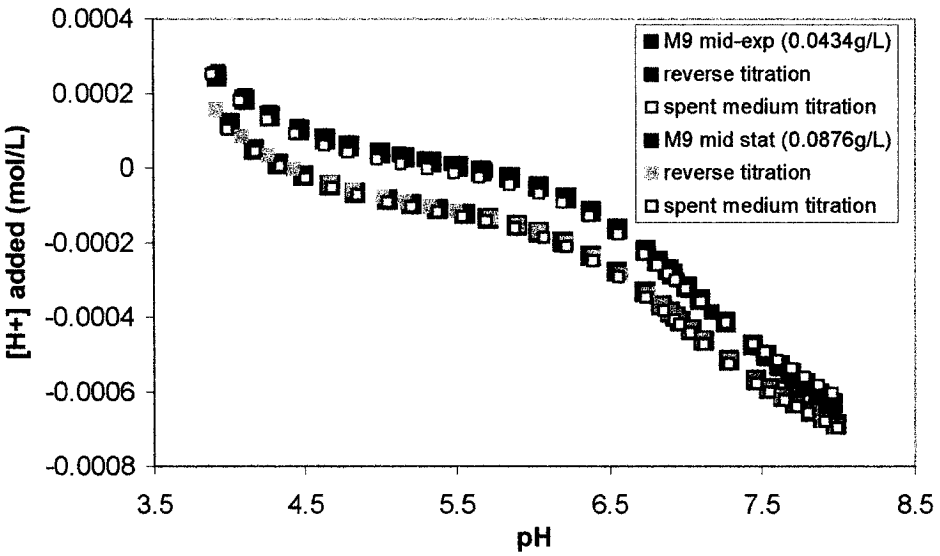

Figure 2.8. Acid base titrations of active *E. coli* cells in mid exponential (blue) and mid stationary growth phase (red), reverse (up pH) titrations and titration of spent medium (without bacteria at the end of growth phase) from two individual experiments.

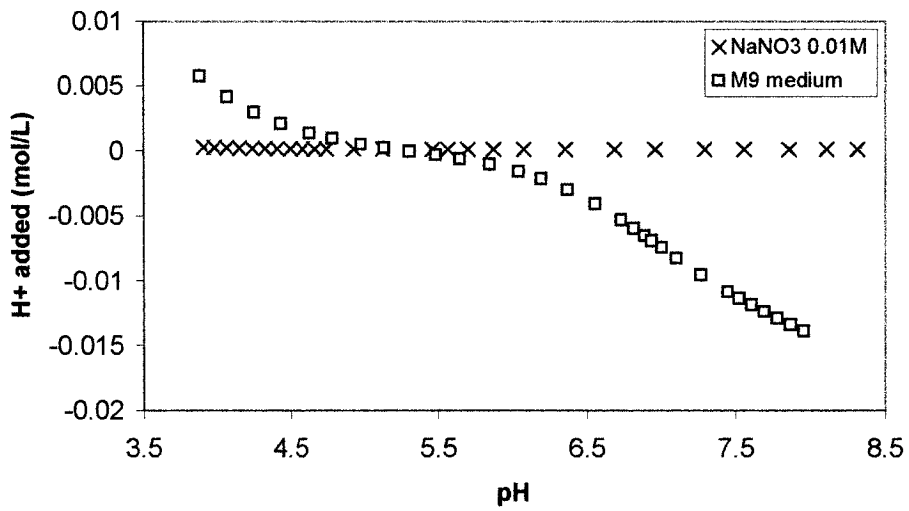

Figure 2.9. Acid-base titrations of 0.01M $NaNO_3$ electrolyte and fresh M9 medium.

Figure 2.10 a shows the titration curves obtained for active cells harvested in their mid-exponential growth phase for various dry weights (between 0.189g/L and 0.273g/L), while Figure 2.10 b shows the titration curves of active *E. coli* cells in their mid-stationary growth phase for various dry weights (between 0.116g/L and 0.396g/L). The results show that for both growth phases, the buffering capacity increased with increasing dry weight. Figure 2.11 a shows the acid-base titration curves of individual non active *E. coli* cell suspensions of similar dry weights during their mid-exponential growth phase (i.e., two hours after being poisoned with streptomycin sulfate) while figure 2.11 b shows the titration curves of non active cells (of similar dry weights) in their mid-stationary growth phase. The results illustrate that independent titration curves (for each treatment) with similar dry weights behaved similarly.

Figure 2.12 shows the difference in buffering capacity (normalized to dry weight) between the various growth phases and metabolic activity of *E. coli* cell suspensions. For each treatment, with the exception of the mid-stationary active cells, there was a fairly good agreement between the curves of independently grown cultures, even though the dry weight varied (see legend in Figure 2.12). However, the curves for the active mid-stationary cells behaved differently, despite being normalized to dry weight and representing the same treatment. The results also indicate that the active cells in their mid-exponential growth phase had the highest buffering capacity, whereas active cells in their mid-stationary growth phase had the lowest buffering capacity (Figure 2.12). Non-active cells in their mid-exponential and mid-stationary growth phases possessed intermediate buffering capacities (Figure 2.12).

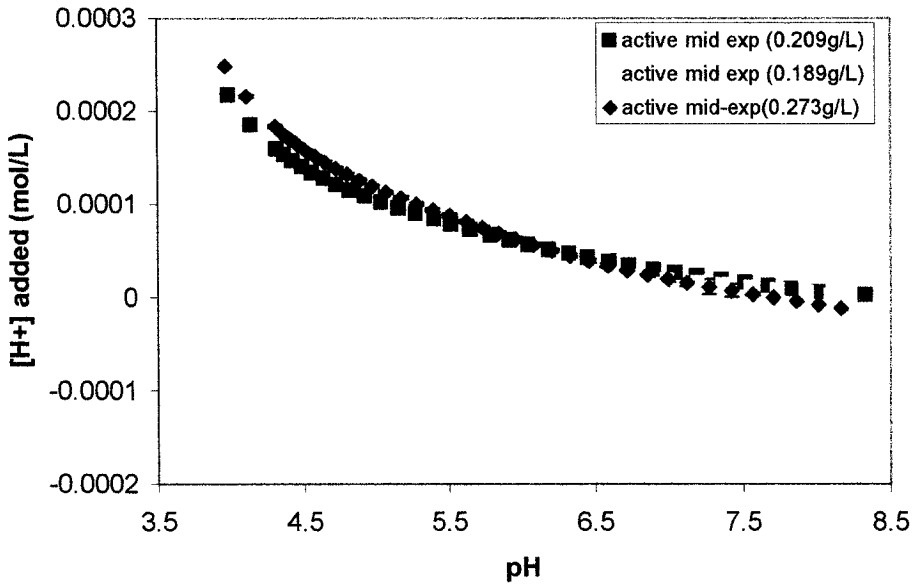

a.

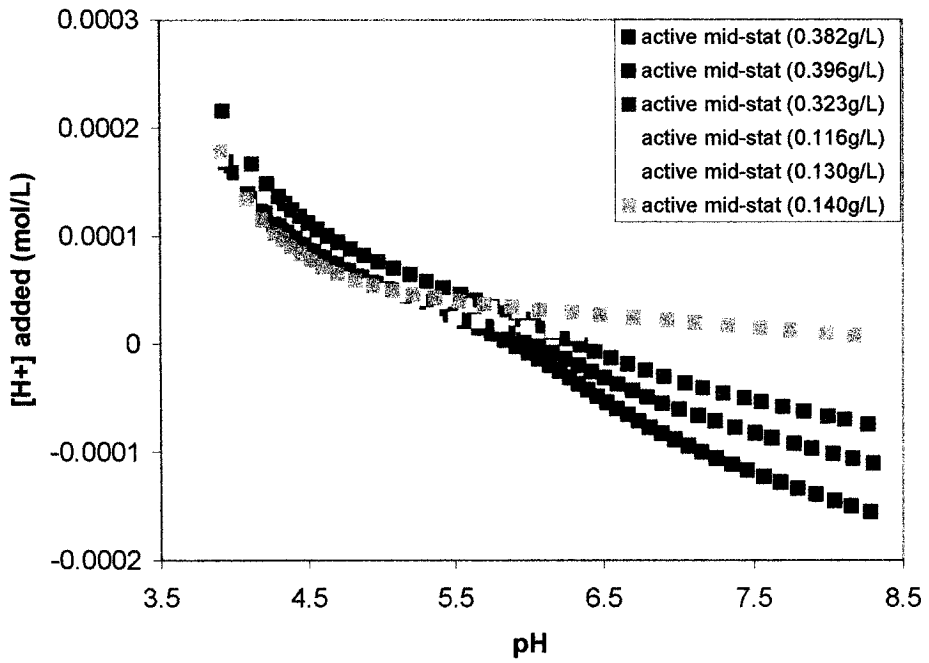

b.

Figure 2.10. a. Acid-base titration curves of active cell suspensions (of various dry weights) harvested in the mid exponential growth phase and re-suspended in 0.01 M $NaNO_3$ electrolyte. **b.** Acid-base titration curves of individual active cell suspensions (of various dry weights) harvested in the mid stationary growth phase and re-suspended in 0.01 M $NaNO_3$ electrolyte.

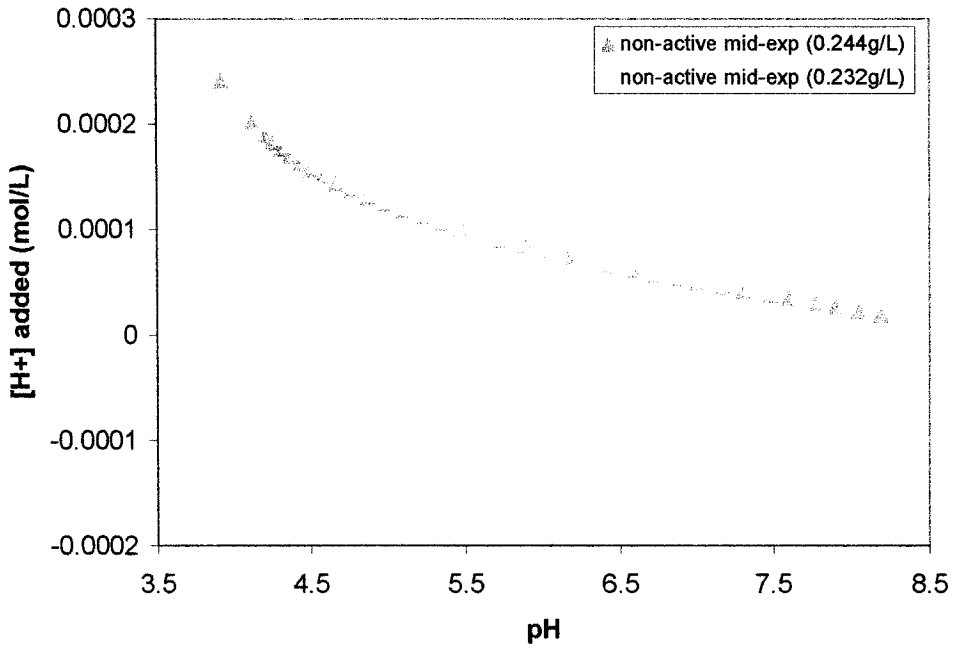

a.

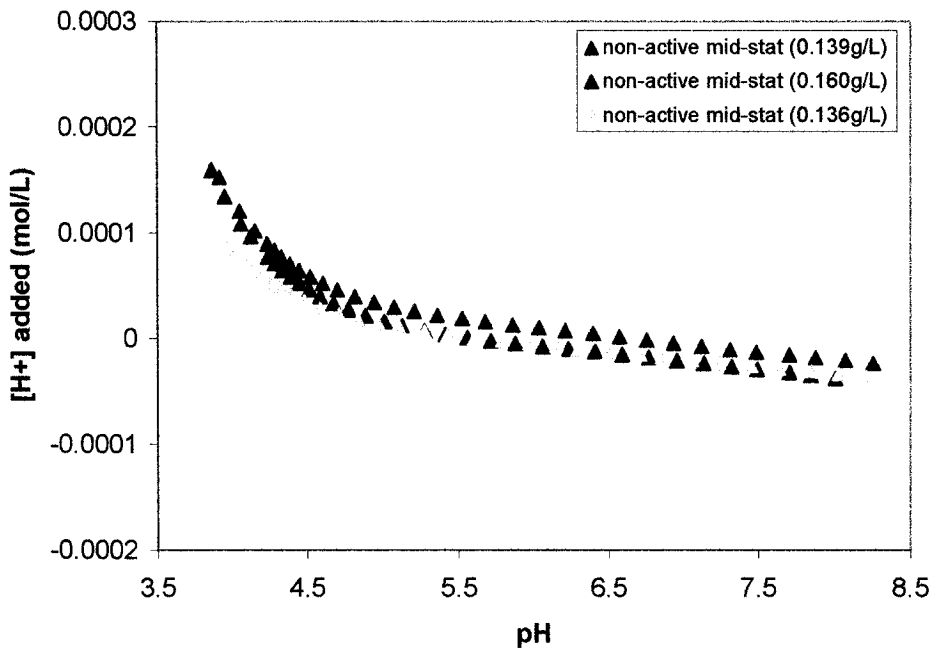

b.

Figure 2.11. **a.** Acid-base titration curves of metabolically inactive and non-reproducing *E. coli* cell suspensions (of similar dry weight) harvested in their mid exponential growth phase and re-suspended 0.01 M $NaNO_3$ electrolyte. **b.** Acid-base titration curves of metabolically inactive and non-reproducing *E. coli* cell suspensions (of similar dry weight) harvested in their mid stationary growth phase and re-suspended 0.01 M $NaNO_3$ electrolyte. 0.1g/100ml of streptomycin was added 2 hours prior to harvesting the cells to stop metabolic activity.

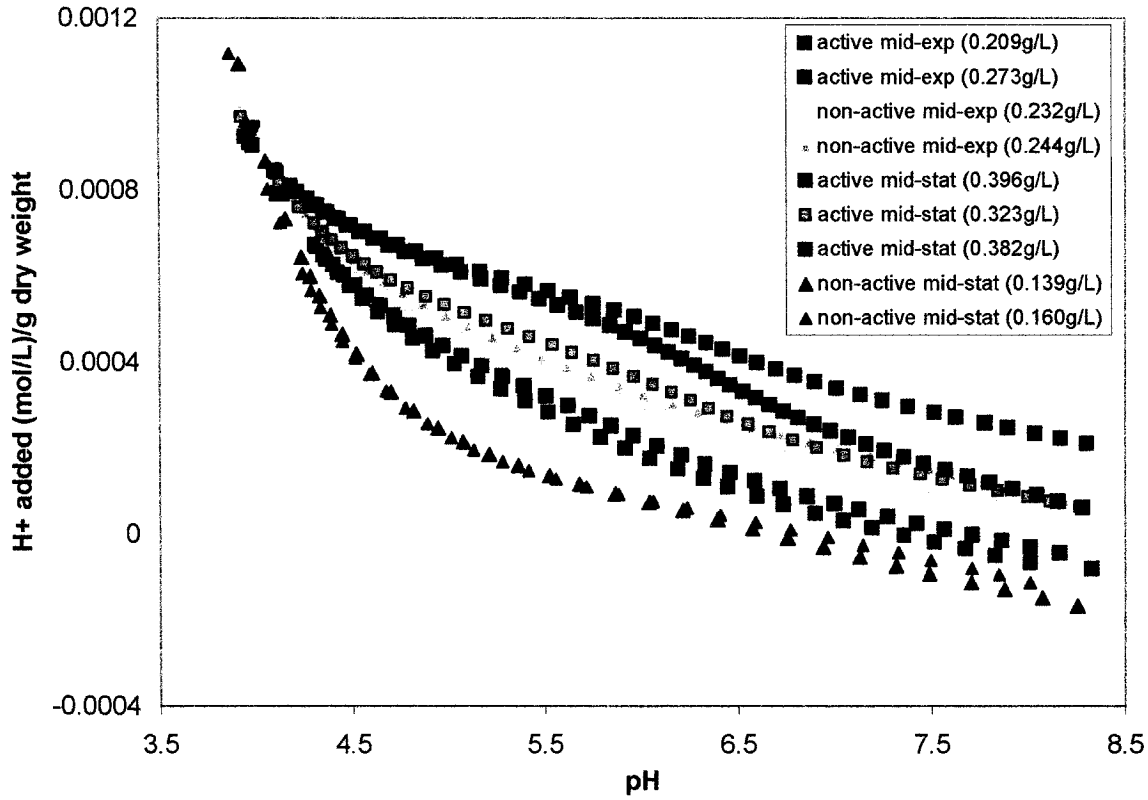

Figure 2.12. Comparison of representative acid-base titration curves (in 0.01 M $NaNO_3$ electrolyte) (normalized to dry weight) of metabolically active and non active *E. coli* cells harvested in their mid-exponential growth phase and in their mid-stationary growth phase. Each curve represents an independently grown culture.

3.5 Acid-Base Titrations of Quartz and Lepidocrocite

3.5.1 Titrations of quartz in $NaNO_3$ electrolyte

Acid-base titrations of quartz were performed in $NaNO_3$ electrolyte at concentrations of 5g/L and 10g/L. The results first indicate that the buffering capacity of quartz is very low in comparison to the *E. coli* cells (Figures 2.12 and 2.13). Figure 2.13 indicates that the quartz titrations were fully reversible for both concentrations. Results in Figures 2.13 and 2.14 also show the theoretical titration curve of water, which further indicates that quartz possesses a very low buffering capacity. The results clearly show

that there were no real differences in buffering capacity between quartz suspensions of various concentrations, i.e., 5g/L and 10g/L (Figures 2.13 and 2.14).

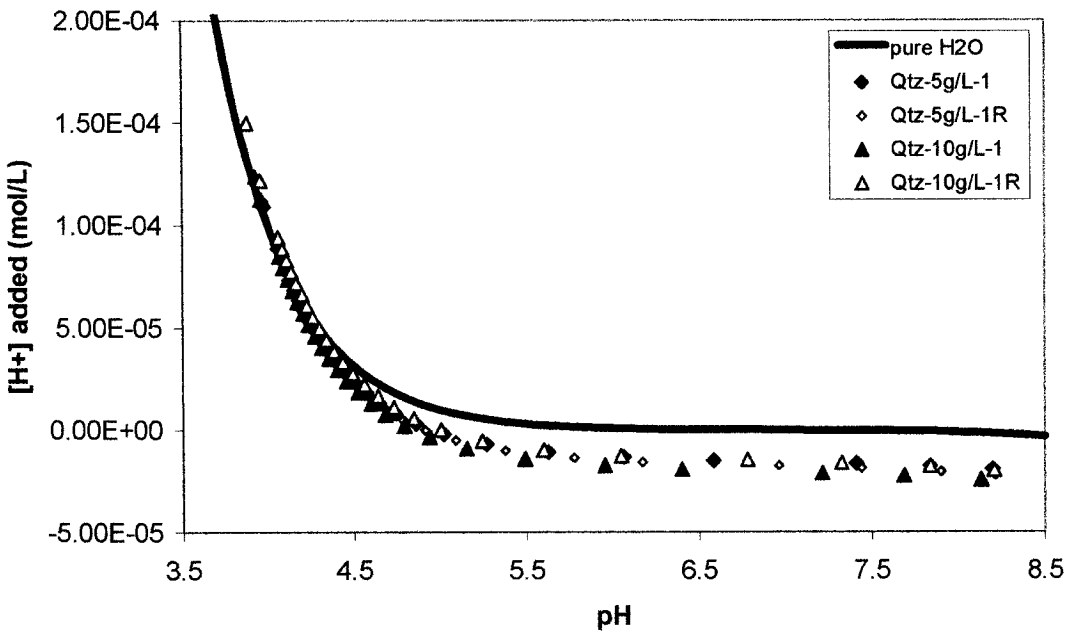

Figure 2.13. Comparison of original (solid symbols) and reverse acid-base titrations (open symbols) of quartz suspensions at concentrations of 10g/L and 100g/L in $NaNO_3$ electrolyte

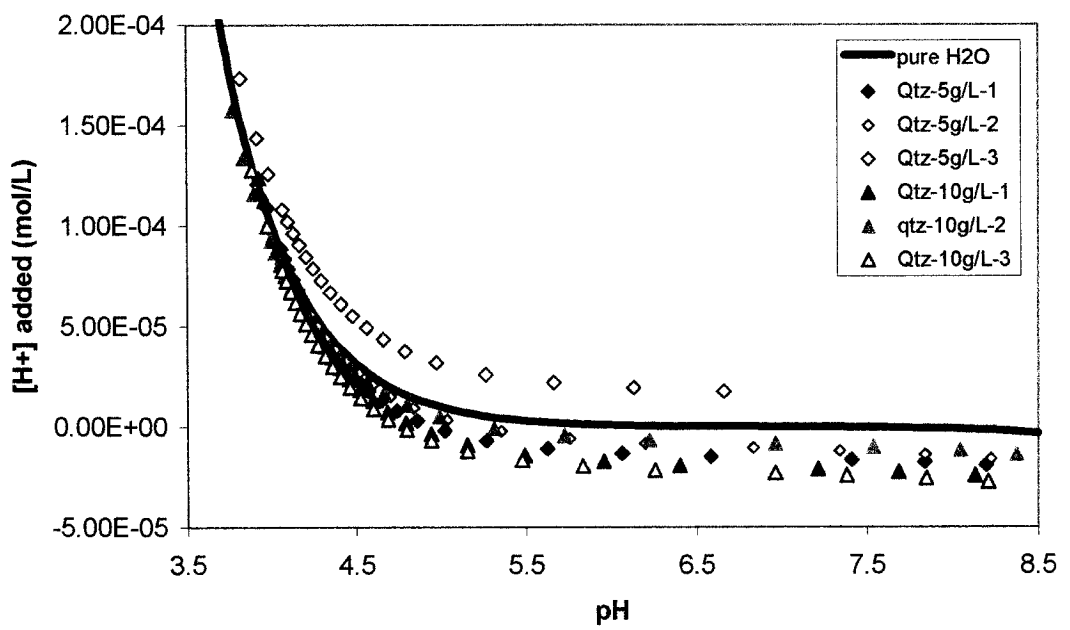

Figure 2.14. Acid-base titrations of quartz at concentrations of 5g/L and 10g/L in $NaNO_3$ electrolyte compared to a theoretical titration curve for pure H_2O.

3.5.2 Titrations of Lepidocrocite in $NaNO_3$ electrolyte

Acid-base titrations of lepidocrocite were performed at concentrations of 5g/L and 10g/L in 0.01M $NaNO_3$. The results first indicate that lepidocrocite had a much higher buffering capacity than both the quartz and *E. coli* cells (Figures 2.12, 2.14 and 2.15). The results also prove that the buffering capacity increased with the quantity of lepidocrocite in suspension, i.e., the 10g/L suspension had a higher buffering capacity than the one at 5g/L (Figure 2.15). The titrations were also reversible for each concentration (Figure 2.16).

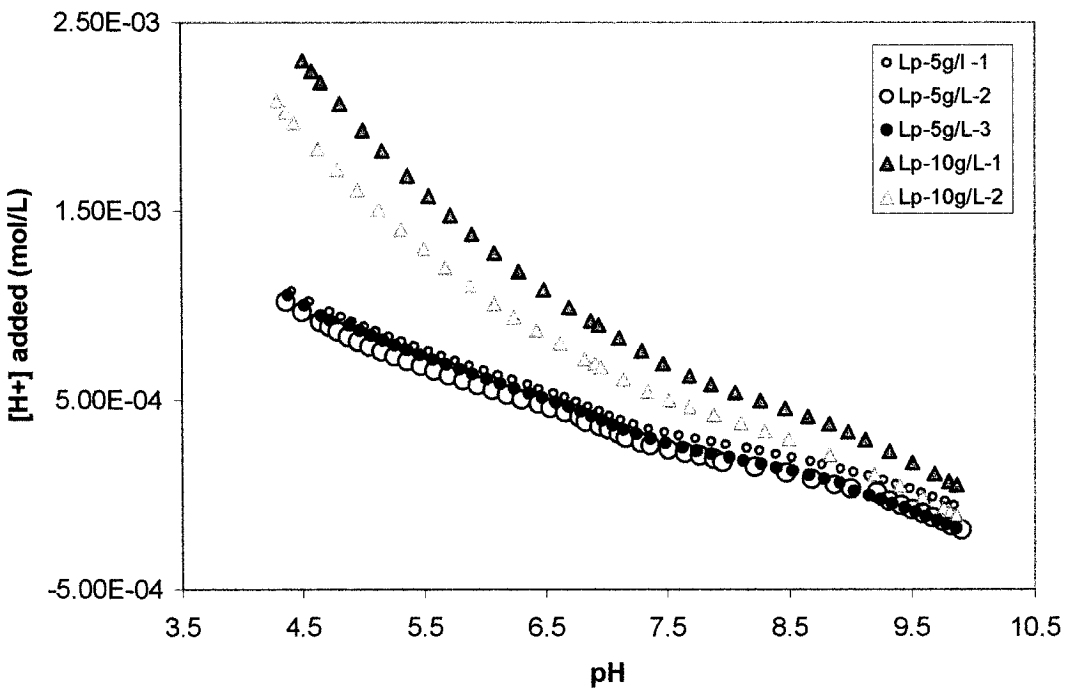

Figure 2.15. Acid-base titrations of lepidocrocite suspensions at 5g/L and 10g/L in $NaNO_3$ electrolyte.

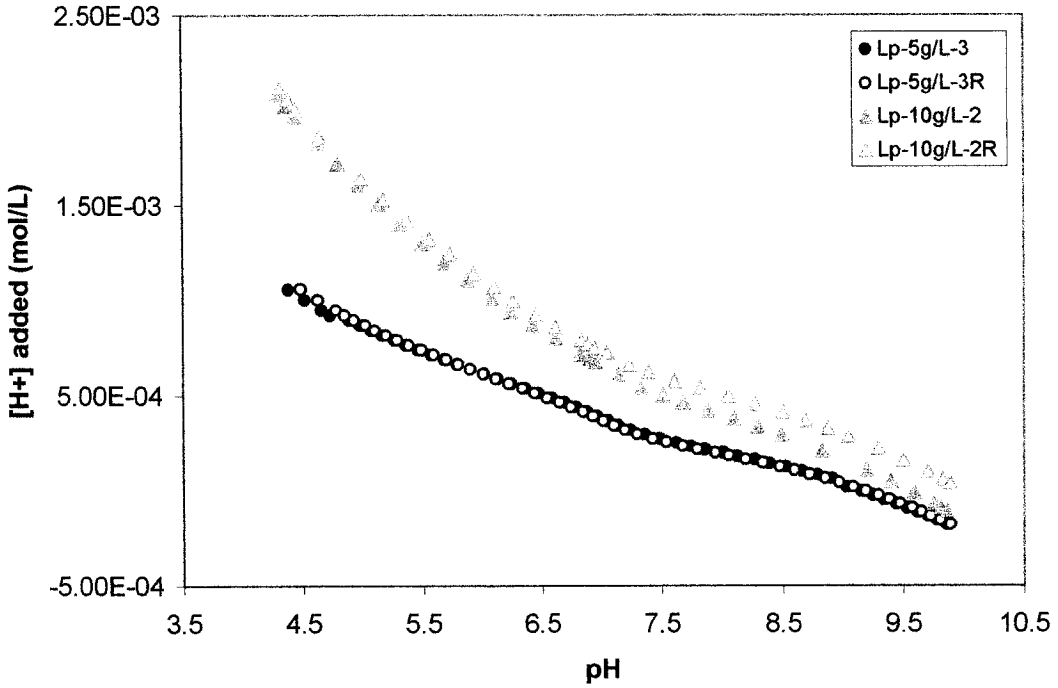

Figure 2.16. Comparison of original (solid symbols) and reverse acid-base titrations (open symbols) of lepidocrocite suspensions at concentrations of 5g/L and 10g/L in $NaNO_3$ electrolyte.

4.0 Discussion

4.1 Chemical changes of the growth medium during *E. coli* growth

The chemistry of the growth medium was monitored during the growth of the cells. The results shown in section 3 (Figure 2.3) show that the final pH of the spent medium after 60 hours was usually around 3.5-4.0, even though the initial pH was approximately 7. This illustrates that the metabolic activity of the cells acidified the medium through the growth of the population. The change in pH may occur through the release of acidifying species such as CO_2 produced by the metabolism of glucose, protons (H^+) and/or organic acids.

The results in Figure 2.4 a and b illustrate that dissolved organic carbon (DOC), provided by the glucose in the medium was used up by the cells during the mid-exponential and mid-stationary growth phases, and that dissolved inorganic carbon (DIC) was produced as a by-product. This assumption is in agreement with the complete oxidation of glucose, which produces CO_2 (eq. 3):

$$C_6H_{12}O_6 + 8O_2 \rightarrow 6CO_2 + 12H_2O \quad (3)$$

The CO_2 dissolves in water and produces carbonic acid, which in turn dissociates to produce bicarbonate (eq. 4):

$$CO_2 + H_2O \rightarrow H_2CO_3 \rightarrow HCO_3 + H^+ \quad (4)$$

This reaction is likely partially responsible for the increased acidity in the spent medium during growth. However, the final pH of the growth medium was near 3.5-4.0, which is lower than the pKa of carbonic acid (~ 5.75). It is then possible that other acidifying compounds were produced during the growth of *E. coli,* such as organic acids originating from the incomplete oxidation of glucose. The presence of such acids was not assessed in the spent medium.

The redox potential also fluctuated, particularly throughout the exponential growth phase indicating that oxygen was consumed. Nitrate and phosphate levels in the spent medium varied as a function of growth phase, as shown in Figure 2.3. The decrease in nutrient concentrations during the exponential phase indicates that the cells were

dividing and using up the nutrients. The increase of soluble NO_3 and PO_4 at the end of the mid-stationary growth phase was most likely caused by the cells dying off and releasing soluble nutrients and organic compounds back into the growth medium.

4.2 Acid-base titrations of *E. coli* cells

4.2.1 Buffering capacity of *E. coli* in M9 medium

The results for the acid-base titrations of *E. coli* cells in the M9 medium (Figures 2.6-2.8) showed that the medium itself had a strong buffering capacity compared to the neutral electrolyte (Figure 2.9). Since the medium contained 2.699 X 10^{-4} mol/L of phosphate (Table 2.1), the highest concentration of ion in the medium next to Na^+, it can be speculated that most of the buffering was caused by phosphate (PO_4^{2-}), according to the following reaction (eq. 5):

$$H_2PO_4^- \rightarrow HPO_4^{2-} + H^+ \qquad (5)$$

As a result, the buffering capacity of the cells alone was not visible and further titrations were performed in neutral $NaNO_3$ electrolyte in order to fully assess the effect of growth phase and metabolic activity on the buffering capacity.

4.2.2. Buffering capacity of *E. coli* in 0.01M NaNO3

Several studies have investigated the proton and metal binding capacity of bacterial cells (Claessens et al, 2004; Fein et al., 1997, Daughney and Fein, 1998, Daughney et al, 1998; Daughney et al, 2001; MacLean and Beveridge; 1990). These studies have shown that the bacterial cell wall of gram-positive and gram-negative bacteria possess binding

sites that can deprotonate, conferring a net charge to the cell. The deprotonation of each site can be described with the following chemical reaction and mass action law (eq. 6, 7):

$$RL_nH^0 = RL_n^+ + H^+ \quad b \tag{6}$$

$$K_n = [RL_n^+]a_{H+}/ [RL_nH^0] \tag{7}$$

where L_nH corresponds to a specific functional group (binding site) attached to the surface R, K*n* represents the stability constant describing the deprotonation, and *a* is the activity of the species RL_n^+ (Daughney et al, 2001). According to several studies (Fein et al., 1997; Daughney and Fein, 1998; Daughney et al., 2000; Daughney et al, 2001) these sites likely correspond to the carboxyl, phosphate, amine and hydroxyl reactive sites within the cell wall. The use of synchrotron techniques (XAFS) has shown that these suspected reactive sites are indeed involved in metal binding (Kelly et al., 2001). These binding sites correspond to exposed reactive sites in the cell wall of gram-negative (mainly from the lipopolysascharide layer (LPS)) and gram-positive (composed of peptidoglycan) bacteria (Daughney and Fortin, 2002 and references therein). Other studies have shown that the cell wall of bacteria could have up to five different types of reactive sites (Cox et al., 1999).

The deprotonation of the reactive sites on the cell wall of bacteria are responsible for the buffering capacity observed during acid-base titrations of bacterial cells. Surface complexation models (SCM) can be used to determine the pKa of each type of sites and quantify the density of sites (Fein et al., 1997). Such an approach was not used in the present study, but the analysis of the buffering capacity behaviour of *E. coli* cells of different metabolic activity and growth stages remains useful to assess their surface charge behaviour in aqueous environments.

The results first show that the titrations were generally reproducible for each treatment. Results from independently grown *E. coli* cultures of various treatments (with variable dry weights) are in good agreement with each other (Figures, 2.11, 2.12), with the exception of the active cells in their mid-stationary growth phase (Figure 2.12). For the latter, it is not clear why reproducible curves could not be obtained. Growth curves of independent cultures (Figure 2.1) showed that the cells reached stationary growth phase within 48 to 60 hours. Given the large span of time to reach stationary growth phase, it is possible that not all individual titration experiments were performed on active cells having reached a complete stationary growth phase (all cells were titrated after 48 hours of growth). It is possible that some titrations were performed on cells in their late mid-exponential growth phase, affecting the overall buffering capacity of the separate cell suspensions.

The results also indicate that the buffering capacity increased with the quantity of cells in suspension (Figure 2.10). This is in agreement with titration results performed on other bacteria, such as *Bacillus subtilis*, a gram-positive bacterium (Fein et al, 1997). The trend of increasing buffering capacity with increasing dry weight was observed for the various *E. coli* treatments, indicating that the buffering capacity of the cell suspension is directly proportional to the quantity of cells in suspension.

The results shown in Figure 2.12 clearly show that buffering capacity is different between active mid-exponential and active mid-stationary cell suspensions, with active *E. coli* cells in their mid-stationary growth phase having the lowest buffering capacity. Cells in their mid-exponential growth phase had the highest buffering capcity. To our knowledge, the effect of metabolic activity and growth phase on the buffering capacity of

E. coli cells has not been previously reported, but recent work by Daughney et al. (2001) found that the buffering capacity of active *Bacillus subtilis* cells was greater for cells in their mid-exponential phase than for cells in their mid-stationary growth phase. The same authors found that *Bacillus subtilis* cells in their mid-exponential growth phase displayed approximately four times more carboxyl sites, than those in their stationary phase. Their findings are in agreement with ours, i.e., active mid-exponential *E. coli* cells had a higher buffering capacity than active mid-stationary cells (Figure 2.12).

Differences in buffering capacity as a function of growth phase were likely caused by changes in the structure and composition of the cell wall as the cells grow. The cells are in turn also affected by changes in the chemical composition of the growth medium (Daughney et al., 2001). According to McLean and Beveridge (1990), the absence of certain components in the growth medium, such as phosphate, can induce changes in the structure of the cell wall of *B. subtilis*. Chemical changes, including a decrease in concentrations of nutrients and a drop in pH were indeed observed during the growth of *E. coli* in the M9 growth medium (Figures 2.3 and 2.4), which might have triggered changes in the structure and chemical composition of the cell wall of *E. coli* during the exponential and stationary growth phases.

To our knowledge, no studies have investigated the effect of metabolic activity on the deprotonation of reactive sites in bacterial cell walls, but some studies have looked at the effect of metabolic activity (starvation) on cell adhesion. Kjelleberg and Hermansson (1984) used seven different marine bacterial strains to determine their ability to adhere to glass during starvation. The study reported changes in cell surface characteristics, most apparently in cell size and cell wall hydrophobicity during starvation, which affected

adhesion. This indicates that metabolic state can induce changes in the cell wall composition, which can then affect their buffering capacity. In our study, mid-exponential non-active cells had a lower buffering capacity than active cells in the same growth phase (Figure 2.12), which suggests that metabolic activity has an effect on the buffering capacity.

4.2.3 Acid Base titrations of quartz and lepidocrocite in $NaNO_3$

The titration curves of quartz in 0.01 M $NaNO_3$ were reproducible and reversible at both concentrations (5g/L and 10g/L) (Figures 2.13 and 2.14. The results also indicate that the buffering capacity of quartz suspensions remained comparable for two different quartz concentrations (Figure 2.13) As in the case of the *E. coli* cells, the mineral surface also contains functional groups which protonate and deprotonate under different pH conditions. The deprotonation of binding sites on quartz can be described by the equation 8 as follows:

$$SiOH \leftrightarrow SiO^- + H^+ \qquad (8)$$

. Unlike *E. coli* cells, quartz only possesses one type of surface site present in the form of SiOH (Yee et al. 2000). The presence of only one type of binding site, and the low surface area of quartz, found to be 0.14 m^2/g by BET surface area analysis (Appendix 2.4a), and 0.2 m^2/g in Yee et al. (2000), account for the low buffering capacity of the mineral. The low buffering capacity of quartz was likely responsible for the lack of differences when two different concentrations were used (Figure 2.14). Bacterial cells on the other hand, have several surface functional groups and a much larger surface area of (approximately 140 m^2/g according to Fein et al, 1997).

The iron oxide titration curves were also reproducible and reversible (Figures 2.15 and 2.16). The titrations of more concentrated iron suspensions (10g/L) led to a sharp increase in buffering capacity (Figure 2.15). The buffering capacity of lepidocrocite was much higher that the one observed for the cells and quartz, indicating that the functional groups on the surface of the iron oxide are more active or that more binding sites are available. Lepridocrocite has a surface area than of approximately 160 m^2/g (Appendix 2.4b), larger in comparison to quartz or *E. coli* cells, and possesses 1 type of binding sites, described by the following reactions, equations 9 and 10 (Morel and Hering; 1993; Stumm and Morgan, 1996;):

$$FeOH_2^+ \leftrightarrow FeOH + H^+ \quad (9)$$

$$FeOH \leftrightarrow FeO^- + H^+ \quad (10)$$

Given the large buffering capacity observed for both *E. coli* cells and lepidocrocite, it can be assumed that surface charge is likely to play a role in the adhesion of the cells onto the iron oxides. The low buffering capacity of quartz might on the other hand greatly limit the adhesion of *E. coli* cells, as discussed in chapter 3.

5.0 Conclusions

The results in this study demonstrate that the growth of *E. coli* cells induces changes in the chemistry of the M9 growth medium, most markedly that the cells acidify the medium over time, likely as a result of the consumption of glucose. The metabolism of glucose resulted in a decrease in DOC and a corresponding increase in DIC. The cells consumed the nutrients (NO_3^-, PO_4^{2-}) in small amounts and then released dissolved nitrate

and phosphate compounds back into the medium when they started to die off in their stationary growth phase.

The acid-base titrations of *E. coli* cells in M9 medium were reproducible and reversible but yielded inconclusive results because the buffering of the growth medium was greater than or equal to the buffering capacity of the cells, because of the high phosphate concentration in the medium. This necessitated the cells to be washed and re suspended in a neutral electrolyte.

Titrations of *E. coli* cells in 0.01M $NaNO_3$ were reproducible and reversible, with the exception of active cells in their mid-stationary growth phase. The results showed that active cells in their exponential growth phase had the greatest buffering capacity, whereas active cells in their mid-stationary growth phase had the lowest one. The results also indicated that the buffering capacity of the cell suspensions increased with increasing quantities of cells in the electrolyte. The titrations of quartz and lepidocrocite yielded very different results. The results showed that the buffering capacity of quartz was extremely low, while that of the iron oxide was very high in comparison.

Based on these results, it can be expected that the adhesion of *E. coli* cells should be different between quartz and lepidocrocite, assuming that adhesion is function of the surface charge of both the minerals and the cells. In addition, changes in adhesion onto each mineral should also be expected between the various growth phases and metabolic state of *E. coli*.

References

Claessens, J; Behrends, T and P van Cappellen. 2004. What do acid-base titrations of live bacteria tell us? *Aquatic Science* 66:19-28

Cornell, R. and Shwertmann, U. 1996. *The Iron Oxides. Structure, Properties, Reactions, Occurrences, and Uses.* VCH, Verlagsgesellschaft, pp. 221-225.

Daughney, C.J., Fein, J.B., Yee, N. 1998. A comparison of the thermodynamics of metal adsorption onto two common bacteria. *Chemical Geology.* 144, 161-176.

Daughney. C. J., Fein, J.B. 1998. The effect of ionic strength on the adsorption of H+, Cd^{2+}, Pb^{2+}, and Cu^{2+} ions by *Bacillus subtilis* and *Bacillus Licheniformis:* a surface complexation model. *Journal of Colloid and Interface science.*198, 53-77.

Daughney, C. and D. Fortin. 2001. Mineral adsorption by bacteria. Encyclopedia of Surface and Colloid Science, Marcel Dekker, Inc.

Daughney, C.J., Fowle and D. Fortin, 2001. The effect of growth phase on proton and metal adsorption by Bacillus subtilus. *Geochim. Cosmochim. Acta*, 65, 1025-1035.

DeFlaun,M.F.; Tamzer, A.S.; McAteer, A.L.; Marshall, B.; Levy, S.B.1990. Development of an adhesion assay and characterization of an adhesion-deficient mutant of *pseudomonas fluorescens. Appl. Environ. Microb.* 56, 112-119.

Fein J.B., Daughney, C.J., Yee, N. and Davis, T.A. 1997. A chemical equilibrium model for metal adsorption onto bacterial surfaces. *Geochim. Cosmochim. Acta,* 61(16), 3319-3328.

Goss, M.J., Barry, D.A.J., Rudolph. D.L. 1998. contamination in Ontario farmstead domestic wells and it's association with agriculture : 1. Results from drinking water wells. . *J. Contam. Hydrol.* 32: 267-293.

Kelly, S.D., Boyanov, M.I., Bunker, B.A., Fein, J.B., Fowle, D.A., Yee, N., and Kemner, K.M. (2001) XAFS determination of the bacterial cell wall functional groups responsible for complexation of Cd and U as a function of pH. *Journal of Synchrotron Radiation*, 8, 946-948.

J. Cox, D. S. Smith, L. A. Warren, and F. G. Ferris, ``Characterizing heterogenous bacterial surface functional groups using discrete affinity spectra for proton binding," *Environ. Sci. Technol.*, vol. 33, 4514-4521, 1999.

McLean R.J.C and Beveridge, T.J. 1990. Metal Binding Capacity of bactieral surfices and their ability to form mineralized aggregates. In *Microbial Mineral Recovery* (eds. H.L. Erlich and C.L. Brierly), McGraw Hill Publishing. pp. 185-222.

Morel, F.M.M. and J.G. Hering. Principals and Applications of Aquatic Chemistry. Pages 65-82. John Wiley & Sons, Inc. New York:1993.

Murck, B.W., Skinner, B.J., and Stephen C. Porter. Environmental Geology. Pages 49-51. John Wiley& Sons, Inc. New York: 1996.

Rudolph, D.D., Barry, D.A.J., Goss, M.J. 1998. Contamination in Ontario Farmstead domestic wells and its association with agriculture: 2. Results from multilevel monitoring well installations. *J. Contam. Hydrol.* 32: 295-311.

Skoog, D.A, West, D.M., and F.James Holler. Chimie Analytique. Pages 33-39. Translation by De Boeck & Larcer s.a. Translation copywrite : 1997.

Stevenson, G., Neal, B., Liu, D., Hobbs, M., Packer, N. H., Batley, M., Redmond, J. W., Lindquist, L. and Reeves, P. 1994. Structure of the O antigen of *Escherichia coli* K-12 and the sequence of its *rfb* gene cluster. *J. Bacteriology*, 176, 4144-4156.

Stumm, W and James J. Morgan. Aquatic Chemistry, Chemical Equilibria and Rates in Natural Waters. Third Edition. Pages 252-271, 571-573. John Wiley & Sons Inc. New York: 1996

Yee, N., Fein, J. 2001. Cd adsorption onto bacterial surfaces: A universal adsorption edge? *Geochim. Cosmochim. Acta*, 65(13): 2037-2042.

Yee, Nathan.; Fein, J.B.; Daughney, C. 1999. Experimental study of the pH, ionic strength, and reversability behaviour of bacteria- mineral adsorption. *Geochim. Cosmochim. Acta,* 64(4): 609-617.

Chapter 3

Effect of growth phase and metabolic activity on the adhesion of *E. coli* K-12 onto quartz and lepidocrocite

Abstract

The adhesion of *E. coli* K-12 to quartz and lepidocrocite (γ-FeOOH) was determined through batch experiments in a chemically defined growth medium (M9) and in 0.01M $NaNO_3$ electrolyte, as a function of pH, growth phase and metabolic state of *E. coli* cells. The adhesion of *E. coli* onto lepidocrocite increased with decreasing pH, while cell adhesion to quartz was not influenced by pH changes since both cells and minerals displayed a net negative charge in the pH range studied. In the lepidocrocite systems, adhesion cells increased with increasing bacteria: mineral ratios. Adhesion to lepidocrocite was greater with cells in their exponential growth phase than in their stationary growth phase, since there are more protonated sites on the surface of the cells during the exponential phase. The results also showed that metabolic state played a role in adhesion. Cells that were not reproducing and not metabolically active tended to adhere better to both minerals, but particularly in the lepidocrocite systems. The enhanced adhesion in the presence of inactive cells was caused in part by the inhibited proton motive force. Overall, electrostatic interactions account for most of the mineral-bacteria interactions observed, with Fe-oxides being the minerals expected to play an important role in *E. coli* transport in natural environments due to their net positive charge under environmental conditions.

1.0 Introduction

The presence of pathogens in natural aquifers is a constant problem in most rural communities (Gagliardi and Karns, 2002; Rudolph et al, 1998; Topp et al, 2003). *Escherichia coli* is a fecal coliform often associated with livestock manure and humans (Byappanahalli et al., 2003). Large quantities of manure produced by agricultural activities are therefore susceptible to leaching by rain and surface water, making *E. coli* a common groundwater contaminant in rural areas (Goss et al, 1998). According to Ontario schedule 1, regulation 169/03 of the Safe Drinking Water Act 2002, levels of total coliforms, fecal coliforms and *Escherichia Coli* should be undetectable.

Adhesion of bacteria to minerals is a very important geochemical reaction that can aid in retarding the movement of bacteria through soil and water. There are several interrelated variables that control the adhesion between bacteria and minerals in soil. These include soil mineralogy, abundance of nutrients, pH, ionic strength, bacterial growth phase and metabolic activity. Adsorption between bacteria and metals has been discussed in many studies (Daughney et al, 2001; Daughney and Fein, 1997, Yee et al, 2000; Fein et al, 1997); however, few studies provide information on the adhesion of *E. coli* to common soil minerals, such as quartz and iron oxides.

It is known that in most natural soil and water conditions (above pH 4), bacterial cell walls carry a negative charge (Fein et al., 1997; Daughney et al., 1998). If a bacterial cell has a negative charge, its adhesion to negatively charged minerals should be minimal due to electrostatic repulsion. This means that negatively charged pathogenic bacteria, such as *E. coli,* can percolate through a soil composed of minerals with negative electrical charges resulting in a risk to environmental and human health. The most common soil

minerals; quartz feldspars, and micas have a net negative charge in the pH range common to natural water conditions (4<pH<9)(Yee et al., 2000). The electrostatic forces for bacterial adhesion to quartz and most soil minerals should, as a result, be unfavourable. On the other hand, iron oxides (which comprise oxides, hydroxides and oxyhydroxides) represent a common soil mineral group and they possess a net positive charge in the pH range of 4-8 (Cornell and Schwertmann, 1996). Iron oxides therefore represent a class of minerals capable of retarding the transport of pathogenic bacteria in soils.

Studies have shown that pH, ionic strength, bacterial species and strain, nutrient availability and mineralogy all influence adsorption and adhesion between bacteria and metals and/or minerals (Ams et al., 2004; Daughney and Fortin, 2002 and references therein). There are comparatively few studies (Stenstrom, 1989; McCaulou et al, 1994) that have examined the interactions between gram-negative bacteria, such as *E. coli,* and common constituent minerals.

Several models have been proposed to quantify adhesion. The Derjaguin-Landau-Verwey-Overbeek (DLVO) theory, which takes into account the long range electrostatic and short range van der Waals forces between charged surfaces and measures the potential energy of interactions between two surfaces as a function of their separation distances (van Loosdrecht et al, 1989), is a commonly used to evaluate adhesion and adsorption in experimental studies. This method can be used for studies that vary the ionic strength since it accounts for the differences in the thickness of the electric double layers associated with the surfaces. However, the theory relies on parameters that have to be measured for each system and is not readily transferable to natural conditions (van Loosdrecht et al, 1989; Yee et al., 2000). Another commonly used model is the chemical

equilibrium surface complexation model (SCM). Because they encompass all the number, type and deprotonation constants for all the functional groups on the cell walls and mineral surfaces, SCMs have been shown to enable quantitative extrapolation to more general and complex natural settings (Yee et al, 2000; Fein et al, 1997; Daughney and Fein, 1997).

The objective of this study is to examine the effect of pH, growth phase and metabolic activity on the adhesion of *E. coli* to quartz and lepidocrocite (γ-FeOOH). The experimental results obtained from the acid-base titrations (Chapter 2), the present data on zeta potential and surface area, and the adhesion experiments can be used in surface complexation models. The models will be used to predict the extent of *E. coli* adhesion to the minerals under the conditions used here and in more complex environments.

2.0 Materials and Methods

2.1 *E. coli* Growth Protocol

E. coli K-12 cells were grown according to the protocol described in Chapter 2. In the M9 medium, at 37°C, the cultures took approximately 20-24 hours to reach the exponential growth phase, and 48-60 hours to reach the stationary growth phase. The mid-exponential and mid-stationary cells were also exposed to various treatments in order to modify their metabolic activity and reproduction (Table 3.1).

2.2 Mineral Preparation

The quartz and lepidocrocite used in the experiments were obtained from Alpha Aesar (Silicon (IV) oxide, 99.995% and Iron (III) hydroxide, gamma FeO(OH)). The minerals were washed 5 times in 0.01M $NaNO_3$ and then dried for 7 days in an anaerobic chamber in a nitrogen environment. Both mineral phases were confirmed to be pure and were identified as quartz (SiO_2) and lepidocrocite (γ-FeOOH) by XRD analysis.

Table 3.1: Treatments of E. *coli* cells.

Growth phase	System	Treatment: streptomycin
Mid-exponential	Inactive and not reproducing	yes
	Active	no
Mid-stationary	Inactive and not reproducing	yes
	Active	no

2.3 Dry weight calibration

Dry weight of bacteria was used as a representation of the number of bacteria present in a suspension for all adhesion experiments; therefore a calibration curve was necessary. The method for creating the dry weight calibration curve is described in detail in Chapter 2, section 2.2.6 (dry weight calibration). A dry weight calibration curve was created from the results, and was used to calibrate all of the titration data. A correlation between optical density and actual cell count was also performed, the method and results for which can be seen in Appendix 3.1.

2.4 Zeta Potential Measurements

Zeta potential is the measurement of the electrical potential that exists across the interface of all solids and liquids, known as electrophoretic mobility. A charged particle will move at a fixed velocity in a voltage field and the zeta potential is measured by tracking particles through a microscope as they move in a voltage field. Zeta potential measurements of *E. coli* cells (of various growth phases and metabolic activity, (Table 3.1) were performed as a function of pH using a Zeta-Meter 3.0+, and a Malvern Zetasizer 3000 (University of Windsor, Ontario). The measurements were performed in 0.01M $NaNO_3$ electrolyte. Zeta measurements were also done with *E. coli* cells suspended in M9 medium, in order to see if the chemical composition of the aqueous solution affected the zeta measurements. Using the acid-base titration data available for quartz, lepidocrocite and *E. coli* (Chapter 2), the measured zeta potential values of *E. coli* and the values available in the literature for quartz and lepidocrocite, and a surface complexation model approach, the surface potential (in volts) of each mineral and the cells was determined as a function of pH.

2.5 Bacteria – Mineral Adhesion Experiments

Batch adhesion experiments with quartz were done in both M9 growth medium (the chemical composition is described in chapter 2) and in 0.01M $NaNO_3$ electrolyte, as a function of pH, growth phase and metabolic state of *E. coli* cells. The mineral-bacteria weight ratio varied between 0.4 and 1.4 for the adhesion experiments with quartz. For the adhesion experiments with lepidocrocite, only the M9 medium was used for the reasons

described below. The weight mineral-bacteria ratio for the adhesion to lepidocrocite was kept at approximately 1.0.

For all adhesion experiments conducted in the growth medium, *E. coli* cells were grown as indicated above and kept in the M9 growth medium. The fresh suspension of a known optical density (approximately 0.270) was then kept under nitrogen atmosphere for the duration of the experiment. The pH was adjusted to the desired values in the range of 4-10 (approximately every 0.5 unit) using small amounts of standardized 1.0M NaOH and 1.0M HCl. Each cell suspension (10 mL) was placed in contact with 0.1g of dry minerals to give a final concentration of 10g of mineral per liter of suspension in 15ml plastic falcon tubes. The pH adjustments and setup of the experiment were also done under N_2 environment. The individual tubes were then placed on a rotator (20 rotations per minute). In each experiment, the bacteria-mineral suspension was allowed to equilibrate for 45 minutes as determined by kinetic experiments (see section 2.5.1).

The adhesion experiments in the electrolyte were performed with *E. coli* cells washed 4 times with the electrolyte and re-suspended in degassed $NaNO_3$. In the quartz system, after adjusting the initial pH adjustment (4 to 10), it was noticed that the pH of each suspension drifted over the course of the experiment. As a result, the pH range for the adhesion experiment in 0.01M $NaNO_3$ ranged between approximately pH 4.5 and pH 7, as it was the value recorded at the end of the equilibration period. It was however impossible to maintain the pH of the lepidocrocite-cell suspensions in the electrolyte because all suspensions (no matter what the original pH was) had a final pH of approximately 4.5.

2.5.1 Kinetic experiments

Kinetic experiments were needed to determine the equilibration time for the adhesion experiments. The kinetic experiments were done using quartz and were prepared as in section 2.5, but with slight modifications. Eight reaction vessels were prepared under a nitrogen environment for each set of experiments, each one containing 0.1g of quartz. The pH of the culture used in the first set of experiments was approximately 4.8 and was not adjusted. The pH of the culture used in the second set of experiments was adjusted to pH 7.0 using 1.0M NaOH. Kinetic experiments were carried out over 4 hours with 10ml of suspension. The reaction tubes were allowed to rotate for fixed amounts of time, after which the optical density was recorded.

2.5.2 Adhesion to quartz

After the pre-determined equilibration period of 45 minutes in both M9 and the electrolyte, the quartz particles were allowed to settle for approximately two minutes after which a small sample of the supernatant was withdrawn from each tube using a Pasteur pipette. The unattached bacterial fraction was determined through the measurement of the optical density (at a wavelength of 600nm) of the supernatant. The percentage of bacteria attached to the mineral was determined by subtracting the optical density of the supernatant after the equilibration period from the original optical density.

2.5.3 Adhesion to lepidocrocite

The adhesion experiment protocol for lepidocrocite in the M9 medium was identical to the one described for quartz. However, the iron oxide particles were finer

than the quartz ones and thus did not settle readily under gravity after the equilibration period. Each suspension was then centrifuged at 500 rpm for three minutes to ensure that all the iron particles settled to the bottom of the tube but that the unattached cells remained in suspension. The percentage of bacteria attached to the mineral was determined by subtracting the optical density of the supernatant after the equilibration period from the original optical density.

2.5.4 Control experiments

Control adhesion experiments were done in the absence of minerals to determine whether cell adhesion to the falcon tubes occurred. One experiment was performed on three separate falcon tubes at pH 4, 7 and 10, while the other included 12 samples ranging from pH 4-pH 10. The control experiments showed that approximately 10% of the bacteria adhered to the sides of the tubes. The amount of bacteria attached to the tubes varied randomly over the experiment with the twelve samples, resulting in a standard deviation of 4.2%.

The effect of pH on the optical density of the bacterial culture was monitored. A bacterial suspension of a given optical density (between 0.2 and 0.6) was separated into several sub-samples that were adjusted to different pH values between 2 and 10 to determine if there was a significant variation of the optical density with pH changes.

3.0 Results

3.1 Optical density and dry weight

Optical density was highly correlated to the dry weight of bacteria (R^2 = 0.997) indicate that the approach is reliable, as indicated by the high correlation coefficient (Figure 3.1). The relationship between the optical density and the number of cells is shown in appendix 3.1.

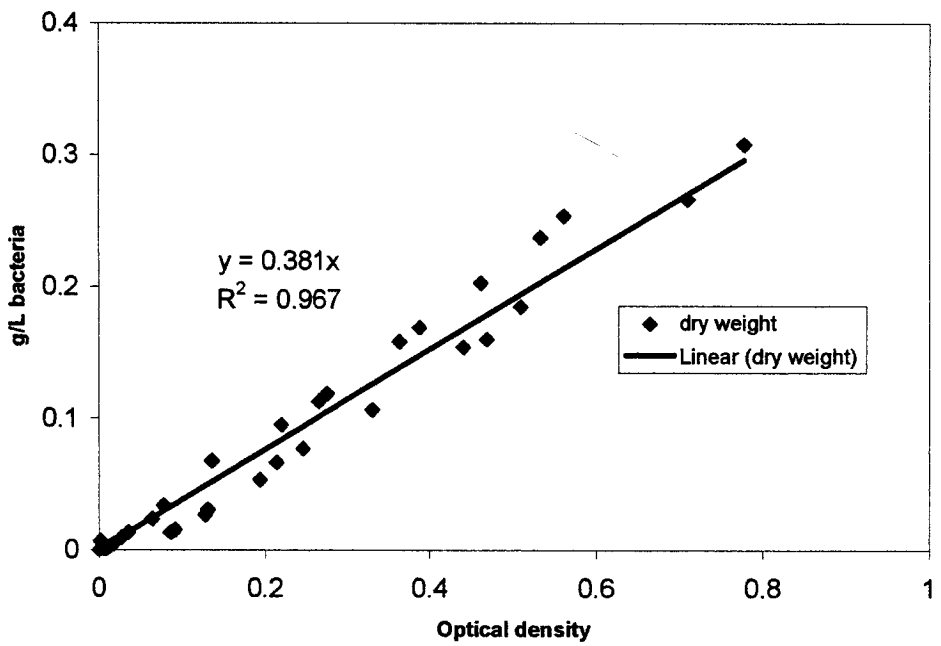

Figure 3.1. Optical Density vs. dry weight of bacteria calibration curve used to determine dry weight of bacteria present in each adhesion experiment.

3.2 Effect of pH on optical density

The results of the effect of pH on the optical density (OD) for 4 individual trials of 4 separately grown cultures at both relevant growth phases are shown in Figure 3.2. The results confirm that there are no considerable changes in OD when the pH is changed.

3.3 Kinetic experiments

Kinetic experiments were done to determine the correct equilibration time needed for adhesion to completely take place. Equilibrium was achieved within approximately 30 minutes with no significant changes in adhesion over the next four hours (Figure 3.3). As a result, adhesion experiments were allowed to proceed for 45 minutes before measurements were taken to ensure that maximum adhesion was obtained in every case.

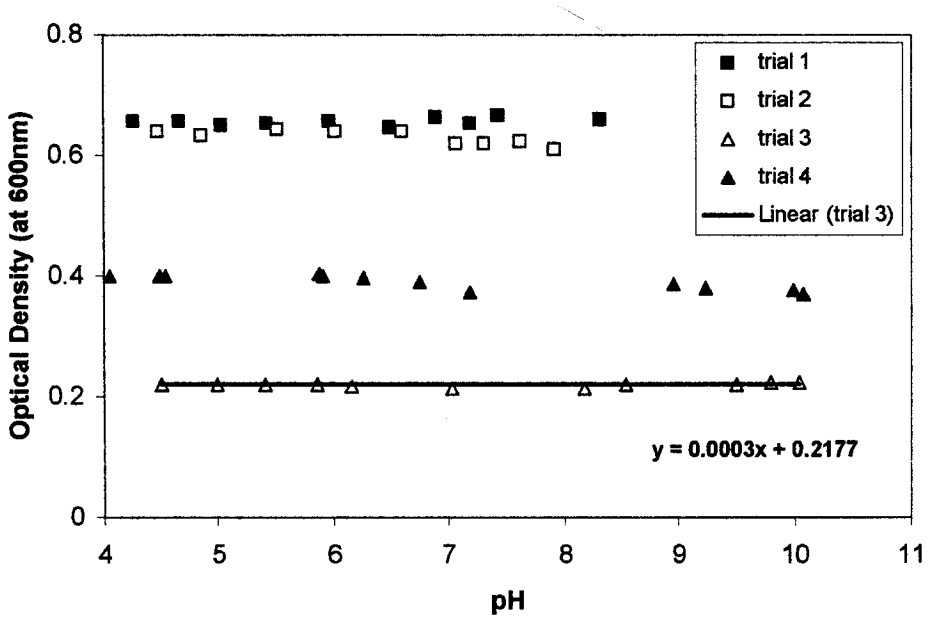

Figure 3.2. Optical density of four separate cell suspensions as a function of pH. Trial 1 and 2 represent cultures harvested at mid-stationary phase. Trials 4 and 5 represent cultures harvested at mid-exponential phase.

3.4 Adhesion to quartz in the growth medium and the electrolyte

There was no adhesion of *E. coli* cells to quartz in M9 medium, whereas some adhesion occurred in the electrolyte (Figure 3.4). *E. coli* adhesion to quartz in $NaNO_3$ electrolyte varied according to growth phase and metabolic activity, as shown in Figure

3.5.. Adhesion in the electrolyte generally varied from 8% to 23% over the pH range and slightly increased with pH in most cases.

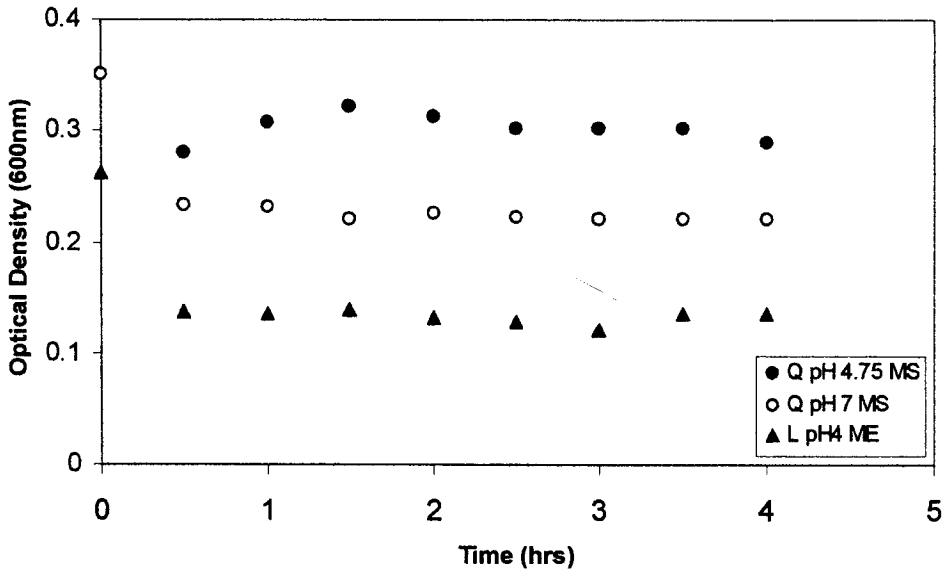

Figure 3.3 Kinetic adhesion equilibration experiment performed with E. coli cells at mid exponential (ME) and mid stationary (MS) phase and quartz (Q) or lepidocrocite (L) in electrolyte $NaNO_3$ 0.01M. Both quartz experiments had a starting optical density of 0.352 (quartz experiments) adjusted to pH 4.75 and pH 7, while the lepidocrocite experiment began with a starting optical density of 0.262 and was adjusted to pH 4.02.

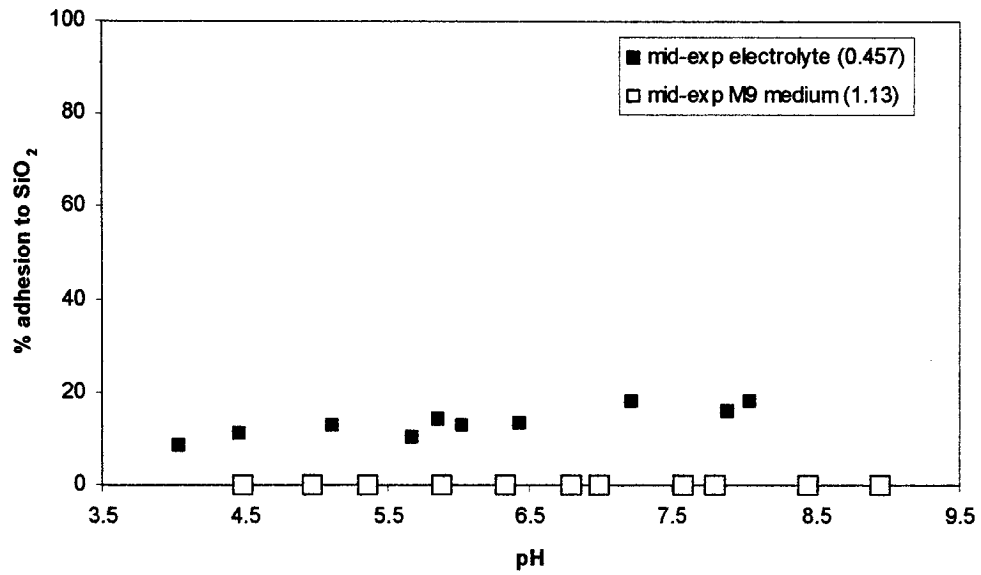

Figure 3.4 Comparison of the adhesion of metabolically active *E. coli* cells in their mid-exponential growth phase to quartz (SiO_2) in $NaNO_3$ electrolyte (solid symbols) and in M9 medium (empty symbols).

Active cells in their exponential phase adhered less to quartz than in their stationary growth phase, especially at higher pH (Figure 3.5a). In addition, non-active *E. coli* cells in their mid-stationary growth phase adhered more to quartz than non-active cells in their mid-exponential growth phase (Figure 3.5b). A comparison of active and inactive cells in the same growth phase indicated that the adhesion was slightly higher for non-active cells than for active cells (Figures 3.5 c and d).

There is a correlation between the weight of bacteria: mineral ratio and the amount of adhesion in the quartz system. Figure 3.6 illustrates that adhesion was greater in systems that had a higher bacteria: mineral ratio.

3.5 Adhesion to lepidocrocite in the growth medium

The adhesion of *E. coli* to lepidocrocite (γ-FeOOH) in M9 medium is shown in Figure 3.7. Adhesion to lepidocrocite was greater than to quartz, reaching almost 80% in certain cases. Furthermore, adhesion to lepidocrocite generally decreased with increasing pH, especially after pH 5-6 (Figure 3.7).

For similar mineral-bacteria ratios, *E. coli* adhesion to lepidocrocite was greater for non-active cells in their mid-exponential growth phase, followed by non-active cells in their mid-stationary growth phase, then active cells in their mid-exponential, while the lowest adhesion was observed for active cells in their mid-stationary growth phase (Figure 3.7).

The effect of weight bacteria-mineral ratios on adhesion was difficult to assess since most of the experiments with lepidocrocite were carried out at a similar ratio of 1.0, however some experiments had slightly lower or higher bacteria-mineral ratio.

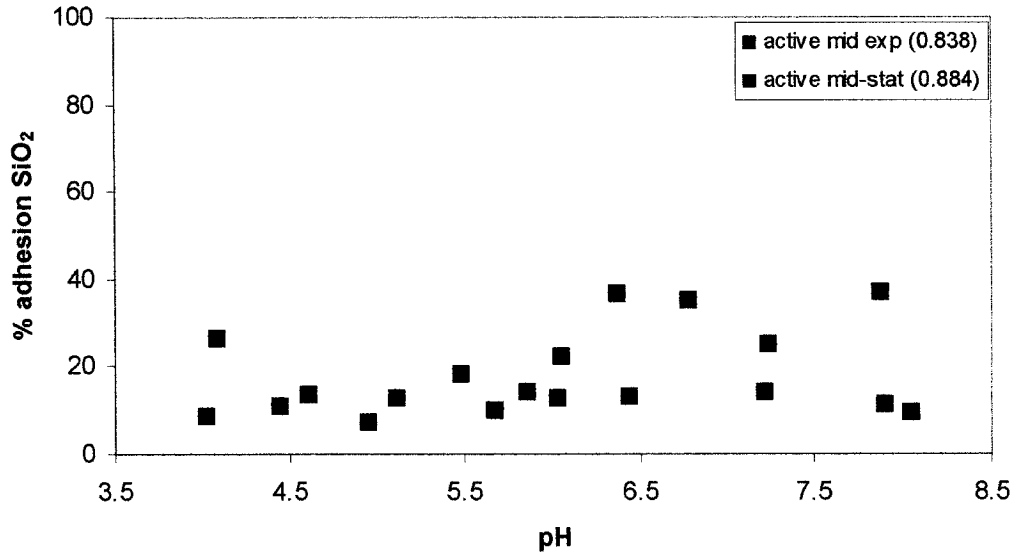

Figure 3.5 **a**

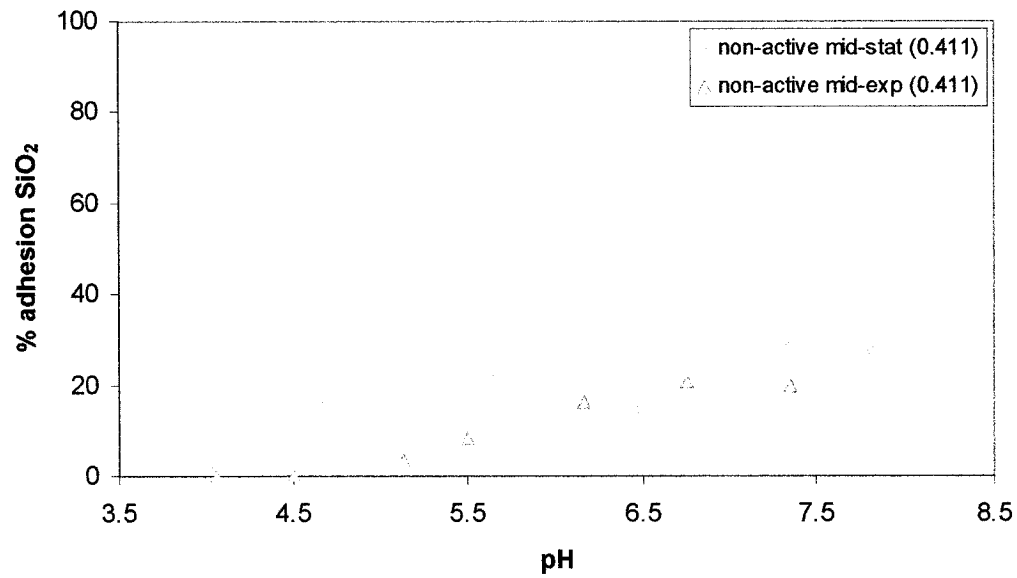

Figure 3.5 **b**

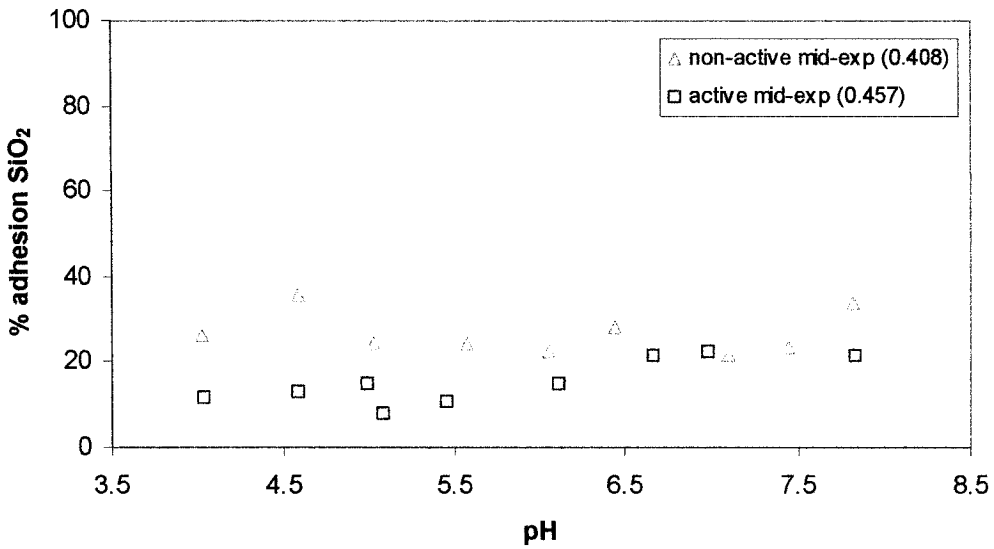

Figure 3.5 **c**

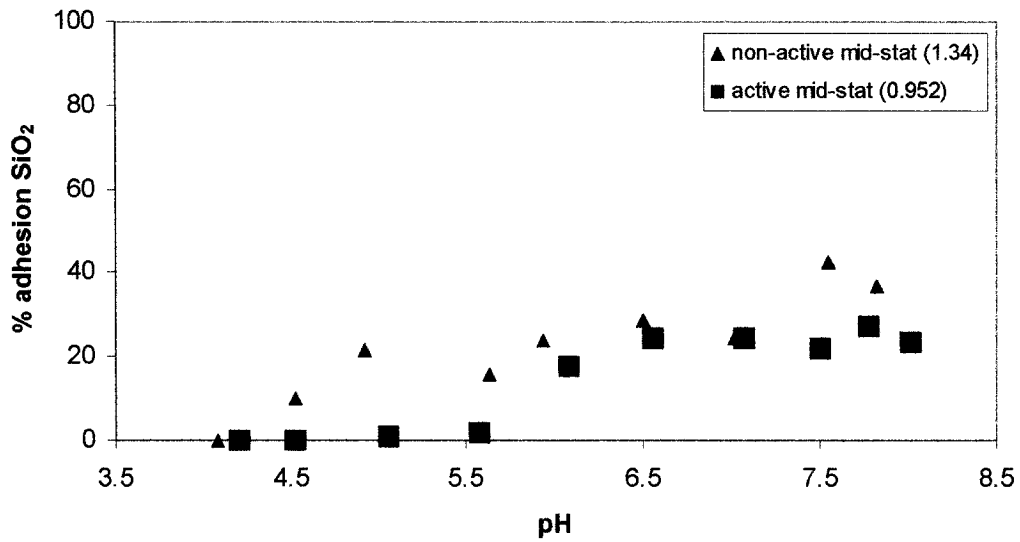

Figure 3.5 **d**

Figure 3.5. Adhesion of *E. coli* cells to quartz in the electrolyte as a function of pH and metabolic state. **a)** Comparison between active cells in the mid-exponential growth phase (blue squares) and mid-stationary phase (red squares) **b)** comparison of non-active cells in the mid-exponential (green triangles) and the mid-stationary phase (pink triangles). **c)** Comparison of active (blue squares) and non-active (green triangles) cells in the mid-exponential phase. **d)** Comparison of active (red squares) and non-active cells (pink triangles) in the mid stationary phase. Bacteria: mineral in each comparison were similar.

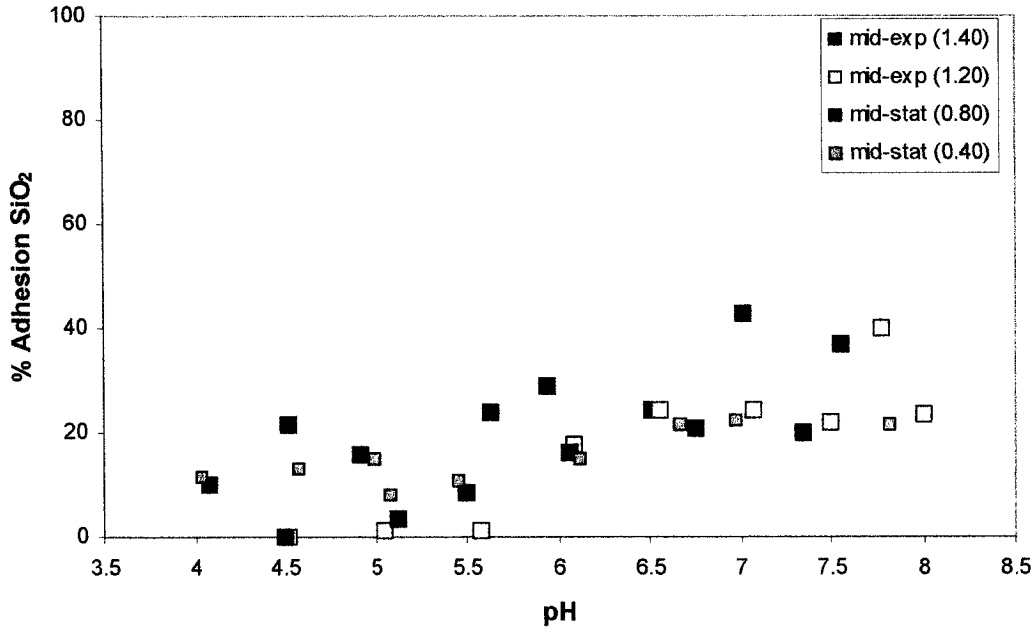

Figure 3.6. Adhesion of metabolically active *E. coli* cells in their mid-exponential and mid- stationary phase to quartz in $NaNO_3$ for various bacteria: mineral weight ratios as shown in the legend.

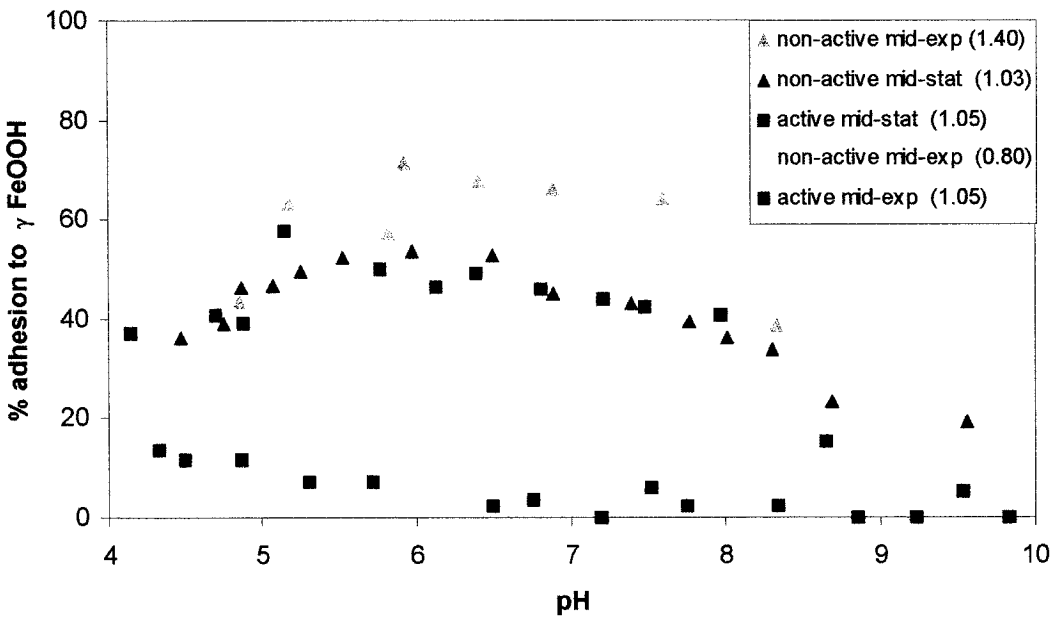

Figure 3.7. Adhesion of *E. coli* cells to γ-FeOOH in M9 medium as a function of pH and metabolic state. Bacteria: Mineral ratios are all close to 1.0 to allow comparison between treatments with the exception of the non-active mid-exponential phase cells (green triangles) as there were no experiments with the same ratios. In this case, two experiments were included, one with a lower ratio (0.80-lighter green) and one with a higher ratio (1.40-darkest green).

Adhesion slightly increased with increasing mineral-bacteria ratio for active mid-exponential cells (Figure 3.8 a) and active mid-stationary cells (Figure 3.8 c). An increase in adhesion with increasing bacteria: mineral weight ratio was observed between the highest and lowest ratios (1.40 and 0.80) for the non-active mid-exponential phased cells (Figure 3.8 b). However, the effect is not as clear between the middle and lowest weight ratios (0.8 and 1.04), perhaps because the ratio's were too similar. The effect of weight bacteria-mineral ratio was however not clear for non-active cells in their mid-stationary growth phases (Figure 3.8 d).

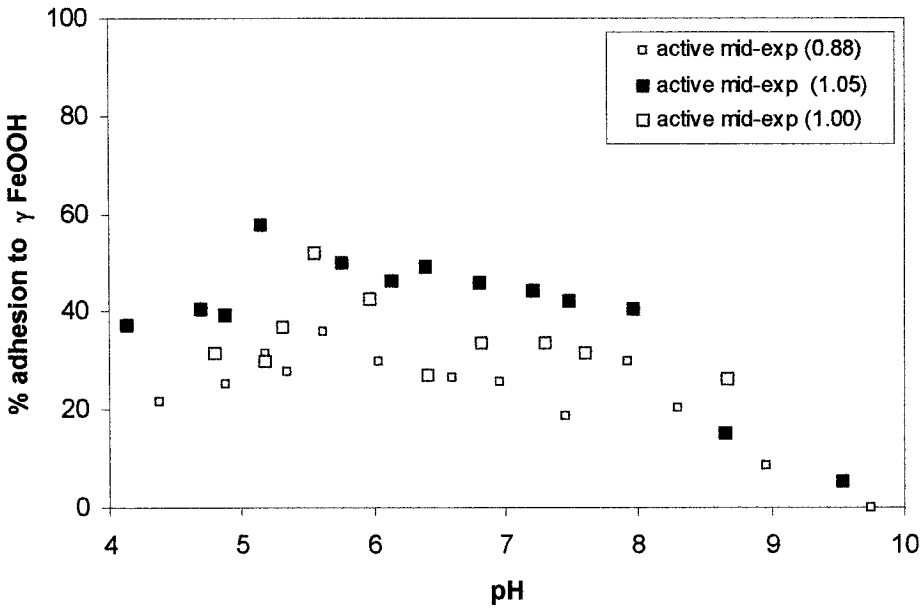

Figure 3.8 **a**

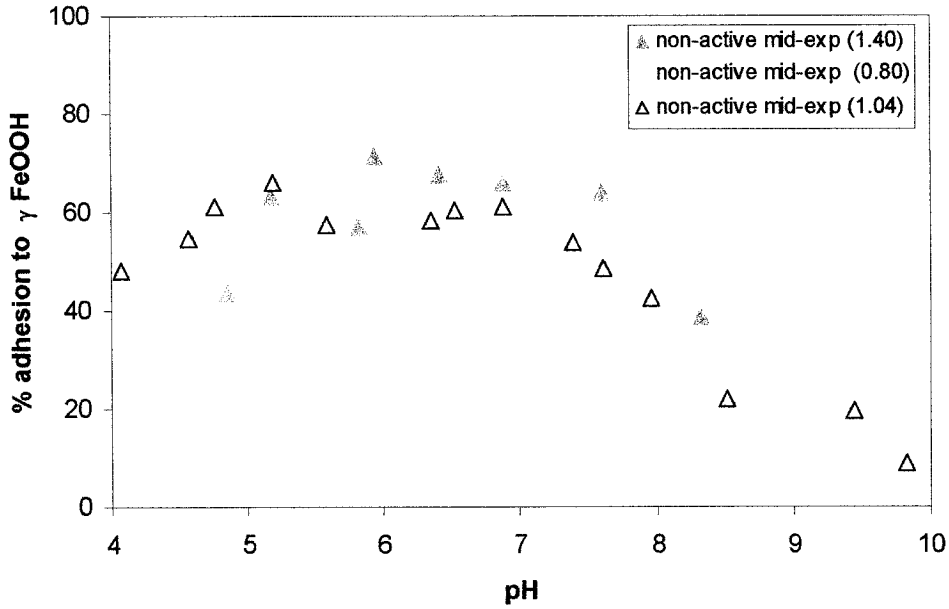

Figure 3.8 **b.**

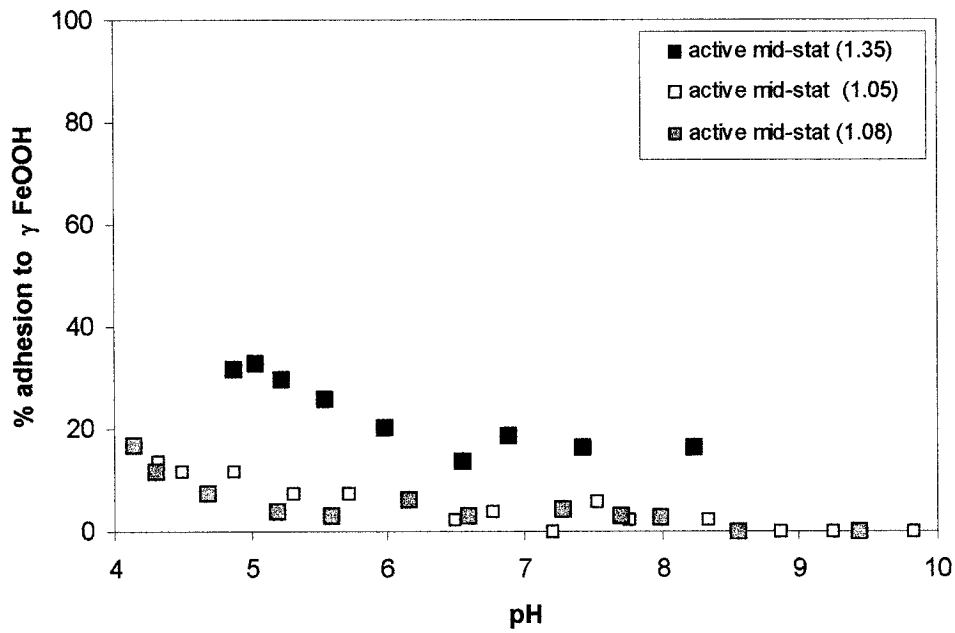

Figure 3.8 **c.**

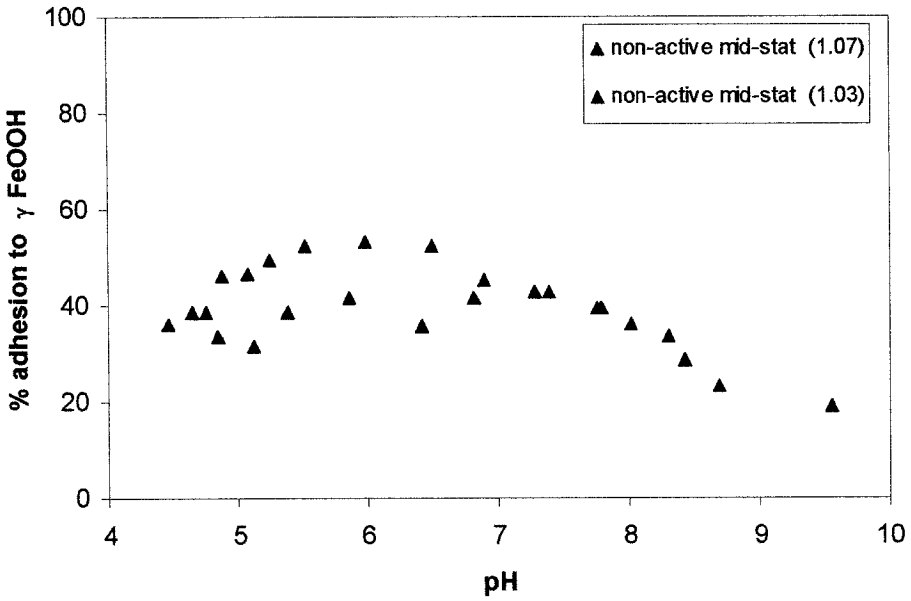

Figure 3.8 **d.**

Figure 3.8. Adhesion of *E. coli* cells to γ-FeOOH in M9 medium as a function of pH, metabolic state and growth phase for various bacteria: mineral ratios as shown in the legends. **a.** Active mid-exponential phase cells. **b.** Non-active mid-exponential phase cells. **c.** Active mid-stationary phase cells. **d.** Non-active mid-stationary cells.

3.6 Zeta measurements and surface charge

Figure 3.9 shows the zeta potential measurements of active *E. coli* cells in the M9 medium as a function of pH for both growth phases and Figure 3.10 presents the measurements for cells suspended in $NaNO_3$ (in their mid-exponential phase). In both cases, the cells display a net negative charge over most of the pH range studied here and that the cells became increasingly negatively charged with increasing pH. The cells did however possess a net positive charge around pH 2.5 in the electrolyte (Figure 3.10). The results show that the growth phase does not appear to affect the overall surface charge of the cells (Figure 3.9).

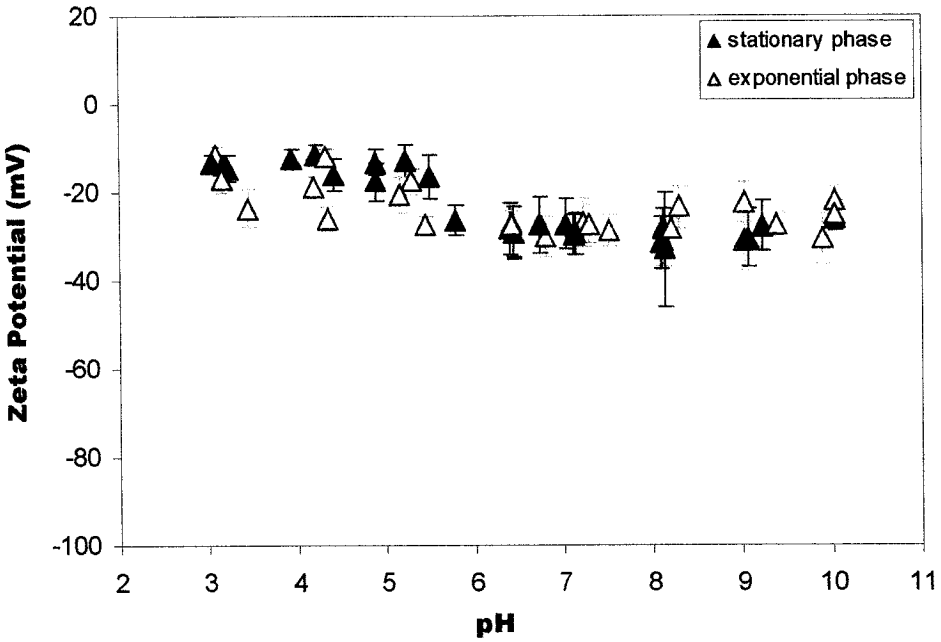

Figure 3.9. Zeta potential measurements of active *E. coli* cells in the M9 medium as a function of pH for both growth phases. Error bars represent two standard deviations.

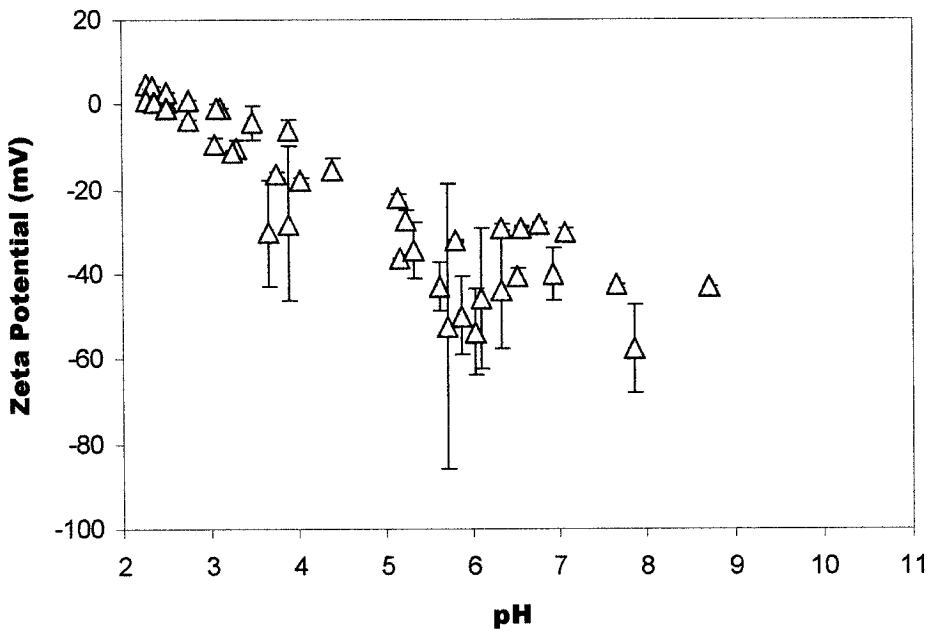

Figure 3.10. Zeta potential measurements of active *E. coli* cells in $NaNO_3$ electrolyte as a function of pH for both exponential cells only. Error bars represent two standard deviations.

Figure 3.11 presents the calculated surface electric potential of metabolically active *E. coli* cells in their mid-stationary and mid-exponential growth phase, inactive cells in their mid-exponential growth phase and quartz and iron oxide, as a function of pH. Calculations for the cells were performed with the measured zeta potentials (Figures 3.9 and 3.10), whereas literature values were used for quartz and lepidocrocite. Quartz has a net neutral to negative surface electric potential over the pH range (i.e., 4 to 10), whereas lepidocrocite possesses a positive electric potential from pH 4 to 8. On the other hand, *E. coli* cells display a net negative electric potential over the entire pH range (i.e., 4 to 8) and it is lower than the one calculated for quartz. The results also indicate that there is no difference between active and inactive cells and growth phases.

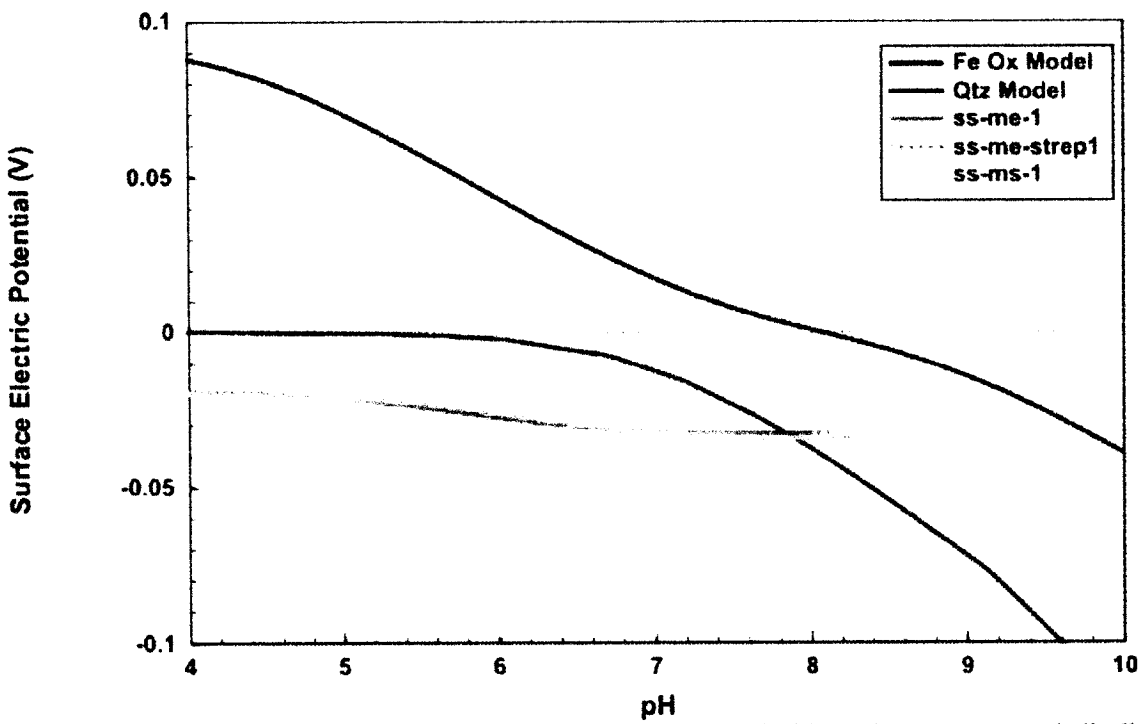

Figure 3.11. Comparison of the modeled surface potential of the lepidocrocite, quartz, metabolically active *E. coli* cells in the exponential growth phase, metabolically inactive cells in the exponential growth phase and metabolically active cells in the stationary phase.

4.0 Discussion

4.1 Effect of chemical composition of M9 medium and electrolyte

In earlier work, adhesion of bacteria onto minerals was thought to be a function of ionic strength (Jewitt et al, 1995). However, in our experiments, ionic strength had very little effect because the M9 medium had an ionic strength of about 0.009 M, and the electrolyte had an ionic strength of 0.01 M.

4.2 Effect of pH

Initially it was found that the surface electric potential of the minerals and cells was pH dependant (Figures 3.9, 3.10 and 3.11). The development of a surface charge on both minerals can be partially explained by the deprotonation of surface reactive sites (equations 1 to 4) (Dzomback and Morel, 1990; Fein et al., 1997; Yee et al., 2000).

$$SiOH_2^+ \leftrightarrow SiOH + H^+ \quad (1)$$

$$SiOH \leftrightarrow SiO^- + H^+ \quad (2)$$

$$FeOH_2^+ \leftrightarrow FeOH + H^+ \quad (3)$$

$$FeOH \leftrightarrow FeO^- + H^+ \quad (4)$$

In the case of bacteria, it has also been shown that the components of the cell wall possess an acid-base behavior, which confers a net surface charge to the cells. Fein et al. (1997) demonstrated that the cell wall of *Bacillus subtilis* (a Gram positive bacterium), possessed at least 3 different types of binding sites which likely correspond to carboxylic (eq. 5), phosphate (eq. 6) and hydroxyl groups (eq. 7) as shown below:

$$RCOOH \leftrightarrow RCOO^- + H^+ \quad (5)$$

$$RPO_4H \leftrightarrow RPO_4 + H^+ \quad (6)$$

$$ROH \leftrightarrow RO + H^+ \quad (7)$$

Surface charge measurements of bacterial suspensions have also indicated that most cells are negatively charged at pH above 2-3 (Fein et al., 1997; Daughney et al., 1998). This is in agreement with our zeta potential measurements (Figures 3.9 and 3.10). Given the surface charge of the minerals and cells, it is likely that it played a major role in adhesion, even though bacteria-mineral adhesion generally depends on both electrostatic interactions and hydrophobicity (Van Loosedrecht et al, 1989). In addition, the surface charge of the mineral may be slightly different in the M9 medium compared to the electrolyte, because some components of the M9 medium, such as phosphate, could adsorb to the mineral surface. However, phosphate is not likely to adsorb onto quartz because both surfaces are negatively charged over the pH range used for the adhesion experiment. On the other hand, phosphate could adsorb onto lepidocrocite because they are oppositely charged. The extent of phosphate sorption was not determined in this study. Adhesion of *E. coli* cells to quartz in the M9 medium was negligible when compared to adhesion in the electrolyte (Figure 3.4), suggesting that the chemical composition of the M9 medium did indeed affect the surface charge of both the cells and quartz.

The experimental data demonstrated that the adhesion of *E. coli* cells onto lepidocrocite was dependant on pH, with the highest adhesion occurring at low pH (Figures 3.7). This trend is in agreement with the surface charge of both the iron oxide and the cells. At low pH (<5), lepidocrocite possessed a net positive charge, whereas E.

coli cells were negatively charged (Figure 3.11). This resulted in a net electrostatic attraction between the two surfaces and to enhanced adhesion. On the other hand, at higher pH (> 8), both surfaces had a net negative charge and the adhesion of *E. coli* cells to lepidocrocite drastically decreased. Similar results were obtained for the adhesion of *Bacillus subtilis* (Gram-positive bacterium) cells onto corundum (Yee et al., 1999).

The adhesion of *E. coli* to quartz particles was less than to lepidocrocite and it did not appear to be dependent at low pH conditions. However, adhesion slightly increased at higher pH values for some treatments (Figure 3.5). The overall low adhesion of *E. coli* to quartz was caused in part net negative surface charge on both surfaces over the pH range (Figure 3.11). The slight adhesion increase at higher pH cannot be explained by electrostatic charges since both surface were negatively charged. This indicates that hydrophobicity might have played a role in adhesion.

4.3 Effect of Growth Phase

Several studies have found that cells adhere best to minerals and cations while they are in their exponential phase (DeFlaun et al., 1990; Fletcher 1977; van Schie and Fletcher, 1999). For instance, DeFlaun et al. (1990) found that *Pseudomonas fluorescens* and *E. coli* (both Gram-negative bacteria) adhered best to fine sandy loam in their exponential growth phase than in their stationary phase.

Daughney et al. (2001) also reported that the cell wall of *B. subtilis* cells in their exponential phase exhibited more surface functional groups than cells in their stationary phase. Specifically, there were four times more carboxyl sites and twice as many phosphate sites. Interestingly, carboxyl sites are the most common surface functional

groups on the cell envelope of *E. coli* and they have been found to be the dominant binding sites for *E. coli* (Appenzeller et al. 2001), although, phosphate groups are also present in LPS and contribute to the negative charge. Hydroxyl groups, also present on the cell wall of *E. coli,* are however protonated at pH up to 8-9, therefore not contributing to the negative charge in the pH range we studied (Appenzeller et al. 2001).

The adhesion results for active and non-active *E. coli* cells onto lepidocrocite (Figure 3.7) are in agreement with the above studies in terms of the effect of growth phase. Cells in their mid-exponential growth phase adhered more to lepidocrocite than cells in their mid-stationary phase. Despite adhesion to quartz being less, cells in their mid-stationary growth phase showed better adhesion than cells in their mid-stationary growth phase (Figure 3.6).

4.4 Effect of metabolic state

Several studies (Kjelleberg and Hermansson 1984; Fletcher, 1977; van Schie and Fletcher, 1999; Despirito et al., 1983; DeFlaun et al., 1990; Humphrey et al., 1983; Meadows, 1971; Daniels, 1980) have reported the effect of cell metabolic state on adhesion. In some cases. metabolically active cells adhere more extensively to minerals than resting cells (Despirito et al., 1983), in other cases, the opposite trend is observed (DeFlaun et al., 1990; Humphrey et al., 1983) and sometimes, no differences exist (Meadows, 1971; Daniels, 1980).

Non-active cells in their exponential and stationary growth phases adhered more to lepidocrocite than active cells over the whole pH range used for the experiment (Figure 3.7). A similar trend was observed for quartz (Figure 3.5c and d) where non-active cells

adhered better than active cells in the electrolyte. During the utilization of energy sources (such as glucose), active cells create a proton gradient on one side of the cells, which is known as the proton motive force. Once established, the proton motive force can perform work, such as generating ATP, rotating flagella, or pumping compounds across the membrane. From our results with *E. coli* cells and lepidocrocite in the M9 medium, the inactive cells (treated with streptomycin) did not pump protons through their cell walls and as a result the adhesion was enhanced. This suggests that the proton motive force somehow changed the surface charge of the cells and inhibited adhesion onto lepidocrocite. In the case of *E. coli* adhesion onto quartz in the electrolyte, the proton force was likely not important since the cells had been washed and re-suspended in the electrolyte prior to the adhesion. The increased adhesion of inactive cells over active cells remains unexplained.

4.3 Effect of Bacteria-Mineral Ratio

Previous investigations (Yee et al. 2000; Shafter et al. 1998) have found that the bacteria: mineral ratio is significant when studying adhesion. Yee et al. (2000) determined that the weight of bacteria (*B. subtilis*) adsorbed onto corundum corresponded directly to the weight of bacteria present in the system, with adhesion increasing linearly with increased weight of bacteria in the system. The linear trend observed by these authors suggested that the mineral surface was not saturated with respect to bacteria. In our systems, the effect of mineral-bacteria mass ratio was not specifically tested, but the use of different weights of bacteria and minerals in the systems allowed us to see that it might have an effect as well in the presence of quartz and lepidocrocite (Figures 3.6 and

3.8, respectively). It is clear that additional work is needed to fully assess if the trend is linear and if the minerals become saturated with bacteria, especially lepidocrocite.

5.0 Conclusions

This study demonstrates that the adhesion of *E. coli* cells to quartz and lepidocrocite is pH dependant and that the extent of adhesion is partially controlled by electrostatic interactions between the cells and the minerals. Under environmental pH conditions (pH 4-8), the cells and quartz both display a net negative charge, which prevent their adhesion. *E. coli* adhesion is enhanced in the presence of lepidocrocite because the mineral possesses a positive charge. Growth phase also had an affect on adhesion, especially in the lepidocrocite system as a result of changes in site density between growth phases might affect the extent of adhesion. Metabolic state was also an important constraint, especially in the presence of lepidocrocite. Non-active cells adhered more to lepidocrocite than active cells over the whole pH range used in the experiments likely due to the absence of proton motive force.

The presence of lippopolysaccharides and their influence on the hydrophobicity of the cell wall was not investigated. It is possible that the cells also produce extracellular polymers that increase adhesion when exposed to streptomycin. In order to fully understand the adhesion of *E. coli* to quartz and lepidocrocite, it is necessary to investigate the hydrophobic properties of the cell wall and mineral surfaces and determine and measure the presence of LPS and EPS. We can conclude that in a natural system, soils containing mainly positively charged minerals such as iron and aluminum

oxides would retain more bacteria than soils rich in negatively charged minerals such as quartz, feldspars, micas and clay.

6.0 References

Ams, D.A, Fein J.B, Dong, H, and P. A. Maurice. Experimental measurements of the adsorption of *Bacillus Subtilis* and *Pseudomonas mendocina* onto Fe-oxide-coated and uncoated quartz grains. *Geomicrobiology Journal.* 21, 511-519

Appenzeller, B. M. R., Duval, Y.B., Thomas F., and J. C. Block. 2002. Influence of phosphate on bacterial adhesion onto iron oxyhydroxide in drinking water. *Environ. Sci. Technol.* 36, 646-652.

Byappanahalli, M., Fowler, M., Shively, D. and Whitman, R. 2003. Ubiquity and persistence of Escherichia coli in a midwestern coastal stream. *Appl. Environ. Microbiol.* 69, 4549-4555.

Cornell R.M. and Schwertmann U. 1996. *The Iron Oxides: Structure, Properties, Reactions, Occurrence and Uses.* VCH, Germany.

Daniels, S.L. Mechanisms Involved in Sorption of Microorganisms to Solid Surfaces. In *Adsorption of Microorganisms to Surfaces*; Bitton, G. Marshall, K.C., Eds.; John Wiley & Sons: New York, 1980; 7-58.

Daughney, C.J. and Fortin, D. 2002. Mineral Adsorption and Absorption by Biological Cells. In Encyclopedia of Surface and Colloid Science, (A. Hubbard, Ed.), Marcel Dekker, NY, pp. 3430-3446.

Daughney.CJ. and Fein, J.B. 1998. The effect of ionic strength on the adsorption of H+, Cd^{2+}, Pb^{2+}, and Cu^{2+} ions by *Bacillus subtilis* and *Bacillus Licheniformis:* a surface complexation model. *Journal of Colloid and Interface science.* 198, 53-77.

DeFlaun,M.F.; Tamzer, A.S.; McAteer, A.L.; Marshall, B.; Levy, S.B. 1990. Development of an adhesion assay and characterization of an adhesion-deficient mutant of *pseudomonas fluorescens. Appl. Environ. Microb.* 56, 112-119.

Despirito, A.A; Dugan, P.R.; Tuovinen, O.H. 1983. Sorption of Thiobacillus ferrooxidans to particulate material. *Biotechnol. Bioeng.* 25, 1163-1168.

Dzombak, D.A. and Morel, F.M.M. 1990.Surface complexation modeling: Hydrous ferric oxide. John Wiley&Sons, New York, USA., 393 p.

Fein, J.B.,Daughney, C.J., Yee, N. and Davis, T.A. 1997. A chemical equilibrium model for metal adsorption onto bacterial surfaces. *Geochim. Cosmochim. Acta*, 61, 3319-3328.

Fletcher, M. 1977. The effects of culture concentration and age, time, and temperature on bacterial attachment to polystyrene. *Can. J. Microb.* 23(1), pp. 1-6

Gagliardi, Joel V. and Jeffrey S. karns. 2002. Persistence of *Escherichia coli* O157:H7 in soil and on plant roots. *Environmental Microbiology.* 4(2): 89-96.

Goss, M.J., Barry, D.A.J., Rudolph. D.L. 1998. contamination in Ontario farmstead domestic wells and it's association with agriculture : 1. Results from drinking water wells.. *J. Contam. Hydrol.* 32: 267-293.

Humphrey B., Kjelleberg, S. and K.C. Marshall. 1983. Responses of marine bacteria under starvation conditions at a solid-water interface. *Appl. Environ. Microb.* 45(1), 43-47.

Jewitt, D.G.; Hilbert, T.A.; Logan, B.E.; Arnold, R.G.; Bales, R.C. 1995. Bacterial transport in labratory columns and filters : influence of ionic strength and pH on collision efficiency. *Wat. Res.* 29(7): 1673-1680.

Kjelleberg, Staffan and Malte Hermansson. 1984. Starvation- induced effects on bacterial surface characteristics. *Appl. Environ. Microb.I* 48(3): 497-503.

McCaulou, D.R., Bales, R.C., and J.F McCarthy. 1994. Use of short-pulse experiments to study bacteria transport through porous media. *Journal of Contaminant Hydrology.* 15: 1-14.

Meadows, P.S. 1971. The attachment of bacteria to solid surfaces. *Arch. Microbiol.* 75; 375-381.

Morel, F.M.M. and J.G. Hering. 1993. Principles and applications of aquatic chemistry. John Wiley & Sons, New York,588 p.

Porter, K.J. and Feig, Y.S. 1980. The use of DAPI for identifying and counting aquatic microflora. Limnol. Oceanogr., 25, 943-948.

Rudolph, D.D., Barry, D.A.J., Goss, M.J. 1998. Contamination in Ontario Farmstead domestic wells and its association with agriculture: 2. Results from multilevel monitoring well installations. *J. Contam. Hydrol.* 32: 295-311.

Schafer, A.; Ustohal; P.; Harms, H.; Stauffer, F.; Dracos, T.; Zendher, A.J.B. 1998. Transport of bacteria in unsaturated porous media. *J. Contam. Hydrol.* 33: 149-169.

Strenstrom, T.A. 1989. Bacterial hydrophobicity, an overall parameter for the measurement of adesion potential to soil particles. *Appl. Environ. Microb.* 55: 142-147.

VanLoosdrecht, M.C.M; Lyklema, J.; Norde. Zehnder. A.J.B. 1989. Bacterial adhesion : a physicochemical approach. *Microb. Ecol.* 17: 1-15.

Yee, N, Fein, J.B. and Daughney, C.J., 1999. Experimental study of the pH, ionic strength, and reversibility behaviour of bacteria- mineral adsorption. *Geochim. Cosmochim. Acta,* 64: 609-617.

Yee, N., Fein, J.B. and Daughney, C.J., 2000. Experimental study of the pH, strength, and reversibility behavior of bacteria-mineral adsorption. Geochim. Cosmochim. Acta, 64, 609-617.

General Conclusions

Adhesion between bacteria and minerals has not been studied very extensively, although it is clear from previous studies discussed in Chapter 1, that several biological, chemical and mineralogical variables can affect bacterial adhesion to soil particulate matter.

The main objectives of this study were to 1) investigate how growing *E. coli* cells change the chemistry of the chemically defined M9 medium, 2) examine the surface reactivity of *E. coli* cell walls and quartz and lepidocrocite surfaces through acid-base titrations, 3) determine the amount of adhesion that occurs between *E. coli* and each of the selected minerals when exposed to one another in suspension.

The results showed that growth of *E. coli* cells caused changes in the chemistry of the M9 growth medium. The cells acidified the medium over time, likely as a result of the metabolism of glucose, which releases protons. Concentrations of nutrients (NO_3^-, PO_4^{2-}) in the medium decreased during the exponential growth phase as they were consumed by the growing cells, and dissolved nitrate and phosphate compounds were released back into the medium when the cells died off.

The acid-base titrations of *E. coli* cells in M9 medium showed that the buffering of the medium exceeded the buffering capacity of the cells, due to the high phosphate concentration in the medium. However, titrations of active *E. coli* cells in 0.01M $NaNO_3$ were reproducible and reversible and showed that the buffering capacity increased with the quantity of cells in suspension. Metabolically active cells in their mid-exponential phase showed the highest buffering capacity, whereas metabolically active cells in their mid-stationary growth phase showed the lowest buffering capacity. Non-active cells had

intermediate buffering capacities. Changes in the structure and chemical composition of the cell wall during growth were likely responsible for the differences. .

Acid-base titrations of lepidocrocite suspended in $NaNO_3$ electrolyte showed that the iron oxide had a higher buffering capacity than quartz, which is consistent with values reported in the literature. Zeta potential measurements indicated that quartz was negatively charged between pH 3 and 9, whereas the iron oxide was only negatively charged above pH 8. These zeta potential results implied that *E. coli* cells should adhere better to lepidocrocite than quartz, because the cells have a net negative charge between pH 3 and 9. This was indeed corroborated by the adhesion results, which first showed that the adhesion was pH dependant and that the extent of adhesion was partially controlled by electrostatic interactions between the cells and the minerals. Under environmental pH conditions (pH 4-8), the cells and quartz both displayed a net negative charge, which limited their adhesion, whereas *E. coli* adhesion was enhanced in the presence of lepidocrocite because the mineral possessed a positive charge. Growth phase and metabolic state also had an affect on adhesion, especially in the lepidocrocite system. Mid-exponential non-active cells adhered more to lepidocrocite than active cells over the whole pH range used for the experiment likely due to the absence of proton motive force.

From the results of this study, it is reasonable to conclude that in natural environment containing water and soil composed of quartz and iron oxides, in a pH range of 4-8, that *E. coli* cells would likely adhere to the iron oxides present in the soil, thus reducing the transport of the cells through any water present in the system. We can further extend this conclusion to a soils containing mainly positively charged minerals such as iron and aluminum oxides, which would likely retain more bacteria than soils rich

in negatively charged minerals such as quartz, feldspars, micas and clay, free of positively charged oxide minerals.

To further study the adhesion between *E. coli* cells and quartz and lepidocrocite surfaces, it would be helpful to study the cell surface in more detail to determine if they secrete any lippopolysaccharides (LPS). The presence of LPS and their influence on the hydrophobicity of the cell wall was not investigated in this study. It is possible that the cells also produce extracellular polymers that increase adhesion when exposed to streptomycin. In order to fully understand the adhesion of *E. coli* to quartz and lepidocrocite, it is necessary to investigate the hydrophobic properties of the cell wall and mineral surfaces and determine and measure the presence of LPS and EPS.

It is thought that changes in binding site density between growth phases might affect the extent of adhesion. A surface complexation model (SCM) would allow for the calculation of the K value for the cells and minerals as well as the type and concentration of binding sites available on the surface of the cell wall and mineral surfaces from the acid-base titration data. Modelling the data would enable a more accurate prediction of the behaviour of the minerals and cells in a natural environment. Due to time constraints in the study, and the necessity for complex modelling software, it was not possible to develop a SCM for the current results, however modelling of the acid-base titration data is planned for the near future.

Appendix 2 - Chapter 2

Appendix 2-1 BET Surface Area Measurement

Appendix 2-1 a. t-Plot Report Quartz

BET Surface Area Report

BET Surface Area:	0.1421	±	0.01911 m^2/g
Slope:	30.612706	±	4.107970
Y-Intercept:	0.013308	±	0.294956
C:	2301.378113		
VM:	0.032652		cm^3/g STP
Correlation Coefficient:	9.740362e-01		
Molecular Cross-section:	0.1620		nm^2

Relative Pressure	Vol Adsorbed (cm^3/g STP)	1/ [VA*(Po/P - 1)]
0.011227593	0.0217	0.524298
0.034565081	0.0314	1.138527
0.069094192	0.0389	1.906473
0.080144679	0.0413	2.107731
0.115147181	0.0335	3.884919

Appendix 2-1 b t-Plot Report Iron

t-Plot Report

Micropore Volume:	0.000629	cm^3/g	
Micropore Area:	4.5336	m^2/g	
External Surface Area:	160.6600	m^2/g	
Slope:	10.386602	±	0.113529
Y-Intercept:	0.406483	±	0.474972
Correlation Coefficient:	9.99642e-01		
Thickness Range:	3.5000 to 5.0000 A		

t = [13.9900 / (0.0340 - log(P/Po))] 0.5000

Surface Area Correction Factor:	1.00
Density Conversion Factor:	0.001547
Total Surface Area (by BET):	165.1935

Relative Pressure	Statistical Thickness, (A)	Vol Adsorbed (cm^3/g)
0.009922252	2.6204	27.8236
0.030615958	3.0062	32.2384
0.059932668	3.3370	35.4939
0.077933445	3.4996	37.0480
0.099903780	3.6776	38.7372
0.119933115	3.8273	40.1755
0.139900177	3.9688	41.5748
0.159903447	4.1052	42.9716
0.179832614	4.2374	44.3283
0.199867936	4.3680	45.6994
0.219930955	4.4972	47.1090
0.249929876	4.6894	49.2665
0.298986906	5.0056	52.9383
0.350979544	5.3503	57.0335
0.400411563	5.6941	61.0751
0.450084027	6.0620	65.2873
0.499995650	6.4620	69.8167
0.550076165	6.9032	74.8554
0.600037325	7.3950	80.6407
0.649969776	7.9544	87.5450
0.699430189	8.5977	96.1995
0.748653452	9.3590	107.4645

Appendix 2.2 pH calibration curve

pH Calibration curve: Prior to each titration, the pH electrode on the automatic titrator was calibrated to pH 4, 7 and 10. These values are shown in cells M 9, 10 and 11. The three points are plotted on a graph and an equation of the line is generated (y=mx+b). "**pH m**" is the slope of the pH calibration curve and "**pH b**" is the "b" value from the equation. These values are used in calculations in the pH column (appendix 2.2).

Appendix 2.2 a. Example of an excel spreadsheet used to create titration curves in Chapter 2. Below the spreadsheet is a pH calibration curve made individually for each experiment using pH standards.

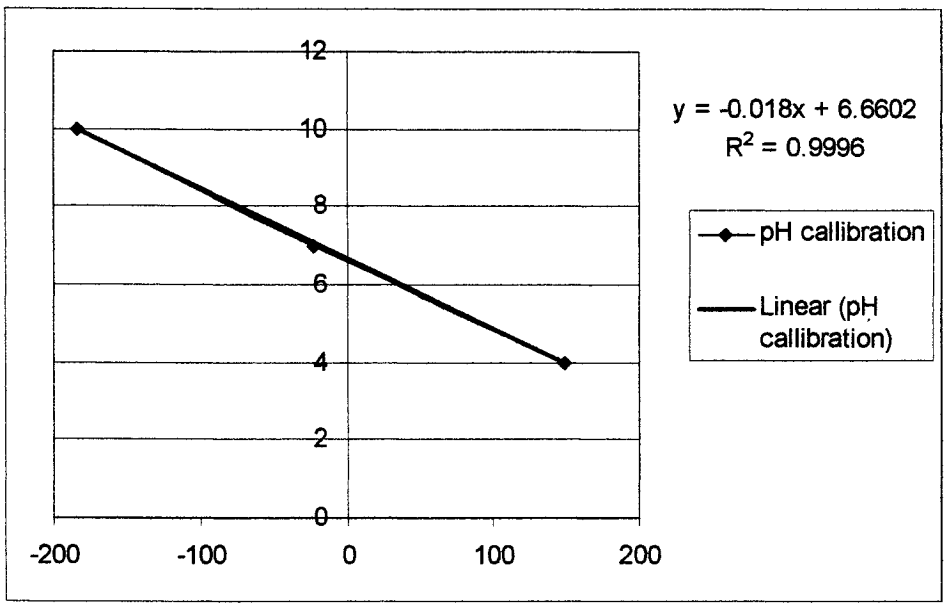

Appendix 2.3 Excel spreadsheet column explanations

mV : Column contains the pH values given on the printout provided by the automatic titrator. It represents the pH values, expressed in millivolts for each amount of base added.

Va: Column contains the volume (ml) of acid (HCl) added initially to adjust the pH to the desired starting value of approximate 4. The concentration of the acid added is accounted for in columns 4,5 and 6)

Vb: Column contains the volume (ml) of base (NaOH) added by the automatic titrator. The concentration of NaOH is accounted for in columns 4.5 and 6.

pH: Column calculates the pH of the solution after each addition of NaOH using the corresponding mV value (column A) and the values from pH m, and pH b (cells H3 and H4 as calculated from the equation from the calibration curve created from the pre-titration calibration) Each cell converts the mV reading from the titrator to the numerical pH based on the following equation:

=A3*$H$3+$H$4

= mV× pH m + pH b

[H+] added (mol/L): Column calculates the [H+] added. TOTAL concentration of protons added to the titration vessel.

[H+] Added = (total concentration of acid in your titration beaker) - (total concentration of base in your titration beaker)

=(0.1*B2/($H$7+B2+C2)-0.01*C2/($H$7+B2+C2))/$H$10

=(0.1*vol acid added/(weight of solution + vol. Acid added+vol base added)

$$=0.1\times\frac{V_{AA}}{\text{Wt of Sol}+V_{AA}+V_{BA}}-0.01*\frac{V_{BA}}{\text{Wt of Sol}+V_{AA}+V_{BA}}$$

[H+] sorb/g wet bug: Column calculations the [H+] sorbed /g wet bug. This represents the H+ interactions with the bacteria and removes the effect of the water interactions,

[H+] Adsorbed = [H+] Added - [H+] + [OH-]

In this equation, [H+] = 10^(-pH) and [OH-] = 10^(pH-14). These are the normal standard relationships between pH, [H+] and [OH-] in water, like:

pH = -log[H+], and [H+][OH-] = 10^(-14).

= (E2-10^(-D2)+10^(-14+D2))/$H$11

$$=\frac{([H+]\text{added}^{pH}+10^{-14+pH})}{\text{Wt Dry Bug/L}H_2O}$$

Appendix 2.3 a. Excel spreadsheet showing raw data used to calculate titration curves of bacteria.

1	A	B	C	D	E	F	G	H	I	J	K	L	M
2	mV	Va	Vb	pH	[H+] add (moles/l)	[H+] sorb/g wet bug							
3	148.5	0.0859	0	3.9872	0.001041924	0.000440441	pH m	-0.018	-55.5556				
4	140	0.0859	0.125	4.1402	0.000887493	0.000382345	pH b	6.6602					
5	130.3	0.0859	0.225	4.3148	0.000764649	0.000335965							
6	127.5	0.0859	0.25	4.3652	0.000734035	0.000324094	wt susp	39.4449	g				
7	124.3	0.0859	0.275	4.4228	0.000703459	0.000312264	wt wet bug	0.084089	g				
8	120.7	0.0859	0.3	4.4876	0.000672921	0.000300395	wt soln	39.36081	g			pH Callibration	
9	116.9	0.0859	0.325	4.556	0.000642422	0.000288313	wt dry bug	0.030938	g			4	149.4
10	112.6	0.0859	0.35	4.6334	0.000611962	0.000276153	wt dry bug/ml H2O	0.000209	g/ml			7	-22.9
11	107.7	0.0859	0.375	4.7216	0.000581539	0.000263888	wt dry bug/l H2O	0.209	g/l			10	-183
12	102.5	0.0859	0.4	4.8152	0.000551155	0.000251361	wt wet bug/l H2O	2.1318	g/l				
13	96.7	0.0859	0.425	4.9196	0.000520809	0.00023866							
14	90.5	0.0859	0.45	5.0312	0.000490501	0.000225723							
15	83.7	0.0859	0.475	5.1536	0.000460231	0.000212596	VOL SAMP	39.233					
16	77.1	0.0859	0.498	5.2724	0.000432416	0.000200336							
17	70.1	0.0859	0.521	5.3984	0.000404633	0.000187935	**O.D = 0.549**						
18	63.5	0.0859	0.543	5.5172	0.000378088	0.000175932							
19	56.3	0.0859	0.567	5.6468	0.000349163	0.000162732							
20	48.6	0.0859	0.591	5.7854	0.000320272	0.00014947							
21	41.4	0.0859	0.612	5.915	0.000295022	0.000137824							
22	34.4	0.0859	0.632	6.041	0.000270998	0.0001267							
23	26.5	0.0859	0.653	6.1832	0.000245799	0.000115001							
24	18.8	0.0859	0.6715	6.3218	0.000223621	0.000104684							
25	11.8	0.0859	0.688	6.4478	0.000203859	9.54735E-05							
26	3.5	0.0859	0.706	6.5972	0.000182318	8.54231E-05							
27	-3.9	0.0859	0.722	6.7304	0.000163187	7.6487E-05							
28	-13.1	0.0859	0.7395	6.896	0.00014228	6.67191E-05							
29	-21.1	0.0859	0.7535	7.04	0.000125568	5.89108E-05							
30	-29.2	0.0859	0.7675	7.1858	0.000108867	5.11094E-05							
31	-38.5	0.0859	0.7825	7.3532	9.09858E-05	4.27653E-05							
32	-47.4	0.0859	0.796	7.5134	7.49043E-05	3.52753E-05							
33	-56.2	0.0859	0.809	7.6718	5.94287E-05	2.80876E-05							
34	-64.8	0.0859	0.822	7.8266	4.3963E-05	2.09302E-05							
35	-75	0.0859	0.836	8.0102	2.73189E-05	1.32906E-05							
36	-92.7	0.0859	0.848	8.3288	1.30617E-05	7.12498E-06							

Appendix 2-4 Calculation of Uncertainty

For each aspect of the calculation performed to obtain the titration curves as seen in chapter 2 and appendix 2-1, the uncertainty (or error) for the calculation was determined according to the following set of equations and rules.

When adding or subtracting values:

$$U_{TOTAL} = \sqrt{U_a^2 + U_b^2 + U_c^2 + ..}$$

When multiplying or dividing values (relative uncertainty)

$$\frac{U_Y}{Y} = \sqrt{\frac{U_a^2}{A^2} + \frac{U_b^2}{B^2} + \frac{U_c^2}{C^2} + ...}$$

Where U_Y is the error on the calculated value Y, and U_{abc} is the error associated with the measured value A, B, C etc.

$$= \text{Conc. acid added} \times \frac{V_{AA}}{(V_{SUSP} + V_{AA} + V_{BA})} - \text{Conc. base added} * \frac{V_{BA}}{(V_{SUSP} + V_{AA} + V_{BA})}$$

$$= 0.1 \times \frac{V_{AA}}{(V_{SUSP} + V_{AA} + V_{BA})} - 0.01 * \frac{V_{BA}}{(V_{SUSP} + V_{AA} + V_{BA})}$$

Simplified

$$= \frac{(0.1)(V_{AA}) - (0.01)(V_{BA})}{V_{SUSP} + V_{AA} + V_{BA}}$$

Example Active Mid-Exp (0.273g/L) – for pH 4.11

Known Values and Associated Error:

Concentration Acid Added [HNO_3] = 0.1M

Error Concentration [HNO_3] = $2.0*10^{-4}$M

Concentration Base Added= 0.01M

Error Concentration [NaOH] = $5*10^{-5}$M

V_{AA}= 0.094g = 0.094ml/1000 = $9.4x10^{-5}$L

Error V_{AA} =0.1mg = $1.0x10^{-4}$g=ml/1000= $1.0x10^{-7}$L (error of balance)

V_{BA}= 0.125ml = 0.125/1000 = $1.25x10^{-4}$L

Error V_{BA}= 5μL=**5**.$0x10^{-6}$L (error of titrator)

V_{SUSP} = 39.13g= 0.03913L

Error V_{SUSP} =0.1mg = $1.0x10^{-4}$g=ml/1000= $1.0x10^{-7}$L (error of balance)

1) <u>error denominator</u>

$$\text{Error } (V+Vaa+Vba) = \sqrt{V_{SUSP}^2 + V_{AA}^2 + V_{BA}^2}$$

$$= \sqrt{(1.0\times10^{-7}\text{L})^2 + (1.0\times10^{-7}\text{L})^2 + 5.0\times10^{-6}\text{L})^2}$$

$$= \sqrt{(1.0\times10^{-14}\text{L})^2 + (1.0\times10^{-14}\text{L})^2 + 5.0\times10^{-11}\text{L})^2}$$

$$= \sqrt{2.50\times10}^{-11}\text{L}^2$$

$$= \mathbf{5.0\times10^{-6}L}$$

<u>Error for (Concentration acid) (volume acid added)</u>:

$$\frac{U_Y}{Y} = \sqrt{\frac{U_a^2}{A^2} + \frac{U_b^2}{B^2} + \frac{U_c^2}{C^2} + \ldots}$$

$$\frac{\text{error}_{(HNO3\times V_{AA})}}{(HNO_3 \times V_{AA})} = \sqrt{\left(\frac{(1.0\times10^{-7}\text{L})^2}{(9.4\times10^{-5}\text{L})^2}\right) + \left(\frac{(2.0\times10^{-4}\text{ mol/L})^2}{(0.1\text{mol/L})^2}\right)}$$

$$= \sqrt{1.13\times10^{-6} + 4.0\times10^{-6}}$$

$$= \sqrt{5.13\times10^{-6}}$$

$$\frac{error_{(HNO3\times V_{AA})}}{(HNO_3 \times V_{AA})} = 2.26\times10^{-3}$$

$$error_{(HNO3\times V_{AA})} = (2.26\times10^{-3})(9.4\times10^{-6}\,L)(0.1 mol/L)$$

$$= \mathbf{2.13\times10^{-9}\ mol}$$

Error for (Concentration base) (volume base added):

$$\frac{error_{((NaOH\times V_{BA})}}{(NaOH\times V_{BA})} = \sqrt{\left(\frac{(5.0\times10^{-6}L)^2}{(1.25\times10^{-4}L)^2}\right)+\left(\frac{(5.0\times10^{=5}mol/L)^2}{(0.01mol/L)^2}\right)}$$

$$= \sqrt{(1.6\times10^{-3})^2+(2.5\times10^{-5})^2}$$

$$= \sqrt{1.63\times10^{-3}}$$

$$= 0.0403$$

$$error_{((NaOH\times V_{BA})} = 0.0403\ mol \times ([NaOH]\times V_{BA})$$

$$= 0.0403 \times (0.01\ mol/L \times 1.25\times10^{-4}L)$$

$$= \mathbf{5.04\times10^{-8} mol}$$

2) Error numerator

Error

$$([NaOH]\times V_{BA})([HNO_3]\times V_{BA}) = \sqrt{(Error\,[NaOH]\times V_{BA})^2+(Error\,[HNO_3]\times V_{BA})^2}$$

$$Error = \sqrt{(2.13\times10^{-8}\,mol)^2+(5.04\times10^{-8}\,mol)^2}$$

$$= \sqrt{4.54\times10^{-16}\,mol^2+2.54\times10^{-15}\,mol^2}$$

$$= \sqrt{2.99\times10^{-15}\,mol^2}$$

$$= \mathbf{5.47\times10^{-8}\ mol}$$

Value Numerator $= ([HNO_3]\times V_{AA})-([NaOH]\times V_{BA})$

$$= (0.1\text{mol/L} \bullet 9.4\times10^{-6}\text{L}) - (0.01\text{mol/L} \bullet 1.25\times10^{-4}\text{L})$$

$$= 9.4\times10^{-6}\text{mol} - 1.25\times10^{-6}\text{mol}$$

$$= \mathbf{8.15\times10^{-6}\ mol}$$

Value Denominator $= V + V_A + V_B$

$$= 0.0391\text{L} + 9.4\times10^{-5}\text{L} + 1.25\times10^{-4}\text{L}$$

$$= \mathbf{0.03935L}$$

$$\frac{\text{val. numer.}}{\text{val. demonim.}} = \frac{8.15\times10^{-6}\text{mol}}{0.0394\text{L}}$$

$$= \mathbf{2.07\times10^{-4}\ mol/L}$$

$$\frac{\text{Final Error}}{\text{Final Value}} = \sqrt{\left(\frac{(\text{error num.})^2}{(\text{value num.})^2}\right) + \left(\frac{(\text{error denom.})^2}{(\text{value denom.})^2}\right)}$$

$$= \sqrt{\left(\frac{(5.47\times10^{-8}\text{mol})^2}{(8.15\times10^{-6}\text{mol})^2}\right) + \left(\frac{(5.0\times10^{-6}\text{L})^2}{2.07\times10^{-4}\text{L}^2}\right)}$$

$$= \sqrt{(0.00671)^2 + (0.0242)^2}$$

$$= \sqrt{(4.50\times10^{-5})^2 + (5.83\times10^{-4})^2}$$

$$= \sqrt{6.28\times10^{-4}}$$

$$= 0.0251$$

$$\frac{\text{Final Error}}{2.07\times10^{-4}} = 0.0251$$

Final Error $= 0.0251 \times 2.07 \times 10^{-4}$ mol/L

Final Error on $[H^+]$ added= 5.19×10^{-6} mol/L

Appendix 2.4a. Titration curve showing error bars. Note that graph needed to be enlarged more than twice it's original size to be able to see the uncertainty.

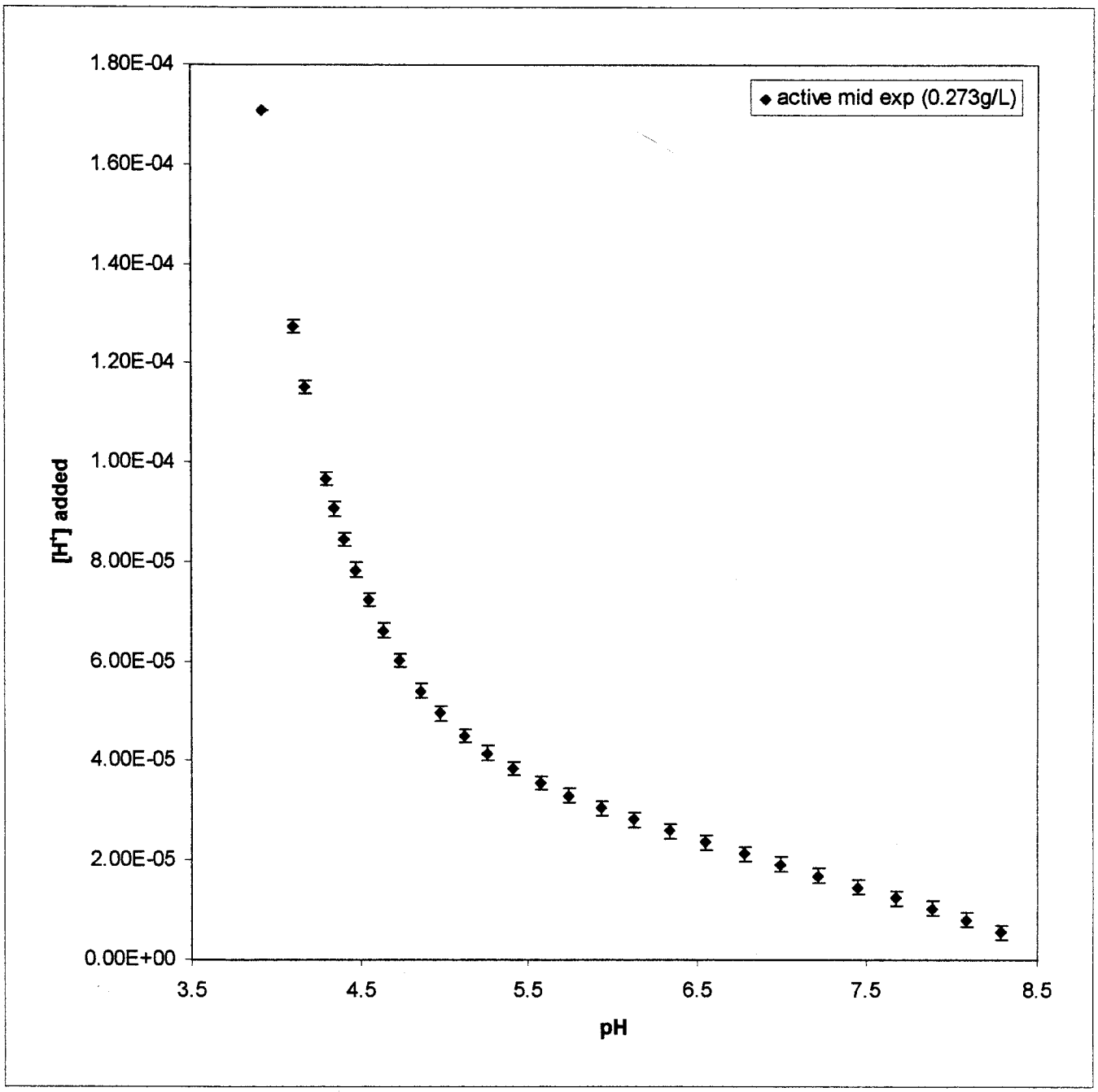

Appendix 3 - Chapter 3

Appendix 3.1 Optical Density vs. Bacterial Cell Count

Appendix 3.1 a. Relationship between the optical density and the number of *E. coli* cells, as determined by DAPI counting.

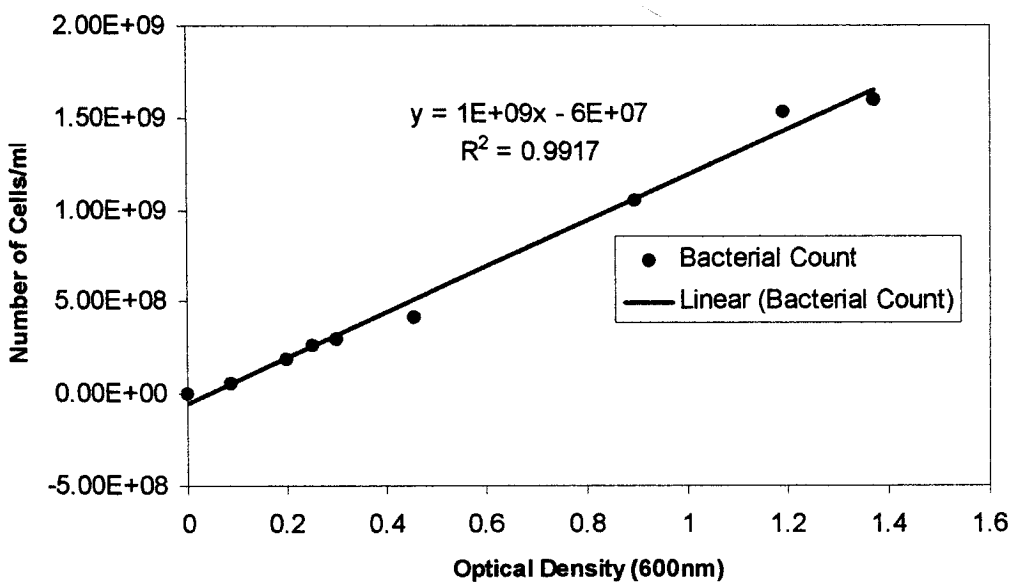

Relationship between the optical density and the number of *E. coli* cells, as determined by DAPI counting.

Method Dry Weight-Cell Count Correlation

In order to determine the number of cells that remained in suspension after each experiment, it was necessary to make a correlation between the optical density, the dry weight of bacteria in g/ml, and the number of cells for each dry weight/optical density. First, a calibration curve was made to correlate dry weight to optical density as described

in chapter 2. Second, a calibration curve describing the relationship between the number of cells and the optical density was obtained. This was accomplished by growing *E. coli* cultures to mid-exponential phase and then pelleting them by centrifugation at 6000rpm for ten minutes. The supernatant was discarded each time and after the final wash, the cells were re-suspended in a given amount of 0.01M $NaNO_3$ to provide an optical density between approximately 0.250 and 1.5. Cell count was done with DAPI (4',6-diamidino-2-phenylindole; Porter and Feig, 1980). The cells were first fixed with aqueous gluteradehyde (Sigma) (final concentration 2% vol/vol). After fixation, the samples were then diluted to 1:100, 1:200, 1:500, and 1:1000 to ensure representative cell counts. Counting was performed with a Jena Zeiss epifluorescence microscope at 1250X magnification with a standard UV excitation filter.

In order to determine the number of cells in a given suspension, first the optical density is measured, and then the following equation is used: $\mathbf{y = 1E+09x - 6E+07}$, where x is equal to the value obtained from the optical density measurement, and y is equal to the number of cells for that given suspension.